Microbial cooperation at high temperatures

By Jacinta van de Grint
MSc Nanobiology
13 July 2020

TU Delft
Erasmus MC
Universitair Medisch Centrum Rotterdam

Microbial cooperation at high temperatures

by

Jacinta van de Grint

to obtain the degree of Master of Science Nanobiology
at the Delft University of Technology,
and the Erasmus MC Rotterdam,
to be defended publicly on Monday July 13, 2020 at 10:00 AM.

Student number:	4447840	
Project duration:	September 7, 2019 – July 13, 2020	
Daily supervisor:	MSc. Diederik Laman Trip	
Thesis committee:	Dr. H. O. Youk,	TU Delft, supervisor
	Prof. Dr. C. L. Wyman,	Erasmus MC, TU Delft
	Dr. G. E. Bokinsky,	TU Delft

An electronic version of this thesis is available at http://repository.tudelft.nl/.

Abstract

Microorganisms can cooperate with each other, meaning that individual cells work together to pursue a common interest. Cooperation can be crucial for microorganisms to survive stressful environmental conditions. In this work, we report on the cooperative behaviour by the yeast *S. cerevisiae* and the bacterium *E. coli*, which stimulates survival and growth at high temperatures.

Our lab had already discovered that genetically identical yeast cells cooperate with each other via the secretion of a public good (the antioxidant glutathione), to extend habitability of high temperatures. However, microbes naturally live in communities, where they coexist with other strains and species. These microbial communities are crucial to the health of an ecosystem, but their habitats are warming up due to climate change. So, understanding their response to a rising temperature may be crucial to keep ecosystems healthy. We take it one step further and study the cooperation between different yeast strains at high temperatures. We found that not only a population of genetically identical cells, but also different strains cooperate with each other, to collectively survive under high temperature conditions. We performed so-called co-existence experiments at high temperatures, where we combined two different yeast strains, one genetically fitter than the other. Depending on the initial composition of the mixed population, we obtained two outcomes. In the first outcome, the genetically fitter strain helps the less fit strain to grow. In the second outcome, vice versa, the less fit strain helps the fitter strain to grow. A mathematical model that reproduces the experimental data, predicts an additional outcome, where both strains would help each other to grow.

Additionally, we discovered a novel cooperative behaviour at high temperatures in the bacterium *E. coli*. We found that *E. coli* cells show similar growth behaviour compared to yeast and we hypothesize that a comparable cooperative behaviour lies at the basis, also regulated by the secretion of a public good. These results suggest that cooperation at high temperatures could be conserved amongst different microbial species.

Acknowledgements

I would like to thank the members of the Youk lab, for the useful suggestions and feedback. Especially, I would like to thank my direct supervisors: Diederik Laman Trip and Dr. Hyun Youk, for allowing me to join the group, for helping me throughout the research process and for the insightful discussions.

Contents

Part 1

Introduction

Microorganisms are extremely diverse, microscopic organisms, living in almost all habitats on earth, ranging from gut flora of animals [1] to seabeds [2]. Like all organisms, microorganisms take part in social interactions with each other. One type of interaction is cooperation, a process of individual cells working together for a common benefit. For example, cooperation between cells has played a crucial role in the transition from unicellular to multicellular life [3]. Also, cooperation can enable a population of cells to perform collective behaviour, such as migration [4] or distribution of labour in metabolism [5]. Additionally, cooperation can be essential for the survival of a population of cells, for example by providing a mechanism that enables the cells to collectively survive harsh environmental conditions [6–8].

We will discuss two main processes that can form the basis of cooperative behaviour, the first being cross-feeding and the second being the secretion of a useful molecule (a so-called public good) [9]. Cross-feeding means that one microbial species converts a primary nutritional resource into an intermediate, which is then used by another microbial species. Initially, it seems that cross-feeding is a selfless trait, as it gives no benefit to the cooperating cell, but only to the receiving cell (i.e. the intermediate is merely a waste product to the first species, but happens to help the second species, called incidental cooperation [10]). However, some cases of cross-feeding, called syntrophy, are mutually beneficial, because the intermediate molecule inhibits the growth of the cooperating cell. Then, the uptake of the intermediate molecule by the receiving cell is beneficial for the cooperating cell as well. A well-known example of microbial syntrophy is the interaction between a methane-producing bacterial species and a bacterial species that produces one-carbon compounds [11]. The latter bacterial species produces H_2, which thermodynamically inhibits its own growth. However, the methane-producing bacteria consume H_2 and thereby promote growth of both species [11].

The second process that can underlay cooperative behaviour is the secretion of a useful molecule (a so-called public good), such as an enzyme or a signalling molecule, which can be used by other cells in the population [9, 12]. For instance, researchers found that yeast cells secrete the sucrose-digesting enzyme invertase, that catalyzes the hydrolysis of sucrose into glucose [13]. So, after the secretion of invertase, glucose is available in the environment of the cells. All cells in the population take up glucose from the environment and use it to grow. Thereby, a population of yeast cells carries out its sucrose metabolism partly as a population rather than as individuals. Here, the cells that secrete invertase cooperate for the greater good of the population, at an individual cost [5]. Namely, the cooperating cell needs to take action, via the production and secretion of the public good, which costs the cell energy [14]. Nevertheless, the benefits of cooperation can outweigh the cost for the individual cell if the cells form a spatial structure, where the cooperating cells group together [5].

Cooperation under stress

Cooperation between microbes can arise under stressful environmental conditions. One of the most well-studied examples of environmental stress is starvation. When starved, the dormant phase of the amoeba *D. discoideum* (called the fruiting body) and the vegetative cells cooperate with each other [6]. The dormant phase is only entered by part of the cells during starvation - the lucky cells. Then, the residual, vegetative cells form a protective layer around the dormant spores, thereby reducing their own chances at survival, but increasing the

chances of survival of the population as a whole. Because these cells sacrifice themselves for the greater good of the population, this is called self-destructive cooperation.

Additionally, microbes cope with the stress caused by high temperatures via cooperation, as will be described in this thesis. Each microbial species has an upper and a lower temperature limit for growth. In between, there is a range of temperatures, called the habitable range, at which the microorganism can survive and proliferate. Above the habitable range, the three major essential constituents of a cell (DNA, proteins and membranes), can become damaged [15] and a cell is likely to go into apoptosis [16]. However, cells do not exist alone, rather, they live in a population. This causes interesting, cooperative behaviour between the microbial cells to occur at the extreme high end of the habitable range [8], revealing that the cells of a population collectively combat the stress caused by high temperatures.

Why do cells cooperate?

As described above, cooperation between microbes can be crucial for the survival of a population. Nevertheless, the evolution of cooperation can be difficult to explain from an evolutionary stand point, as it favors the population but comes at a cost for the individual [17]. By cooperating with each other, microbes increase the chance of survival of the population as a whole, because it facilitates propagation of the same set of genes. Therefore, cooperative behaviour can arise between cells that are sufficiently genetically related. Cells recognize other cells with the same genome, called their kin, and only show cooperative behaviour to these cells, which is called kin selection [18]. During kin selection, cells recognize shared genes in a non-specific way via receptor binding and biochemical reactions or via quorum sensing, a communication mechanism that enables microbes to 'measure' the density of the population in their neighbourhood via the concentration of a certain signalling molecule [18]. As an example, damaged yeast cells go into apoptosis, because it is beneficial for the rest of the population, which they recognize as kin [19]. Namely, if cells with damaged genetic material would keep proliferating, a large part of the population would become damaged, whereas the death of a single, damaged cell would block the damaged genetic material. This example illustrates one of the goals of cooperation: facilitating the propagation of a cell's genome, by increasing the chance that the population survives.

Alternatively, the goal of cooperation can be to receive a benefit that outweighs the cost for the cooperative behaviour [14]. This disproportionality can be achieved when cells coexist in a spatial structure, because a spatial structure provides the required positive feedback between two cooperative acts of cells [14]. For example, *C. aggregatum* is a complex of two bacterial species (one non-motile, photosynthetic bacterium and the other a motile proteobacterium), forming in stratified lakes. The non-motile bacteria stick to the motile bacteria to reach their optimal depth in the lake. In return, the motile bacteria benefit from the presence of the photosynthetic, non-motile bacteria because they provide fixed, organic carbon. The spatial stucture of the complex results in a benefit for both species that outweighs the cost of cooperating [20]. This example illustrates that cooperation does not only arise between genetically related cells, but also between cells that coexist in a spatial structure [14].

Cooperation between different species or biological kingdoms

As will be described in this thesis, not only cells within the same population, but also cells from different genetic variants of the same species, called strains, can cooperate with each other. This shows that cooperation does not only exist between genetically identical cells, but also between cells that do not share the same genome.

In nature, different microbial species [4] or even microbial species from different biological kingdoms [21], such as fungi and bacteria, are found to cooperate with each other, despite their limited genetic relatedness. The bacterial complex called *C. aggregatum* [20] described above, is a well-studied example of cooperation between different microbial species. Cooperation between different biological kingdoms occurs for example in biofilms, which are spatially structured microbial communities, where the microbes stick to each other and to a surface via self-produced extracellular polymers [22]. For example, dental plaque consists of bacterial and fungal species [21]. The biomass of a biofilm consisting of both fungi and bacteria is larger than the sum of the single-species biofilms, which suggests that the species stimulate each other's growth via an unknown cooperative mechanism.

This thesis

In this thesis, we will study the cooperation between microbial cells that arises under the stressful condition of high temperatures. We will study two different model organisms. The first model organism is the eukaryotic yeast *S. cerevisiae*. In yeast, the cooperative behaviour between genetically identical cells has been studied before [8]. This study revealed that yeasts cooperate via the secretion of a public good - the antioxidant glutathione, which is crucial for survival at high temperatures. In nature, microbes live in communities, coexisting with other strains and species. Therefore, we aimed to mimic the natural situation partly, by combining two different strains of yeast and study the cooperation between them. We did this via co-existence experiments, experiments in which we combine two populations from two different yeast strains and separately track their growth, to determine whether they cooperate to survive heat.

To discover whether the cooperative behaviour by yeast cells is conserved among microbial species, we studied a second model organism, namely the prokaryotic bacterium *E. coli*. The cooperation between *E. coli* cells at high temperatures has not been studied before. Therefore, we started at the basis and studied the cooperation between genetically identical cells, belonging to the same population. We found that *E. coli* cells indeed make use of a similar type of cooperation to combat high temperatures. Possibly, *E. coli* cells also cooperate via secretion of a public good, carrying out similar functions compared to glutathione in yeast.

This thesis is structured as follows: first, we discuss the results from co-existence experiments with yeast. Furthermore, we present a mathematical model that recapitulates the experimental results. Then, we discuss the results from experiments with *E. coli*, where we study the cooperation between genetically identical cells. Next, the results of both model organisms are summarized and placed in current scientific consensus. Finally, an overview of the materials and methods is given.

Part 2

Cooperation in yeast at high temperatures

1 Introduction

The following chapter is focused on the model organism yeast, specifically the budding yeast *Saccharomyces cerevisiae*, which is well-known for its role in the food industry and in science. At a temperature of $\sim 30\,℃$, yeast grow optimally. However, at temperatures above $\sim 36\,℃$ [8], yeasts experience heat stress, caused by the cell being exposed to heat-induced damage. The primary stress resulting from heat is oxidative stress [23], which is caused by reactive oxygen species (ROS). ROS are chemically reactive molecules that contain oxygen, such as peroxides or superoxides, formed for example by disfunction in the respiratory chain within mitochondria [24]. Reactive oxygen species are toxic to the cell and can cause lethal damage to essential cellular components such as DNA, proteins and lipids. For example, ROS can cause errors in the DNA sequence, denaturation of proteins and unwanted permeability of lipid membranes [15].

To repair heat-induced damages, a cell can apply a series of rapid changes in gene expression, called the heat shock response system. Activation of this system results in a lower expression level of genes for protein synthesis and a higher expression level of cytoprotective genes, which encode for example the heat shock proteins (HSPs) [16]. The main role of the HSPs is to act as molecular chaperones and prevent proteins from aggregating, by helping proteins retain their native structure. Also, the heat shock response system causes cell cycle arrest, slowing down the cell's replication rate [8]. Above a sufficiently high temperature, the heat shock response system becomes insufficient [16], leading to organisms failing to replicate and eventually going into apoptosis [15]. The survival of yeast cells was conventionally thought to depend on a cell's ability to autonomously repair the heat-induced damage using its heat shock response system [8]. This means that at the optimal temperature, a cell replicates, but at a sufficiently high temperature, a cell fails to replicate and goes into apoptosis, because the heat shock response system insufficiently improves the cell's stressful condition (see Figure 1A).

Interestingly, a recent study [8] discovered that the conventional view is incomplete and the survival of a cell does not solely depend on its heat shock response, as cells do not exist alone, but rather they exist in a population. Accordingly, cells can cooperate with each other via density-dependent cell-to-cell communication, and thereby collectively reshape habitability of high temperatures [8]. The yeast cells cooperate by producing and secreting the antioxidant glutathione (see Figure 1B). Glutathione can deactivate reactive oxygen species via redox reactions [25], reducing oxidative stress of the cells, thereby promoting survival and growth of the population (see Figure 1C). Glutathione must be available in the extracellular environment, but it needs not be imported into the cell, for the cells to survive and replicate [8]. So, the secretion of glutathione, resulting in a detoxified environment, enables the cells to survive and replicate.

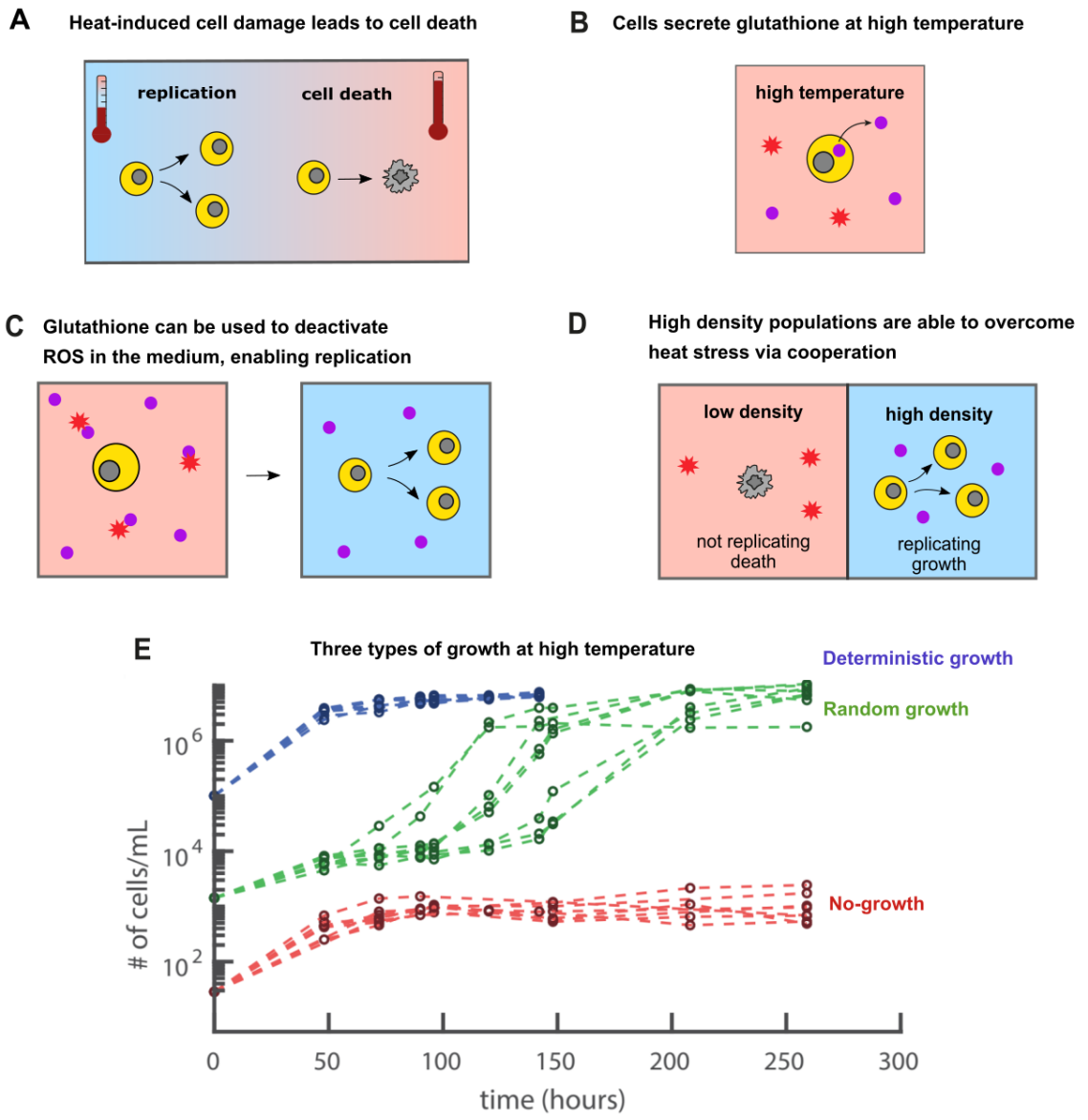

Figure 1: Growth behaviour of yeast at high temperatures. **A)** At optimal temperature ($\sim 30℃$), a cell survives and replicates, whereas at a high temperature ($\sim 40℃$), the cell dies. **B)** At high temperatures, ROS (red) arise in the medium and yeast cells secrete the antioxidant glutathione (purple). **C)** Glutathione deactivates ROS, resulting in a detoxified medium that promotes survival and growth. **D)** On the population-level, a culture with low cell density goes extinct, because the medium remains toxic, whereas a culture with high cell density grows at the same conditions, because the accumulated concentration of glutathione detoxifies the medium. **E)** Population density over time, showing density-dependent growth at 38.5 ℃. At high initial density, all populations grow (blue curves), at intermediate initial cell density, random growth occurs (green curves) and at low initial cell density, no population grows (red curves) (n=8 biological replicates per colour).

As a result, a sufficiently dense population is able to survive high temperatures - that the single cells or a less dense population would not survive (see Figure 1D). Namely, if the initial cell density is sufficiently high, glutathione is accumulated quickly, the medium is detoxified and a large fraction of the cells survives the heat to start replicating, resulting in deterministic growth (blue curves in Figure 1E). However, if the initial cell density is low, the accumulated concentration of glutathione is not sufficient, the medium remains toxic and the population is unable to grow (red curves). In between the initial cell densities that result in deterministic growth and in non-growth, there is a range of initial cell densities that results in random growth: growth after an unpredictable amount of time of stasis, a state in which the population size remains stable (green curves). Overall, this study [8] shows that the cooperation between cells can be crucial for survival.

In conclusion, yeast cells secrete a public good (the antioxidant glutathione) at high temperatures at a cost for the individual cell, namely the cost of production and secretion. Then, glutathione detoxifies the growth medium, which is not only a benefit for the individual cell, but for the whole population, promoting survival and replication of the cells. So, the cells in a population cooperate to increase the chances of collectively surviving the heat. This cooperative behaviour results in density-dependent growth, because the initial density of the population determines whether the environment can be detoxified before the population goes extinct.

Strains in a co-existence experiment

In nature, many different microbial species and strains coexist within a microbial community. Interactions occur not only within the same population, but also between different species and strains, which grow at different rates, secrete public goods at different rates and respond to them differently. This naturally raises the question of how the interactions between different species and strains influence the ability of a population to survive high temperatures. In this thesis, we evaluate the cooperative behaviour of a population consisting of two different yeast strains, as a first step towards understanding natural, microbial communities and their cooperative methods of dealing with heat stress.

To this end, we use a system of yeast strains and combine two different strains in a so-called co-existence experiment, a growth experiment where two strains share a growth medium and we separately monitor their growth. Additionally, as part of a co-existence experiment, the strains are grown separately, to characterize their growth behaviour without the influence of the other strain. Our system consists of a 'weak' strain and a 'strong' strain. The weak strain is genetically manipulated to produce a fluorescent protein, which causes it to have less resources and energy left to grow [26], whereas the strong strain is not (or to a lesser extent) manipulated to produce a fluorescent protein (see Figure 2A). As a result, the strong strain is able to grow, whereas the weak strain is unable to grow under the same conditions (see Figure 2B).

We use a phase diagram to indicate under which conditions (initial cell density and temperature) a strain grows or not. The phase diagrams were characterized for multiple yeast strains (strong and weak), expressing GFP at different levels (see Figure 2C,D). The difference in the phase diagrams indicates that GFP expression forms a metabolic burden for the cells [26], causing the strain to be weaker (i.e. under identical conditions, the strong strain grows, whereas the weak strain does not). The exact, molecular mechanism that gives a metabolic burden to a strain that expresses a fluorescent protein, requires a follow-up study.

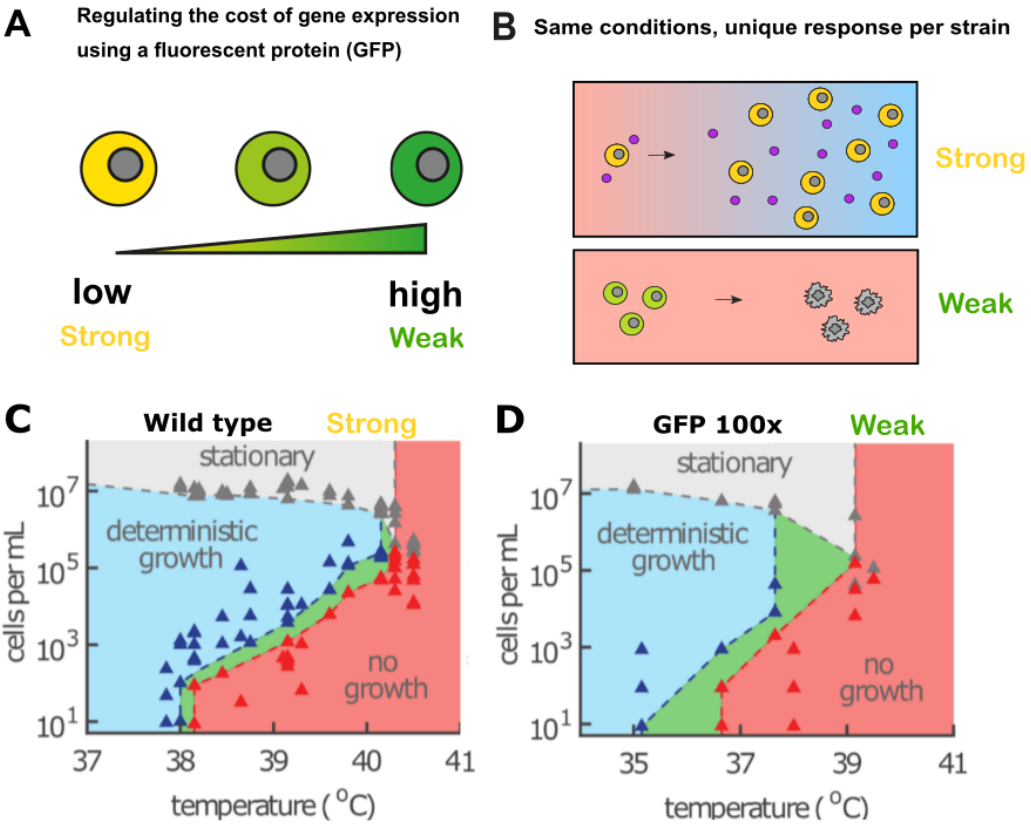

Figure 2: We combine a wild-type yeast strain (strong) and a GFP-expressing yeast strain (weak) in a co-existence experiment. **A)** The level of GFP expression can be genetically tuned (see also supplement section S1.1). **B)** The different strains have a unique response to high temperatures. **C-D)** Phase diagrams (adopted from [8]) that indicate the conditions (temperature and initial cell density) under which **C)** the wild type (strong strain) is able to grow or not. **D)** DHY5 (relative GFP expression 100x, weak strain) is able to grow or not. Green regions indicate random growth.

Outcomes of a co-existence experiment

In this thesis, we will study the outcome of co-existence experiments, growth experiments where two strains share a common environment and we separately monitor their growth. A co-existence experiment can have various outcomes. These outcomes are classified into three non-trivial scenarios: the strong strain profiting from the weak strain, the strong strain helping the weak strain or both strains helping each other to grow (see Figure 3). Here, we excluded outcomes based on two theoretical limitations: firstly, if the strong strain is unable to grow, then the weak strain is also unable to grow under identical conditions and secondly, if the weak strain is able to grow, then the strong strain is also able to grow under identical conditions. Also, we excluded trivial outcomes, where the pure cultures behave in the same way as the mixture (e.g. the strains both grow in the mixture, but also in the pure cultures). Excluding outcomes that contradict these requirements, results in the three scenarios described above. In the first scenario (see Figure 3A-C), a pure culture consisting of cells from only the strong strain would not grow (Figure 3B), but by adding cells of the weak strain, it is stimulated to grow (Figure 3C). So, the strong strain profits from the weak strain, as these cells cooperate with the strong strain and help to accumulate glutathione. In the second scenario (see Figure 3D-F), a pure culture consisting of cells from the weak strain is unable to grow (Figure 3E), but by replacing part of the population with cells from the strong strain, it is stimulated to grow. So, the strong strain helps the weak strain to grow in the mixture (Figure 3F). Finally, in the third scenario (see Figure 3G-I), the pure cultures of both strains are unable to grow (Figure 3H), but by combining them, they are stimulated to grow (Figure 3I). We expect that the cooperation between

strains is based on the secretion of glutathione, detoxifying the common growth medium.

Overall, we aim to answer the following research question: Can cooperative behaviour between different yeast strains result in the three scenarios described above: profiting from the weak strain, helping the weak strain and helping each other? Finding these scenarios as an outcome of a co-existence experiment would be the first step towards understanding cooperation at high temperatures in a microbial community.

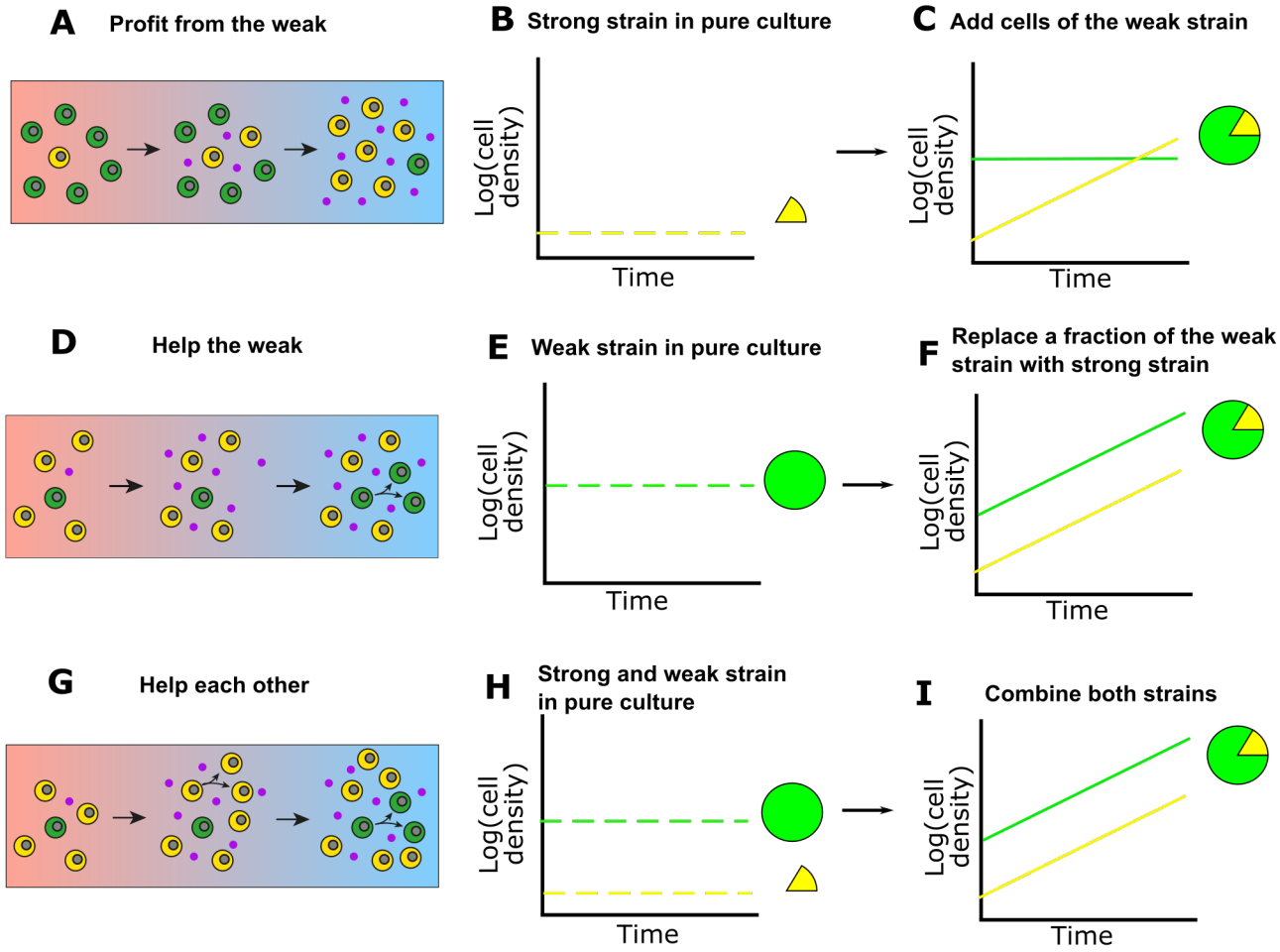

Figure 3: Three possible outcomes of a co-existence experiment. **A)** Schematic representation of the scenario called profit from the weak. **B)** The strong strain is unable to grow in a pure culture, but when we add cells of the weak strain, **C)** the strong strain grows. **D)** Schematic representation of the scenario called help the weak. **E)** The weak strain is unable to grow in a pure culture, but when we replace part of the weak strain by the strong strain, **F)** the weak strain grows. **G)** Schematic representation of the scenario called help each other. **H)** In this scenario, both strains are unable to grow in a pure culture, but when combined, **I)** both strains grow.

2 Results

In this section, the results of co-existence experiments are presented. Two different generations of strains were used. The first generation was already available, whereas the second generation was constructed specifically for this thesis. First, the results that were obtained using the first-generation strains are described, then, the results obtained with the second-generation strains and finally, we discuss the results and outline useful follow-up experiments.

2.1 First-generation strains

The first generation of strains consists of a wild-type strain (called W303), three GFP-expressing strains (called DHY3, DHY4 and DHY5), each expressing GFP at a different level (relatively 1x, 10x and 100x), and a strain with inducible GFP expression (called TT7) (see supplementary Figure S1). The GFP expression of the inducible strain TT7 is regulated by and increases as a function of the concentration of the small molecule doxycycline in the growth medium (see supplementary Figure S2).

2.1.1 Proof of concept

The first generation of strains was used to prove the concept of cooperation between different yeast strains at high temperatures, in the form of one of the three scenarios described above. We measured the cell densities of pure populations and of a mixture of two strains over time using flow cytometry (see Figure 4A). We started with a population of wild-type cells with a sufficiently low initial cell density such that they are unable to grow (Figure 4B). Then, we performed an experiment in which we co-incubated this low initial density wild-type population with cells from a GFP-expressing strain (relative expression level 10x), creating a mixed initial population consisting of different strains (see Figure 4C). In the mixture, we separated the two strains using their relative level of GFP expression (see supplementary Figure S5A). We found that in this mixed initial population, the wild type was able to grow. This suggests that the low initial density wild-type population that is unable to grow on its own, can grow when cells of another strain are added to the initial population. Thus, we found that the wild-type strain (strong strain) can profit from co-incubation with cells from a GFP-expressing strain (weak strain), which is characterized as scenario 1: profit from the weak. We were able to reconstruct this scenario with a different strain, the TT7 strain, not induced to express GFP (see Figure 4D,E).

In this scenario, the strong strain profits from the glutathione produced by the weak strain. Namely, in isolation, the strong strain does not produce and secrete a sufficient amount of glutathione on its own to detoxify the medium, but the additional glutathione produced by the weak strain detoxifies the medium sufficiently to stimulate growth of the strong strain. The weak strain is unable to grow, even though the strong strain grows, because it needs a more detoxified environment to grow compared to the strong strain. Additionally, the strong strain might deplete the nutrients in the medium before the weak strain is ready to start growing and the weak strain might go extinct before the glutathione concentration is sufficiently high. Consequently, with the same amount of glutathione in the medium, the strong strain can grow, whereas the weak strain cannot. Overall, these results provide the proof of concept that different yeast strains can cooperate with each other at high temperatures.

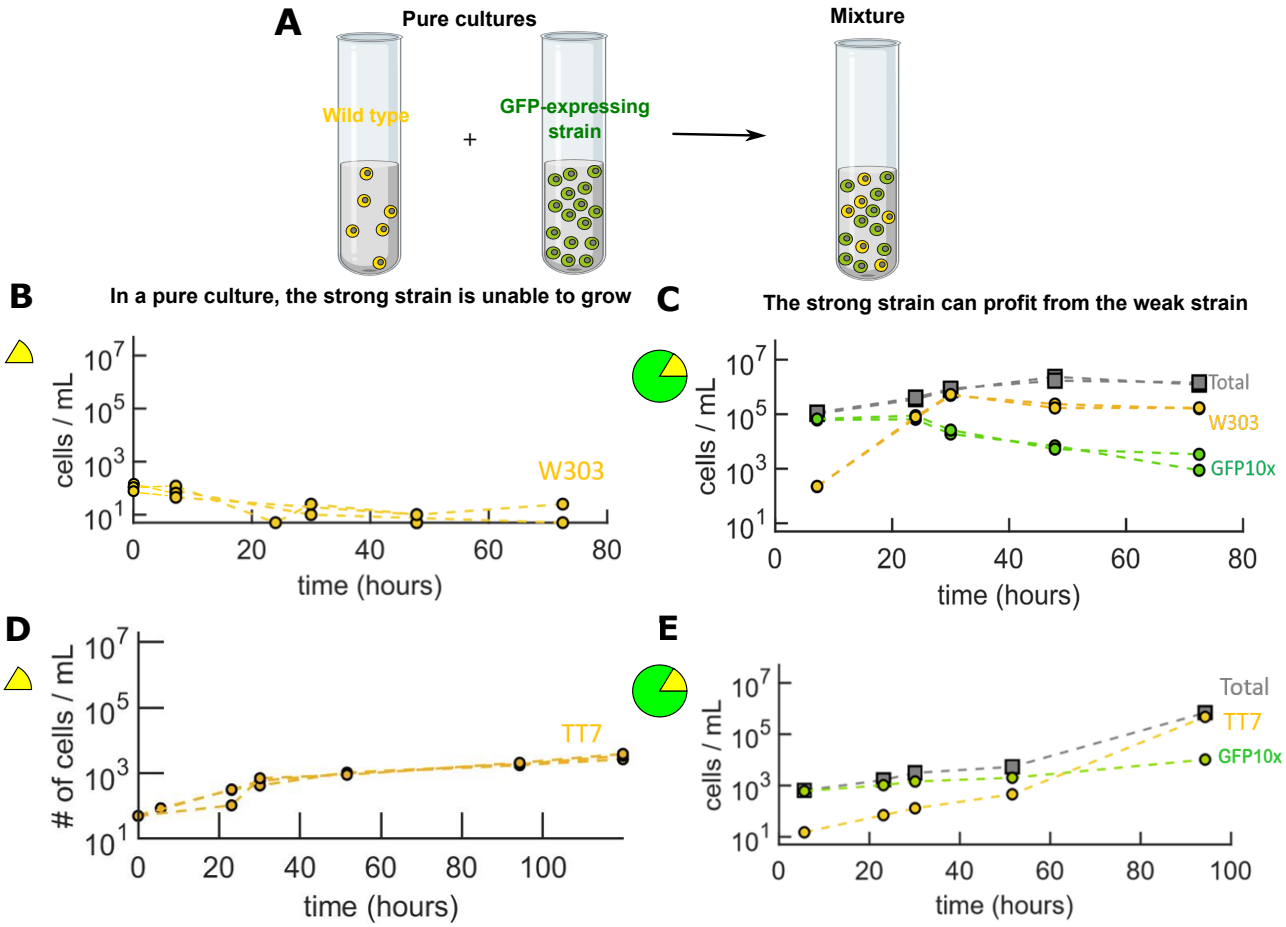

Figure 4: The strong strain profits from the glutathione secreted by the weak strain at $38.2℃$. A) Schematic of a co-existence experiment: the two strains are grown separately and in a mixture. **B)** Population density of the wild-type population over time (initially ~ 100 cells/mL). **C)** Population density over time for a mixed population of wild type w303 and DHY3 (10x relative GFP). Grey, dotted lines give the total population density. Yellow, dotted lines give the wild-type population density. Green, dotted lines give the DHY3 population density. **D)** Population density of the TT7 (non-induced to express GFP) population over time (initially ~ 50 cells/mL). **E)** Population density over time for a mixed population of TT7 (non-induced to express GFP) and DHY3 (10x relative GFP). Here, yellow, dotted lines give the TT7 population density.

2.2 Second-generation strains

Using the expression of two fluorescent proteins instead of one would enable us to mix strains with a similar expression level, but expressing a different fluorescent protein, thereby still being able to separate them. Additionally, it would simplify the separation between two strains in a co-existence experiment, because we would have two channels to use for separation, where the strains are only fluorescent in one of the channels (GFP or mCherry) (see supplementary Figure S5B,C,D). To that end, we constructed a second generation of strains, including strains that express GFP and strains that express mCherry, each at five different levels.

2.2.1 Characterization of the strains

To characterize the engineered yeast strains, we measured their relative fluorescence and maximum growth rates (at the optimal temperature of 30℃). First, we used a flow cytometer to quantify the relative fluorescence of the constitutively expressed GFP and mCherry of each strain (see Figure 5A,B and supplementary Figure S4A,B). Correspondingly, we chose the strain names to correlate with their relative expression levels (Figure 5C).

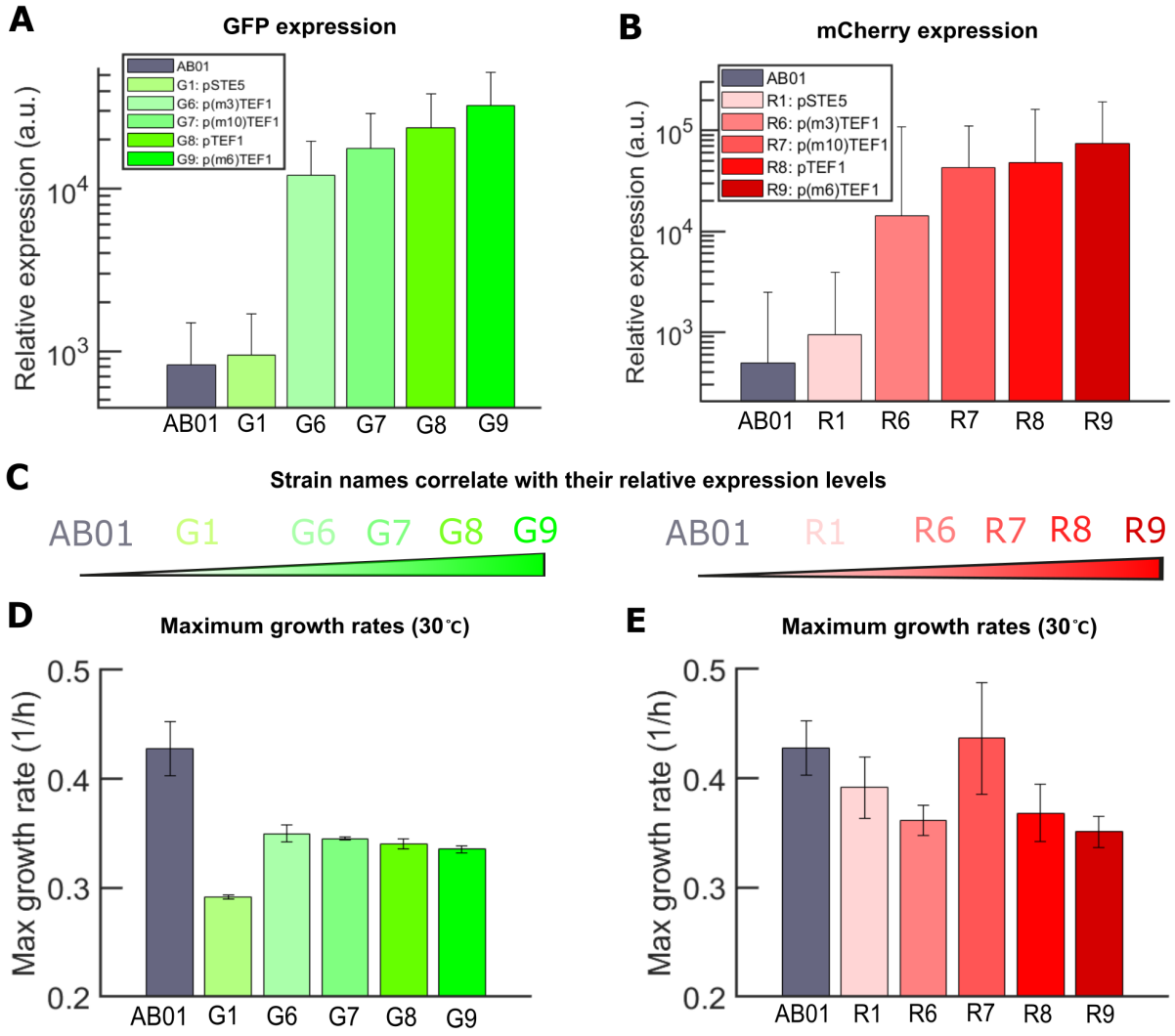

Figure 5: Characterization of fluorescence and maximum growth rate of constructed strains at $30\,^{\circ}C$. AB01 is the parent strain of the second-generation strains. **A)** Relative GFP expression of engineered yeast expressing constitutive GFP. Expression is regulated by strength of constitutive promoters. Data represents the geometric mean and error bars represent standard deviation within the population. **B)** Relative mCherry expression of engineered yeast expressing constitutive mCherry. Data represents the geometric mean and error bars represent standard deviation within the population. **C)** The strain names correlate with their relative expression levels of GFP or mCherry. **D)** Maximum growth rates of the GFP-expressing strains. **E)** Maximum growth rates of the mCherry-expressing strains. Error bars represent standard error of the mean (six biological replicates).

Next, we used a spectrophotometer, which measures the OD (optical density) of the culture every 10 minutes, to quantify the maximum growth rates of the engineered strains. The measured OD is directly proportional to the cell density of the culture. By performing a linear fit to the growth curves (Figure S4C,D), we calculated the maximum growth rates of the strains (see Figure 5D,E).

A large expression level of GFP or mCherry is expected to result in a low growth rate, because the expression of a fluorescent protein costs energy and resources (such as ribosomes and polymerases) [26], leaving less energy and resources for growth. Indeed, we observe that for the GFP-expressing strains, the maximum growth rate decreases slightly for an increasing GFP expression level, with the exception of strain G1 (see Figure 5D). For the mCherry-expressing strains, the growth rate also mostly decreases for a larger expression level, with the exception of strain R7, which has a relatively large maximum growth rate, even larger than that of parent strain AB01, which does not express a fluorescent protein at all (see Figure 5E). This may be the result

of an experimental error, such as condensation on the plate, which temporarily resulted in a lower OD, and consequently, in a larger measured growth rate after the condensation disappeared. So, we conclude that, apart from the exceptions G1 and R7, the expression level indeed correlates with the maximum growth rate, with a larger expression level resulting in a lower growth rate. Also, we observe that the standard deviation of the maximum growth rate is much larger for the mCherry-expressing strains compared to the GFP-expressing strain (see Figure 5D,E). In the future, the experiment should be repeated to conclude whether this is due to an experimental fluctuation, such as noise in the growth curves or condensation, or due to a property of the strains.

2.2.2 Co-existence experiment

With the engineered strains we can precisely choose the relative expression levels of GFP and mCherry. Using the second-generation strains, we performed new co-existence experiments to test the possible outcomes (see Figure 6A). Similarly to the previous experiment, we chose the initial cell density of the pure population of the weak strain (G6) such that it is unable to grow (see Figure 6B). The pure culture of the strong strain (R9) grows having the same initial cell density (Figure 6C). Then, we performed an experiment in which we replaced a fraction of the pure, weak culture, with cells of the strong strain, creating a mixed initial population. In the mixture, we separated the two strains using their relative level of GFP and mCherry fluorescence (see supplementary Figure S5B-D). We found that in this mixed population, both of the strains grow and coexist (Figure 6D), most likely because the glutathione accumulated by both strains is sufficient to enable growth of both strains. This experiment illustrates that a co-existence experiment can result in the outcome that the strong strain helps the weak strain, resulting in both strains co-existing.

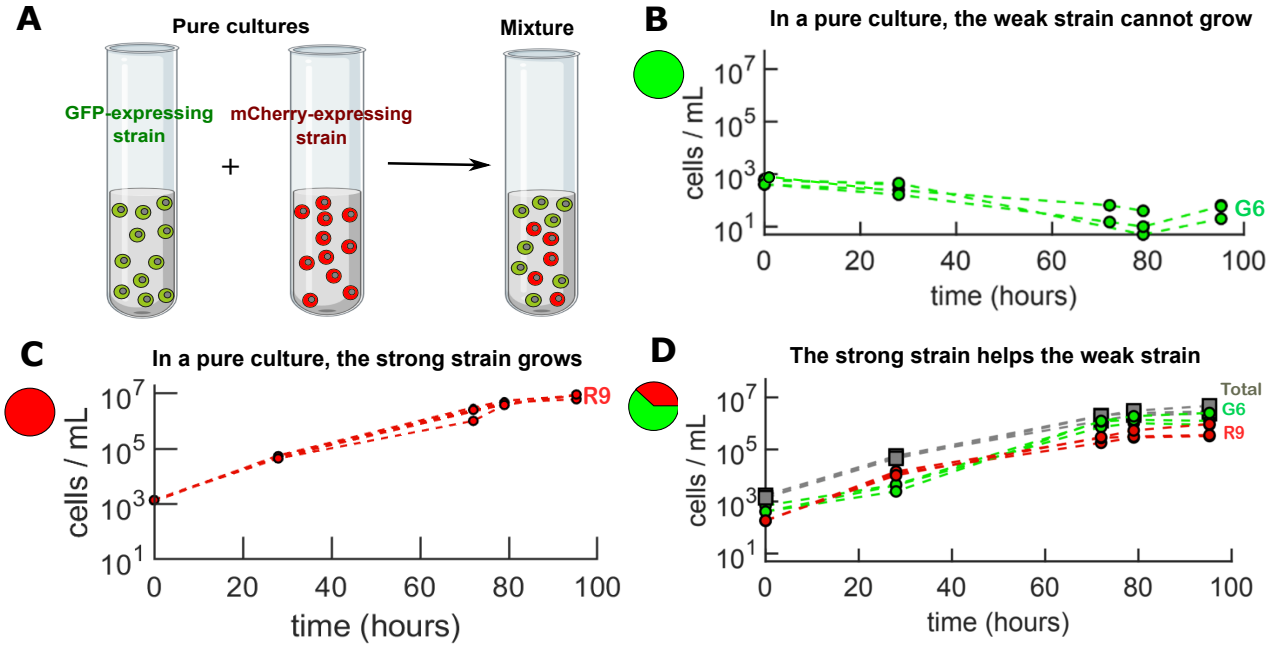

Figure 6: The strong strain helps the weak strain to grow at $39.1\mathcal{C}$**. A)** Schematic of the experiment, where we grow pure cultures of two strains, both expressing a different fluorescent protein and combine them in a mixture. **B)** Population density of the weak strain (G6, relative GFP expression 6x) over time (initially ~ 1000 cells/mL). **C)** Population density of the strong strain (R9, relative mCherry expression 9x) over time (initially ~ 1100 cells/mL). **D)** Population density over time of the mixed population of engineered cells expressing GFP (relative 6x) or mCherry (relative 9x). Shown is the total population density (grey, dotted lines), GFP-expressing strain density (green, dotted lines) and mCherry-expressing strain density (red, dotted lines) (n=4 replicates per strain).

In this experiment, R9 is the strong strain and G6 is the weak strain (because R9 grows whereas G6 does not with the same initial density), even though the expression level of R9 is higher than the expression level of G6 (see Figure 5A,B). We can explain this result from the maximum growth rates of strains R9 and G6. Namely, the maximum growth rate of R9 is slightly larger than the maximum growth rate of G6 (see Figure 5D,E), suggesting that R9 is indeed 'stronger' than G6.

2.3 Cheater strain

In microbiology, cheater cells are those who use a public good for their own, selfish benefit, without providing something in return. To study the effect of cheating in a co-existence experiment, we constructed a cheater strain that is unable to produce glutathione due to deletion of the GSH1 gene. Therefore, it needs an external source of glutathione to grow, because glutathione is crucial for survival, even at low temperature [8]. So, in a pure culture, the cheater strain (called CR6) is unable to grow (see Figure 7B). We chose the initial cell density of a pure culture of a GSH-producing strain (G9) such that the population grows (Figure 7C). Then, we combined the cheater strain with the GSH-producing strain in a co-existence experiment (see Figure 7A). To enable separation of the strains, the cheater strain is constructed to express mCherry and is combined with a GFP-expressing strain (see supplementary Figure S5B-D). Consequently, we expected that in the mixture of both strains, the cheater strain profits from the glutathione produced by the other strain. However, the cheater strain is still unable to grow in the mixture (see Figure 7D). This means that the cheater strain does not profit from the glutathione provided by the GSH-producing strain. An explanation for this result could either be that the cheater cells have gone extinct before the accumulated concentration of glutathione in the medium is sufficiently large or that the cheater strain needs a larger concentration of glutathione than available to grow.

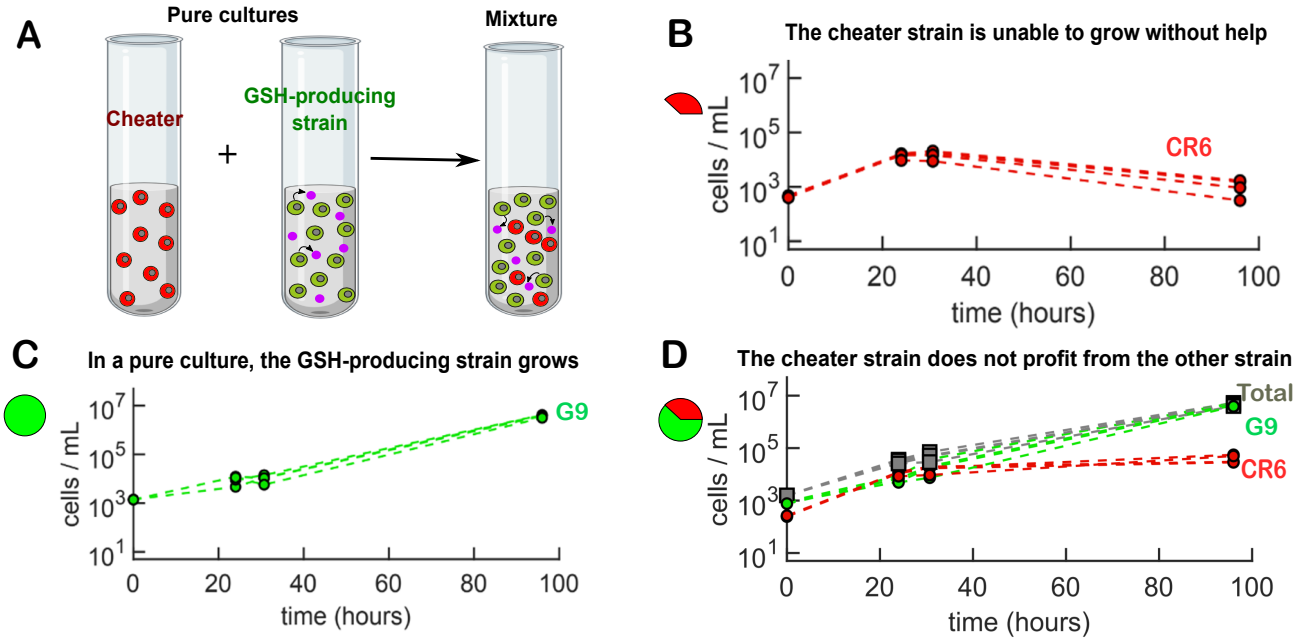

Figure 7: Co-existence experiment with cheater strain CR6 and G9 at $39.1\,℃$. A) Schematic of the experiment, where we combine a cheater strain with a GSH-producing strain. **B)** Population density of the cheater strain (CR6, GSH1 knock-out, relative mCherry expression 6x) over time (initially ~ 1800 cells/mL). **C)** Population density of the GSH-producing strain (G9, relative GFP expression 9x) over time (initially ~ 2400 cells/mL). **D)** Population density over time of the mixed population of engineered cells expressing GFP (relative 9x) or mCherry (relative 6x). Shown is the total population density (grey, dotted lines), GSH-producing strain density (green, dotted lines) and cheater strain density (red, dotted lines) (n=4 replicates per strain).

To find the reason why the cheater strain does profit from the glutathione secreted by the other strain, a follow-up experiment is required in the future. In this follow-up experiment, we would add a certain concentration of glutathione to a culture of CR6 cells to measure what the minimum, but sufficient concentration of glutathione is to enable the strain to grow. Once we have established this threshold, we can measure how much glutathione is secreted by the GFP-expressing strain and determine whether it is sufficient for the cheater strain to grow. If it is not sufficient, we should increase the initial cell density of the GFP-expressing strain and repeat the co-existence experiment.

3 Discussion

In this chapter, we studied the cooperation between different yeast strains at high temperatures. Specifically, we studied whether and how cells in a mixture of different yeast strains cooperate with each other to combat high temperatures. For this, we used engineered yeast constitutively expressing a fluorescent protein (GFP or mCherry) at a given, relative level. We combined two different strains in a so-called co-existence experiment and studied the outcome. We found that two scenarios can arise as outcome. The strong strain (with a low expression level) can profit from the efforts of producing and secreting glutathione of the weak strain (high expression level) and vice versa, the strong strain can help the weak strain to grow by producing and secreting glutathione.

Based on the theoretically possible behaviour of the strong and the weak strain, we suspect that there is another scenario possible: the scenario where the strains help each other to grow. However, we have not observed this scenario experimentally. Likely, this scenario is the most difficult to obtain, because there are only a few combinations of strains and initial cell densities for which this behaviour occurs. Namely, the replacement of a small fraction of the weak strain by cells from the strong strain must stimulate growth of both strains. So, the cooperative effect has to be very strong in order for this scenario to occur. To investigate whether the third scenario could exist, we developed a mathematical model (see next chapter) to simulate co-existence experiments.

We found that an identical expression level of a different fluorescent protein surprisingly results in different growth behaviour, even though the proteins are similar in length, size and mass. The expression of a fluorescent protein forms a metabolic burden for a cell, because it costs the cell extra energy and resources, such as ribosomes, mRNA subunits and amino acids [26]. This results in a weak strain (with a high expression level) to be unable to grow, whereas a strong strain (with a low expression level) grows under identical conditions, which can be visualized using a phase diagram (see Figure 2C,D). We expected that the expression of GFP or mCherry would give a similar metabolic cost to the cell, because the GFP and mCherry protein have a similar length, size and mass (see Table 1). However, we found that the same expression level of GFP and mCherry does not result in the same growth behaviour. This suggests that GFP and mCherry do not give an equal metabolic burden to the cell.

To explore this further, we hypothesized that the amino acids used to synthesize the tripeptide glutathione (see Figure 8), which is essential for growth at high temperatures, are instead partly depleted for the synthesis of GFP or mCherry. Then, more of these non-essential amino acids would have to be synthesized by the cells for the production of GSH, costing extra energy and possibly slowing down growth. The synthesis of glutathione is known to be limited by the concentration of cysteine [25]. Therefore, we studied the number of cysteine copies in

the sequence of GFP and mCherry (see Table 1). The mCherry protein contains no copies of cysteine, while the GFP protein contains two cysteine copies in its sequence. Therefore, we concluded that the synthesis of a GFP protein requires more cysteine than synthesis of a mCherry protein, thereby drawing away these resources from the cell. Thus, the cells that express GFP have less cysteine copies left to use for the synthesis of glutathione. Even though the difference is minimal, this may explain why the metabolic burden from GFP and mCherry is not be equal. Furthermore, cysteine contains thiol groups, which are one of the most easily oxidized residues. Thus, GFP proteins may give the cell additional oxidative stress, as GFP contains more of these thiol groups in its amino acid sequence, whereas mCherry proteins would not cause additional oxidative stress [23]. In short, we propose that expressing GFP is a non-trivial burden for the cell, as the synthesis of GFP draws away resources that are required for glutathione synthesis and possibly increases oxidative stress. This might explain why a strain that expresses mCherry in a certain level is actually fitter than a strain that expresses GFP in a lower level (as shown in the experiment in Figure 6).

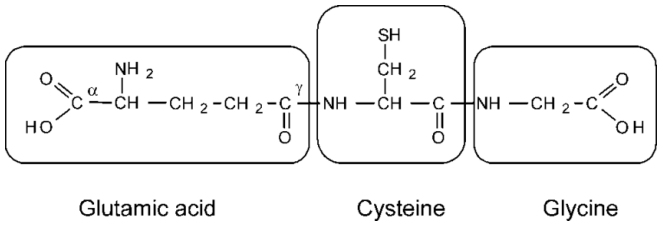

Figure 8: Structure of the tripeptide glutathione (GSH) [25]

Table 1: Size, mass, absorbing wavelengths and sequence information of GFP and mCherry [27, 28]

	GFP	**mCherry**
Length gene (number of bp)	717	711
Length protein (number of a.a.)	238	236
Mass protein (kDa)	26.9	26.7
Number of cysteine copies in sequence	2	0
Number of glutamic acid copies	16	24
Number of glycine copies	22	25

Overall, our results illustrate that not only genetically identical yeast cells [8], but also cells from different strains can cooperate with each other to survive high temperatures, resulting in complex co-existence scenarios. This brings us one step closer to understanding cooperation at high temperatures in the natural situation, where microbes live in communities with many other strains and species.

Part 3

Mathematical model

We developed a mathematical model that describes the growth behaviour of yeast cells at high temperatures, with the goal to find the possible outcomes of a co-existence experiment, to clarify how they arise and to study single-cell behaviour. We modified an already existing, population-level, discrete, non-linear, stochastic model [8] to develop a model that is continuous in time and additionally describes the single-cell behaviour. Also, we extended the previous model to incorporate a carrying capacity and to describe the behaviour of two different yeast strains. Compared to the old, discrete model, there are three main advantages. Firstly, the model presented here is more realistic, as time is continuous rather than divided into fixed, discrete time steps. Additionally, the growth of a population attenuates once the population density is close to the saturating density, because we incorporated a carrying capacity. Finally, with the model presented here, it is possible to track the behaviour of individual cells. In this chapter, we will describe the model and discuss the results.

1 Foundation of the model

In this section, the foundation of the model is described, both on the level of individual cells and on the population-level. Also, the parameters and variables are defined.

1.1 Individual cells

We will first model a population of genetically identical yeast cells at high temperatures. We assume that the cells in the population replicate and die with certain, constant rates, independent of the other cells in the population (see Figure 9A). Then, we follow the individual cell replications and cell deaths over (continuous) time. For this, we consider the waiting times of cell replication and cell death. The waiting time for cell replication is the time between successive replications of an individual cell. The waiting time for cell death is the time between cell birth and cell death. For simplicity, we assume that the waiting time for replication is appropriately modelled by an exponentially distributed random variable X, with some rate μ, such that $X \sim Exp(\mu)$. Beside replicating, we assume that cells die with a certain rate, called the death rate λ (see Figure 9A), such that the waiting time for cell death is appropriately modelled by an exponentially distributed random variable Y, with rate λ: $Y \sim Exp(\lambda)$.

In our model, we determine the characteristics of a cell as soon as it is born, using the parameters μ and λ. So, each cell in the population receives two waiting times as soon as it is born: the waiting time until its first replication: $t_1 \sim Exp(\mu)$ and the waiting time until its death: $t_2 \sim Exp(\lambda)$. If the first waiting time is shorter than the latter ($t_1 < t_2$), then the cell replicates and we create a new waiting time until the cell first replicates again, compare it to the time of death, and so on. When the cell dies, it is removed from the population. Overall, this accounts for asymmetric cell division, where the mother cell keeps all old content, such as damages and produces a 'clean' daughter cell. In other words, the mother cell keeps her own properties including her time of death when dividing. The daughter cell starts from a clean slate and her first replication time and time of death depend on the conditions at the time she is born. In actual yeast cells, the division also occurs in an asymmetric manner [29].

The life of a cell can be shown on a timeline (see Figure 9B), with cell replication events occurring at exponentially distributed waiting times and death of the cell occurring after another exponentially distributed waiting time. The chronological life span (L_{chron}) of a cell is defined as the lifetime of a cell, and the replicative life span (L_{repl}) of a cell is defined as the amount of times the cell replicated [30]. In summary, we described the behaviour of single yeast cells within a population, by describing the waiting times for cell replication and cell death.

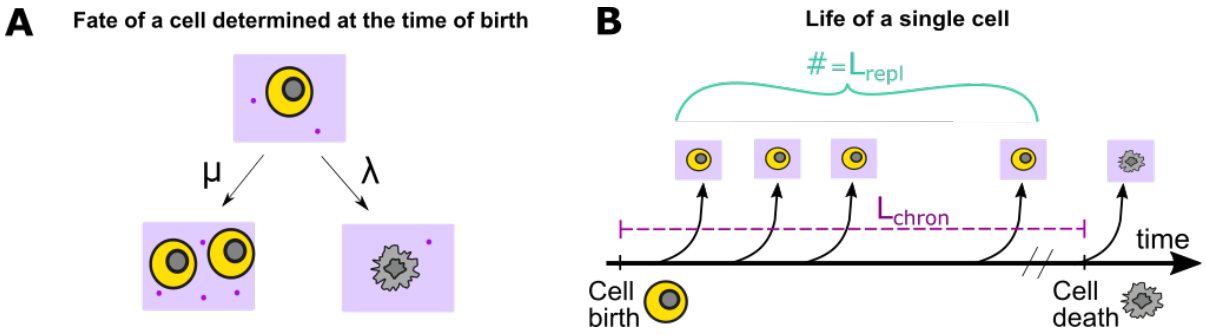

Figure 9: Mathematical model. A) A cell in our model can replicate and die with certain rates: the growth rate μ and the death rate λ. **B)** The life of a cell shown on a timeline, where the cell replicates a certain number of times (equal to L_{repl}) and the cell dies after a certain time, called L_{chron}.

1.2 Population-level

Now that we described the behaviour of individual cells in our model, we next consider the entire population of cells. To model the behaviour of population, we are interested in the first cell in the population to replicate, because then, a new cell is added to the population. Each cell in the population, labeled $i = \{1, \ldots, A_t\}$, has its own waiting time for cell replication X_i. We calculate the minimum of the waiting times X_i for cell replication and call it Z_t, corresponding to the first cell in the population to replicate. So, Z_t is calculated as follows:

$$Z_t = min_i(X_i) \tag{1}$$

Thus, in the population, the waiting time between two successive replication events in the population is given by Z_t. The random variable Z_t is, like X_i, exponentially distributed, as derived next.

Assume that we have two independent random variables, corresponding to the waiting times of two cell replications. Both random variables are exponentially distributed, i.e. $X_1 \sim Exp(\mu_1)$ and $X_2 \sim Exp(\mu_2)$. Then, the minimum of these two random variables is also exponentially distributed, with the sum of the two individual parameters as parameter [31]: $Z = min(X_1, X_2) \sim Exp(\mu_1 + \mu_2)$. In our case, we have a large number A_t of cells that can all independently replicate. So, Z_t is exponentially distributed with the sum of the growth rates as parameter (μA_t):

$$Z_t \sim Exp\Big(\sum_{i=1}^{A_t} \mu\Big) = Exp(\mu A_t) \tag{2}$$

For simplicity (and different from a conventional Gillespie algorithm [32]), we only observe the population of cells at fixed times. We count how many cell replications occur within a certain time step δt, and update the number of cells in the population accordingly after the time step, before starting a new time step. For an exponentially distributed variable $Z_t \sim Exp(\mu A_t)$, the number of events that occur within time δt can be modelled

as a Poisson distribution [33], with parameter $\mu \cdot A_t \cdot \delta t$. We define the variable W_t, which describes the number of cell replications that occur within one time step δt as follows:

$$W_t \sim Poisson(\mu A_t \delta t) \tag{3}$$

After each time step, the newly born cells are added to the population and we repeat the cycle.

Regarding cell death, each cell has its own waiting time for cell death (called Y_i). We are again interested in the minimum of the waiting times for cell death, representing the first cell in the population to die, to remove the dead cell from the population. Then, the waiting time between successive cell deaths in the whole population (Q_t) is exponentially distributed [31], with parameter λA_t. This is described in equation 4.

$$Q_t = min_i(Y_i) \sim Exp(\lambda A_t) \tag{4}$$

We only observe the population at fixed times. Analogously to the cell replications in the population, we obtain the number of cell deaths that occur within one time step δt, defined as D_t,

$$D_t \sim Poisson(\lambda A_t \delta t) \tag{5}$$

By summing up, we can write down the stochastic equation of the number of living cells in the population as follows:

$$A_{t+\delta t} = A_t + W_t - D_t \tag{6}$$

We can write equation 6 as a differential equation. Thus, we can follow the population behaviour over time using the following stochastic differential equation.

$$\frac{dA}{\delta t} = \frac{A_{t+\delta t} - A_t}{\delta t} = \frac{1}{\delta t}(W_t - D_t) \tag{7}$$

This implies that during each time step δt, a number of newly born cells W_t is added to the population, and a number of dead cells D_t is subtracted from the population. Finally, we calculate the expectation value of $\frac{dA}{\delta t}$, corresponding to the average behaviour of a population. Here, we use the fact that the expectation value of a Poisson distribution is equal to its parameter.

$$E[\frac{dA}{\delta t}] = E[W_t] - E[D_t] = \frac{1}{\delta t} \cdot (\mu A_t \delta t - \lambda A_t \delta t) = A_t(\mu - \lambda) \tag{8}$$

This result can be used to describe the average population dynamics. Also, the model can be rewritten as a deterministic equation with stochastic, Gaussian noise. This is explained further in supplement section S2.2. The ability to split the deterministic part from the noise, brings new possibilities. Namely, it enables us to determine the average behaviour of a culture with only one simulation.

1.3 Growth and death rate

Now, we will describe how the growth and death rates used in the model depend on experimental conditions, such as population density, temperature and nutrient availability.

Growth rate

First, we consider the growth rate μ. Matching previous work [8], the growth rate μ changes over time and depends on the extracellular glutathione concentration and the concentration of available nutrients in the environment. We define the concentration of extracellular glutathione as M_t. The antioxidant glutathione is secreted by each living cell at a constant rate equal to 1 h^{-1}. Therefore, the extracellular concentration of glutathione M_t increases with the number of living cells A_t (see equation 9). Thus, we describe M_t and the corresponding differential equation $\frac{dM}{\delta t}$ as follows:

$$M_{t+\delta t} = M_t + A_t \cdot \delta t \tag{9}$$

$$\frac{dM}{\delta t} = \frac{M_{t+\delta t} - M_t}{\delta t} = \frac{A_t \cdot \delta t}{\delta t} = A_t \tag{10}$$

Also, all living cells consume nutrients with a certain rate, equal to 1 h^{-1}. Cells consume one unit of nutrients per time step from a finite pool of C nutrients. So, C is a measure for the total amount of nutrient units available in the medium. Notice that the number of secreted glutathione units is equal to the number of consumed nutrient units. So, we can use M_t to follow both variables. Then, we use M_t to incorporate a carrying capacity in our model. We need a carrying capacity, because the population density should stay below a certain saturating cell density, like it does in experiments. The amount of used nutrients, M_t, is compared to the carrying capacity C. When all nutrient units are used up, the population can maximally grow to the saturating cell density cc. We define a parameter K, which defines the extracellular concentration of glutathione, M_t, that the cells minimally need to grow.

Now that we described the accumulation of extracellular glutathione and the depletion of nutrients, we consider how the growth rate depends on these quantities. Based on previous work [8], we assume that the growth rate μ depends on the concentration of glutathione M_t via a sigmoidal Hill function: $\frac{M_t^n}{K^n+M_t^n}$ [8] (see equation 11 and Figure 10A). The Hill function is a commonly used response curve, that represents the cellular response to the binding of a certain ligand (in our case glutathione). It is a classic, sigmoidal curve, that captures the behaviour of many biological processes that involve a ligand and a macromolecule or cell. As the Hill coefficient n increases, the response curve becomes steeper and more step-like (see supplementary Figure S7D). In general, the Hill coefficient is chosen to be equal to its standard value 1 in this thesis, unless stated otherwise. Alternatives for the Hill function as response curve, are discussed in the supplementary information (see supplement section S2.3). The Hill function is chosen as response curve, because it recapitulates the experimental results best.

Next, we assume that the growth rate scales with the concentration of available nutrients (i.e. $\mu \sim \left(1 - \frac{M_t}{C}\right)$). The longer the experiment is running, the larger M_t is, and the closer it comes to the carrying capacity C. Therefore, the growth rate μ decreases once M_t approaches C and when the culture's density is getting close to the saturating density cc (see equation 11). Thus, the population density can never exceed the saturating cell density cc and we have successfully built in a carrying capacity in the model.

Finally, we define μ_{max} as the maximum growth rate of a strain (genetic variant). The maximum growth rate is measured at a temperature of $\sim 36℃$, where the death rate λ can be approximated to be 0 and the cells start to secrete glutathione [8]). The maximum growth rate is assumed to be a constant function of temperature (even though in reality it slightly decreases with temperature [8]), and it is given in units of h^{-1}. The growth rate μ can never exceed μ_{max}. The maximum growth rate of the wild type approximately equals $\mu_{max} = 0.25h^{-1}$ [8],

meaning that its maximum doubling time is around $2.8h$ when the death rate $\lambda = 0$. Altogether, the growth rate is given by the following equation:

$$\mu(t) = \mu_{max} \frac{M_t}{K + M_t} \left(1 - \frac{M_t}{C}\right) \tag{11}$$

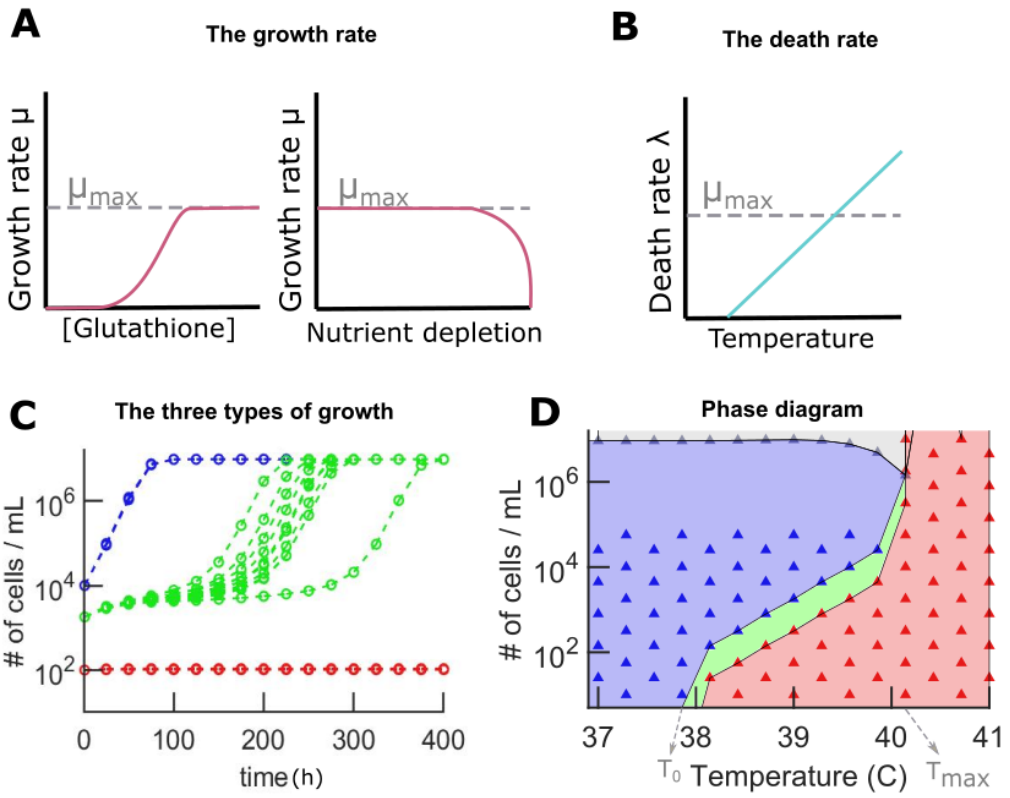

Figure 10: The growth and death rate in the model and the resulting growth behaviour. A) The growth rate depends on the glutathione concentration via a Hill curve and on the nutrient depletion via the carrying capacity C. **B)** The death rate depends linearly on temperature. **C)** The three types of growth: deterministic (blue), random (green) and non-growth (red) (n=10 simulated replicates per colour). **D)** Phase diagram, indicating the conditions at which deterministic, random or non-growth occurs (n=10 simulated replicates per data point). Strain parameters: $T_0 = 37.9℃, T_{max} = 40.2℃, K = 30000, \mu_{max} = 0.25h^{-1}, C = 2 \cdot 10^7$.

Death rate

Now that we described the growth rate, we will describe how the death rate of a population depends on the parameters of the model. We assume that a cell is more likely to die at a higher temperature and that the rate of death λ depends linearly on temperature (see equation 12 and Figure 10B). Namely, how the death rate depends on temperature, does not qualitatively change the behavior of the model, but merely when it displays what kind of behaviour. Therefore, the simplest assumption is that the death rate linearly increases with increasing temperature [8]. We define the maximum temperature at which a population can still grow, as T_{max} and the temperature at which all populations are able to grow, regardless of their initial cell density, as T_0. The death rate is equal to the maximum growth rate at temperature T_{max} and the death rate is equal to 0 at T_0. So, the following equation describes the death rate of a population:

$$\lambda(T) = \mu_{max} \frac{T - T_0}{T_{max} - T_0} \tag{12}$$

In summary, we have found a description of cell replication and cell death on the single-cell level and on the population-level. Also, we described how the growth rate μ depends on the extracellular concentration of glutathione and the available nutrients (see equation 11) and how the death rate λ depends on temperature (see equation 12).

2 Model dynamics

Now that we have constructed the model, we will show simulation results, revealing the dynamics of the model.

Using the described model, we simulated growth of yeast populations at high temperatures for different initial densities. Matching our experimental observations and previous work [8], we find three different types of growth: deterministic growth, random growth and non-growth, as illustrated in Figure 10C. Deterministic growth occurs when the initial cell density is sufficiently large and means that the population will always grow under these conditions, regardless of how often the simulation is repeated. During deterministic growth, the growth rate exceeds the death rate, i.e. $\mu(t) > \lambda(T)$, already shortly after the experiment started, because the concentration of glutathione is accumulated quickly. Random growth occurs at intermediate initial cell density and means that the population sometimes grows, sometimes does not grow and that the time before the population starts growing, is unpredictable. In a randomly growing culture, the glutathione concentration approaches the threshold concentration required for growth (K) and $\mu(t) \approx \lambda(T)$ by the time that there are only very few surviving cells left, whose stochastic replications or deaths subsequently determine the faith of the population. Therefore, noise plays an important role in determining the outcome of a randomly growing culture. In other words, the resilience of the population is low during random growth. Finally, non-growth occurs at low initial cell density (which obey a condition for non-growth, described in the supplement section S2.5). Non-growth means that the population cannot grow under certain conditions, regardless of how often the simulation is repeated. In the case of non-growth, glutathione does not accumulate sufficiently, $\mu(t) < \lambda(T)$ at all times t, and on average, the population size decreases. Also, the population is guaranteed to go extinct after some time.

In short, the growth of a population depends on the initial cell density of the population and we observe three different growth types. We can summarize the growth behaviour of a yeast strain in a phase diagram (initial density versus temperature) (see Figure 10D). The phase diagram shows the regions in which the different types of growth occur, as a function of temperature (deterministic growth in blue, random growth in green and non-growth in red). Also, it shows the region where the nutrients in the growth medium are depleted and the population is unable to grow (in grey). We find that, as temperature increases, the saturating cell density of the culture decreases (see Figure 10D), because the population grows slower (as the death rate increases with temperature) and thus, the population needs more time and more nutrients to grow than at low temperatures. The phase diagram and growth curves (Figure 10C,D) are compatible with the results obtained with the previous model [8].

Furthermore, yeast growth at high temperatures can be viewed as a dynamical system, a system that is in an evolving, time-dependent state, described by the temperature and the cell density of the population. Then, the fixed points of the system are points in the phase diagram that map onto themselves. A further analysis of the fixed points in the phase diagram is given in the supplement (see supplementary section S2.4 and Figure S8). Also, the parameters of the model described in this section have an influence on the phase diagram. We elaborate on this concept in the supplementary information section S2.6.1 (see supplementary Figure S9).

3 Extension of the model: two strains

In the above, we have developed a model that successfully simulates the behaviour of a population of genetically identical yeast cells in the form of growth curves and a phase diagram. Now, we want to simulate co-existence experiments, where two different yeast strains, each with their own parameters, are combined. To this end, the model was extended to simulate the behaviour of two different yeast strains. Instead of simulating a population of identical cells, we assign a strain to each of the cells in the model, where each strain behaves according to a different growth and death rate. We estimated the parameter values from experiments (for further explanation and an overview of the parameters and variables in the model see supplementary section S2.1). Importantly, the two strains share two variables: the extracellular concentration of glutathione and the amount of available nutrient units in the growth medium: both described using M_t (see Figure 11A).

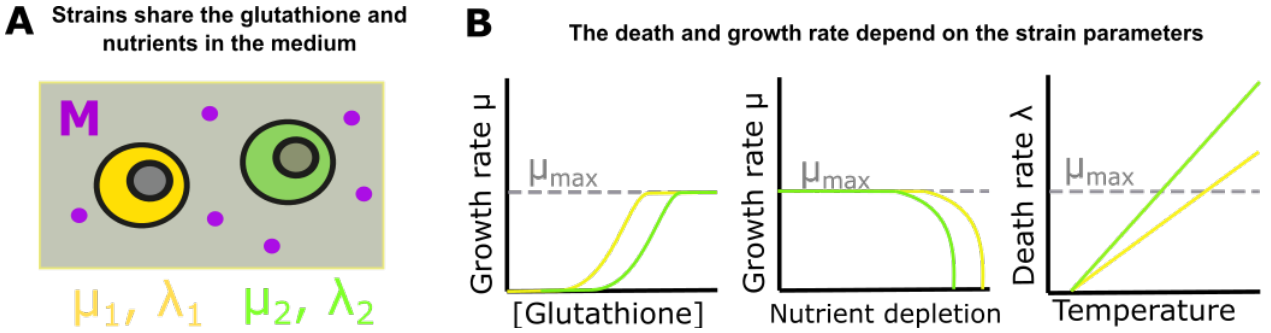

Figure 11: Two strains in the model. A) The strains have their own parameters, but they share the glutathione in the growth medium. **B)** The growth rate is shifted for different strains. The death rate has a different slope for different strains.

For two strains to be different, one or more of the following parameters can be tuned: the minimum and maximum temperature (T_0 and T_{max}), the maximum growth rate μ_{max}, the sensitivity to glutathione K, the Hill coefficient n and the carrying capacity C. By tuning these parameters, various different, synthetic yeast strains are modelled, each with their own growth and death rate (Figure 11B) and with their own phase diagram that indicates the conditions required for growth (e.g. see supplementary Figure S9). For these strains, one or more of the parameters have changed compared to the wild type. In this thesis, we considered strains that express a fluorescent protein. The strains in the model that represent strains expressing a fluorescent protein at a certain level, are saddled with an extra metabolic cost [26]. Therefore, we consider them by decreasing T_0 or T_{max} compared to the wild type. Decreasing T_0 or T_{max} results in a weaker strain, because they represent the temperatures where death plays a role. Alternatively, the strains that produce a fluorescent protein can be modelled to have an increased value for K compared to the wild type, such that they need a larger concentration of glutathione to grow.

4 Simulation Results

We have defined our model and extended it to simulate two different strains in a co-existence experiment. Now, we will consider the outcomes of simulated co-existence experiments and see whether the outcomes that we envisioned are indeed possible.

4.1 Confirm the three scenarios

Using the model, we aimed to confirm the existence of the three scenarios as outcome of a co-existence experiment: profit from the weak, help the weak and help each other. In each simulation, we varied one of the parameters for the weak strain, accommodating the expression of a fluorescent protein, compared to the strong strain, which has the standard parameters, corresponding to the wild-type strain. We chose to vary only the parameter T_0 between the two strains and to keep all the other parameters constant and fixed for the simulations. Then, we adjusted the initial cell densities of both strains until the three scenarios were obtained. We simulated the strain's growth behaviour in pure conditions and in a mixture of both strains, resulting in the growth curves shown in Figure 12.

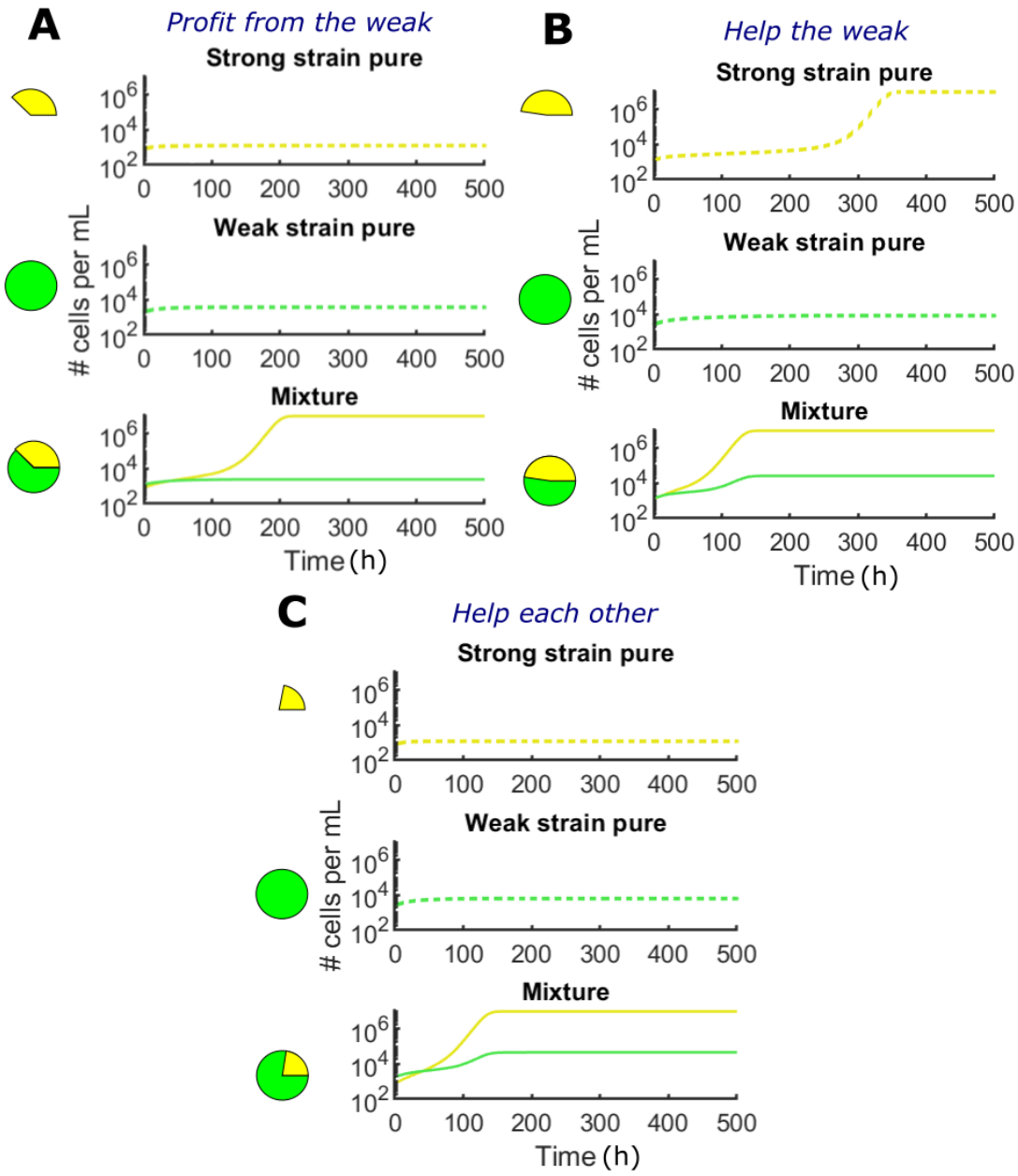

Figure 12: Simulation results displaying the three scenarios as outcome of the model at $T = 39℃$. In this example, T_0 is varied between the two strains (representing a wild-type strain and a strain that expresses a fluorescent protein: $T_0^1 = 37.9℃$ and $T_0^2 = 36.5℃$). Only the initial cell densities of the two strains are varied to obtain the three scenarios. **A)** Scenario 1 (profit from the weak): initially $A_0 = 900$ cells/mL and $B_0 = 1300$ cells/mL. **B)** Scenario 2 (help the weak): initially $A_0 = 1400$ cells/mL and $B_0 = 1500$ cells/mL. **C)** Scenario 3 (help each other): initially $A_0 = 900$ cells/mL and $B_0 = 2000$ cells/mL.

For variations in the parameters of the weak and the strong strain, representing both strains to express a fluorescent protein, the same results were obtained (see supplementary Figure S11). This indicates that a rather broad range of T_0 (corresponding to different combinations of strains) can result in one of the scenarios as outcome of the model. We visualized the range of parameter values for T_0, resulting in interesting outcomes, in the form of a phase diagram (see Figure 13B), where the colours represent the three scenarios (Figure 13A). Here, we varied only T_0 between the two strains, which determined which of the strains is the strong strain (with the more beneficial parameter for growth), and which of the strains is the weak strain (with the less beneficial parameter for growth). We assigned initial cell densities to the strong and weak strain accordingly before running the simulation (800 cells/mL for the strong strain and 2000 cells/mL for the weak strain). So, if the parameter T_0 shifts in such a way that the strong and the weak strain are reversed, then so are the initial cell densities. Similar results were obtained by varying one of the other parameters: T_{max} or K. We visualized the range of parameter values resulting in interesting behaviour for these parameters as well (Figure 13C,D). Additionally, we constructed a phase diagram that indicates the scenarios as a function of the initial densities of the strains (Figure 13E). Here, we kept the parameters of both strains constant and varied only the initial cell densities. Overall, these results indicate that the results in Figure 12 are not rare examples of interesting behaviour, but rather, they are merely exemplary for a characteristic phenomenon in the model. In the future, these results could be useful to predict the experimental conditions that result in a desired outcome of a co-existence experiment.

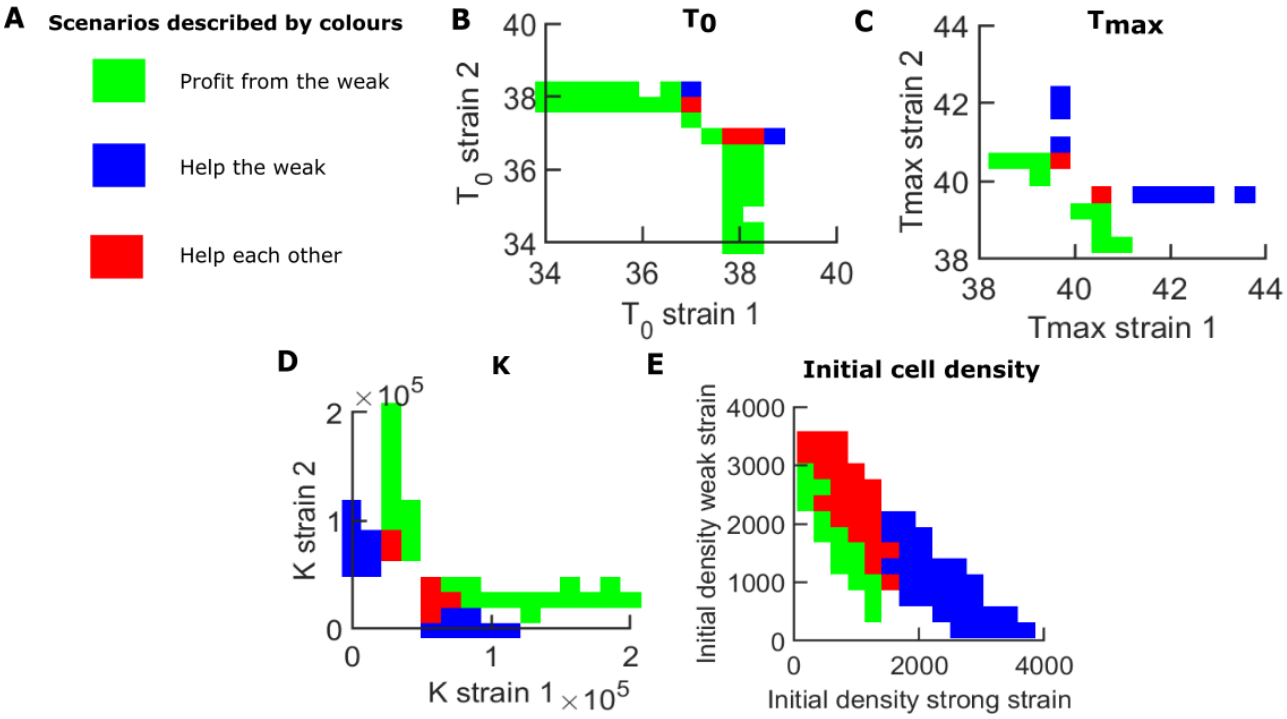

Figure 13: Phase diagrams indicating the scenarios as outcome of the co-existence experiment with one variable parameter at $T = 39℃$. Initial densities: strong strain 800 cells/mL, weak strain 2000 cells/mL. **A)** The scenarios are indicated using a colour code. **B-D)** The outcomes of the model as a function of the only variable parameter between the two strains: **B)** T_0, **C)** T_{max}, **D)** K. **E)** Outcomes of the model as a function of the initial densities of the strains. Here, strain 1 is chosen to be the strong strain and strain 2 is the weak strain. We chose to vary K as follows: $K_1 = 30000, K_2 = 80000$, but varying another parameter (T_0 or T_{max}) gives a similar pattern.

To conclude, we constructed a simple model in which we defined the behaviour of cells, without defining the population-level behaviour, corresponding to a bottom-up approach. As a result, we obtained the population-level behaviour that we also observe in experiments. Importantly, our simulation results confirm that there are

indeed three interesting outcomes of a co-existence experiment, two of which we have already observed in experiments.

4.2 Cheater strain

A cheater strain is a strain that does not produce or secrete glutathione, but is able to take up glutathione from the medium. We expect that a cheater strain can profit from the glutathione secreted by other strains and can grow when co-cultured with another strain. However, we did not find this outcome experimentally. Instead, we found that the cheater strain is unable to profit from the glutathione secreted by the other strain. To test this observation, we modelled the behaviour of a cheater strain.

With a small modification in our model, we can also simulate the behaviour of a cheater strain. The cheater strain does not produce or secrete glutathione, so we define a secretion rate s and set it to zero: $s_2 = 0\ h^{-1}$. Then, we define the rate at which the strain uses up nutrients r, which remains the same as before: $r_2 = 1\ h^{-1}$. The cheater strain is unable to grow in a pure culture, because glutathione is necessary for growth (i.e. without glutathione, the growth rate is equal to zero). The cheater strain can be used in a co-existence experiment, where it can take up glutathione produced by the other strain and we expect that the glutathione secreted by the other strain helps the cheater strain to grow (see Figure 14A). Now, we need two variables instead of one (M_t) to keep track of the glutathione concentration and the consumed nutrients of the population. We take N_t to equal the consumed nutrients, and G_t to equal the concentration of glutathione in the medium. Then, we get the following equations for the co-existence experiment:

$$N_{t+1} = N_t + r_1 A_t \delta t + r_2 B_t \delta t \tag{13}$$

$$G_{t+1} = G_t + s_1 A_t \delta t + s_2 B_t \delta t \tag{14}$$

$$\frac{dN}{\delta t} = r_1 A_t + r_2 B_t \tag{15}$$

$$\frac{dG}{\delta t} = s_1 A_t + s_2 B_t \tag{16}$$

$$\mu(t) = \frac{G_t}{K + G_t}\Big(1 - \frac{N_t}{C}\Big) \tag{17}$$

In the resulting simulation, the cheater strain grows in a mixture with another strain (see Figure 14B), which means that the cheater strain can indeed take advantage of the glutathione produced by the other strain. In fact, we obtained the outcome that the cheater strain grows in the mixture whenever the GSH-producing strain is able to grow in a pure culture, indicating that this is a frequently occurring outcome. These results suggest that the experimental cheater strain could be able to profit from the glutathione produced by another strain as well, even though we did not confirm this experimentally (see Figure 7). In the future, the mathematical model could be used to predict the experimental conditions for which the cheater strain is able to grow in the mixture. Then, the co-existence experiment with the cheater strain could be repeated with those conditions, to confirm the existence of the scenario where the cheater strain profits from the other strain.

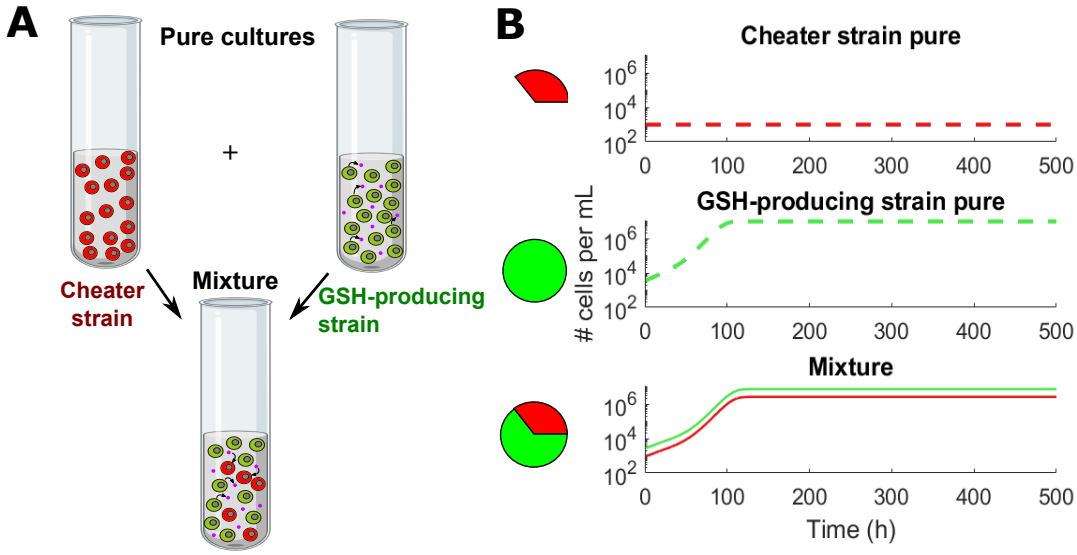

Figure 14: Simulation results with a cheater strain at $T = 39℃$. A) Schematic of the situation. The cheater strain does not produce glutathione (GSH), but in a mixture with another strain, it can take up the glutathione from the environment to grow. **B)** Population densities over time for the pure cultures and the mixture of the cheater strain (red) and the GSH-producing strain (green). The strains have the same parameter values, except the secretion rate of glutathione (which is zero for the cheater strain: $s = 0\ h^{-1}$ and one for the GSH-producing strain: $s = 1\ h^{-1}$). Initially $A_0 = 1000$ cells/mL, $B_0 = 3000$ cells/mL.

5 Prediction of the outcome of a co-existence experiment

We showed that the mathematical model reproduces all experimental results and additionally predicts more interesting outcomes of a co-existence experiment. Now, we aim to classify the outcomes of a co-existence experiment based on solely the parameters of the model. Then, we can use the physical properties of the cells and the initial conditions of the co-existence experiment to predict what the outcome will be. This bears resemblance to the phase diagram for a single strain, as it also predicts the outcome of an experiment from the physical properties of the cell and the initial conditions.

5.1 One variable parameter

We will start by trying to find a quantity that can predict the outcome of a co-existence experiment where one of the parameters is varied between the two strains. To find such a quantity, we will use the concepts of chronological and replicative ages of a cell. The chronological age of a cell is equal to a cell's life time and the replicative age of a cell is equal to the number of times it replicates in its life time (see Figure 9B). We will compare the expected replicative age of both strains to each other, which is a measure for the amount of offspring that a strain creates. With all other parameters and conditions constant, a strain that creates more offspring than another strain (but at the same rate), will dominate in a co-existence experiment, meaning that in the end of the experiment, the mixture consists of almost only cells from that strain. Similarly, if one strain creates offspring faster (but equally many in total), it will also dominate in the co-existence experiment. So, we can use the expected replicative age and the growth rates of the strains to try to predict the outcomes of co-existence experiments. To find the expected replicative age, first, we will describe the expected chronological age.

The chronological age of a cell is a random variable equal to the waiting time of death Y_i. As explained in

the beginning of this chapter, we take the waiting time of death to be exponentially distributed with parameter λ. So the chronological age of the cell is described as follows:

$$L_{cron} = t_{death} - t_{birth} \sim Exp(\lambda) \tag{18}$$

Thus, the chronological age of a cell is an exponentially distributed random variable, with parameter λ. Therefore, the expectation value of L_{chron} is defined as follows:

$$E[L_{cron}] = \frac{1}{\lambda(T)} \tag{19}$$

The replicative age L_{repl} counts the number of cell replications in the life time of a cell (L_{chron}). As described in the beginning of this chapter, cell replication has a waiting time that is exponentially distributed with parameter μ. So, the number of replications in the life time of a cell is Poisson distributed:

$$L_{repl} \sim Poisson(\mu L_{chron}) \tag{20}$$

The expected replicative age depends on the chronological life span of a cell, which itself is a random variable. Therefore, we use the law of total expectation to calculate the expectation value of L_{repl}:

$$E[L_{repl}] = E[E[L_{repl}|L_{chron}]] \tag{21}$$

The number of replications that a cell undergoes during its life time depends on its chronological life span. Thus, first, we calculate the conditional expectation value of L_{repl}, given that the cell lives a certain amount of time L_{chron}. The conditional expectation value is equal to:

$$E[L_{repl}|L_{chron}] = \mu L_{chron} \tag{22}$$

Then, we substitute equation 22 into the law of total expectation (equation 21) and again take the expectation value to find the expected replicative age of cells.

$$E[E[L_{repl}|L_{chron}]] = E[\mu L_{chron}] = \mu E[L_{chron}] = \mu \cdot \frac{1}{\lambda} = \frac{\mu}{\lambda} \tag{23}$$

Summarizing equation 21$-$23, the expected replicative age of a cell is equal to the growth rate μ divided by the death rate λ:

$$E[L_{repl}] = \frac{\mu(t)}{\lambda(T)} \tag{24}$$

Now, we can express the expected replicative age of the cells in terms of the parameters of the model:

$$E[L_{repl}] = \frac{\mu(t)}{\lambda(T)} = \frac{M_t(T_{max} - T_0)}{(K + M_t)(T - T_0)}\Big(1 - \frac{M_t}{C}\Big) \tag{25}$$

Next, we define γ_{repl}, where $E[L^1_{repl}]$ is the expectation of the replicative life span of strain 1 and $E[L^2_{repl}]$ of the

replicative life span of strain 2:

$$\gamma_{repl} = \frac{E[L^1_{repl}]}{E[L^2_{repl}]} \tag{26}$$

The quantity γ_{repl} can help to predict the outcome of a co-existence experiment. However, γ_{repl} only provides the relative, average replicative life spans of the strains, and not the rates of cell division. Therefore, it is not enough to only know γ_{repl} to predict the outcome of the co-existence experiment. Additionally, we need to know the growth rate μ of the strains. Then, we know how many times the cells of both strains on average replicate in their life span, and we know at what maximum rate they replicate. We used the maximum growth rate as a measure for the growth rate $\mu(t)$ of the strains, because it is fixed and it represents the upper bound of $\mu(t)$. For example, if $\gamma_{repl} > 1$ and $\mu_{max,1} = \mu_{max,2}$, strain 1 dominates, because the cells of strain 1 divide more often in their lives, while both strains replicate at the same rate. If $\gamma_{repl} = 1$ and $\mu_{max,1} > \mu_{max,2}$, strain 1 dominates as well, because both strains replicate the same number of times, but strain 1 does so at a higher rate. However, if $\gamma_{repl} < 1$ or $\mu_{max,1} < \mu_{max,2}$, strain 2 dominates. Importantly, we assume that the initial cell densities of both strains are equal. So, the independent parameters γ_{repl} and μ_{max} can be used to predict the outcome of a co-existence experiment, where the strains differ in only one parameter and have the same initial cell density.

We fill in the parameters of both strains in the equation for γ_{repl} to get the following:

$$\gamma_{repl} = \frac{(T^1_{max} - T^1_0)}{(T^2_{max} - T^2_0)} \frac{(T - T^2_0)}{(T - T^1_0)} \frac{\frac{M_t^{n_1}}{(K_1^{n_1} + M_t^{n_1})}}{\frac{M_t^{n_2}}{(K_2^{n_2} + M_t^{n_2})}} \frac{(1 - \frac{M_t}{C_1})}{(1 - \frac{M_t}{C_2})} \tag{27}$$

As an example, by varying only the parameter T_{max} between the two strains and keeping all other parameters, especially the maximum growth rate μ_{max}, equal, we can use γ_{repl} to predict the outcome of a co-existence experiment. We first simplify the formula for γ_{repl}, as many of the terms drop out:

$$\gamma_{repl} = \frac{(T^1_{max} - T^1_0)}{(T^2_{max} - T^2_0)} \tag{28}$$

Then, we can easily determine which of the strains will dominate the experiment, where other parameter are kept constant. If $T^1_{max} > T^2_{max}$, then $\gamma_{repl} > 1$ and strain 1 will dominate, whereas if $T^1_{max} < T^2_{max}$, then $\gamma_{repl} < 1$ and strain 2 will dominate. In Table 2, the resulting expression for γ_{repl} and the consequences for the co-existence experiment are summarized for each parameter.

Table 2: The parameter that is varied between the two strains, the resulting expression for γ_{repl} and the consequences that it has for the outcome of the co-existence experiment.

Parameter	**Expression for γ_{repl}**	**Consequences**
T_0	$\gamma_{repl} = \frac{(T^1_{max}-T^1_0)}{(T^2_{max}-T^2_0)} \frac{(T-T^2_0)}{(T-T^1_0)}$	If $T^1_0 > T^2_0$, then $\gamma_{repl} > 1$, so a larger value for T_0, is beneficial for the ability of the strain to grow in a co-culture
T_{max}	$\gamma_{repl} = \frac{(T^1_{max}-T^1_0)}{(T^2_{max}-T^2_0)}$	If $T^1_{max} > T^2_{max}$, then $\gamma_{repl} < 1$, so a large T_{max} is beneficial
K	$\gamma_{repl} = \frac{(K^n_2+M^n_t)}{(K^n_1+M^n_t)}$	If $K_1 > K_2$, then $\gamma_{repl} < 1$ for small M_t. So, for small M_t, a small K is beneficial. For $M_t >> K$, the parameter K has no influence on the outcome, as $\gamma_{repl} = 1$
C	$\gamma_{repl} = \frac{(1-\frac{M_t}{C_1})}{(1-\frac{M_t}{C_2})}$	For small M_t, the parameter C has no influence on the outcome of the experiment, as $\gamma_{repl} = 1$. However, for intermediate M_t, a larger C is beneficial. Namely, if $C_1 > C_2$, then $\gamma_{repl} > 1$
n	$\gamma_{repl} = \frac{\frac{M_t^{n_1}}{(K^{n_1}+M_t^{n_1})}}{\frac{M_t^{n_2}}{(K^{n_2}+M_t^{n_2})}}$	If $n_1 > n_2$, then $\gamma_{repl} > 1$ for $M_t \geq K$, so a large n is beneficial

In summary, there are five parameters that can differ between the two strains and can change the outcome of a co-existence experiment via γ_{repl}: T_0, T_{max}, n, K, and C. Additionally, μ_{max} can differ between two strains and influence the outcome of a co-existence experiment. In a co-existence experiment with one variable parameter, we can use γ_{repl} and μ_{max} to predict the outcome, using only the physical properties of the strains and the conditions of the experiment. So, we can predict the growth behaviour of a mixture of strains without running a simulation, which can be useful for predicting the conditions and strain parameters that result in a desired outcome.

5.2 Discussion

Overall, we defined a quantity γ_{repl} that can be used to predict the outcome of a co-existence experiment in combination with the growth rate μ. Namely, γ_{repl} describes the amount of offspring that a strain produces relative to another strain and the growth rate μ describes the rate at which the offspring is produced. Together, these quantities can predict which of the two strains dominates in a co-existence experiment where one parameter is varied between the two strains, meaning that in the end of the experiment, that strain will mainly be present in the culture.

However, we can only vary one parameter between the two strains and the initial cell densities of the strains are assumed to be equal. In a co-existence experiment, we usually choose different initial densities for the strains and this helps to obtain one of the three scenarios as an outcome (e.g. see Figure 13E). Therefore, this is a shortcoming of this result. In the future, we could explore other quantities, that could predict the outcome of a co-existence experiment from the parameters and conditions, also for different initial cell densities of the strains. Additionally, the strains that we actually have and use in the lab, differ from each other in more than one parameter. For example, the strain DHY3 (relative GFP expression level 100x), differs in at least three parameters from the wild type: T_0, T_{max} and μ_{max}, as observed from its experimental phase diagram (see Figure S3) and growth curves [8]. Varying more than one parameter in the model could be interesting, but only if one of the parameters is μ_{max}, because in that case, both γ_{repl} and μ_{max} would differ between the two strains, whereas otherwise, only γ_{repl} would differ and that could be achieved by varying only one parameter as well. However, if γ_{repl} and μ_{max} simultaneously differ between the two strains, it becomes more complicated to predict the outcome of the co-existence experiment. Also, all of the three scenarios were already obtained by varying

one parameter between the strains and we only obtain the same scenarios by varying multiple parameters (see supplementary Figure S12). Therefore, varying more than one parameter in the model is not considered useful.

6 Single-cell analysis

So far, we have defined a model via a bottom-up approach, meaning that we started at the single-cell level, and we used it to study population-level dynamics. Also, we derived a quantity that allows us to predict outcomes. An important advantage of the model described in this thesis is that it can be used to describe the growth behaviour of single cells within a population. We will use this feature of the model to study the chronological and replicative age of the cells.

We followed the replicative life span and the chronological life span of the cells over time for different cultures, which show the three different types of growth at a high temperature (deterministic growth, non-growth and random growth) (see Figure 15). We found that the chronological age is always more or less constant around its fixed expected value, whereas the replicative age initially strongly increases due to the buildup of extracellular glutathione, causing the cells to divide more frequently. When the culture reaches the saturating cell density, the nutrients are depleted and the cells stop dividing, but still die. Therefore, the expected replicative age of the cells decreases to zero after reaching the saturating cell density (Figure 15).

Additionally, we observed that both the chronological and the replicative age of the cells are short relative to the duration of the growth experiment (see Figure 15). The average chronological age is around eight hours, so we can conclude that the turnover of cells in the population is high, meaning that the cells are replaced by new cells rather quickly. The replicative life span does not exceed two (see Figure 15), so cells replicate on average at most two times in our model. A low value for the replicative age is also observed experimentally [34]. Every time a yeast cell buds, it forms a bud scar on its cell wall. The researchers stained and counted the bud scars on yeast cells, revealing that yeast cells rarely divide more than three times in their life [34], corresponding to our theoretical result that the average replicative age of a cell does not exceed two.

Finally, we observed that the chronological and replicative age vary more from their average for randomly growing or non-growing cultures (see Figure 15B,C,D) compared to deterministically growing cultures (Figure 15A). Especially the variance of the chronological life span is large, due to the small sample size (number of living cells). Namely, when the sample size decreases, the variability with respect to the expectation value increases. Analogous to the expectation values, we derived the variances of the chronological and replicative age of the cells.

$$Var[L_{repl}] = \frac{1}{\lambda^2}(\mu\lambda + \mu^2) \tag{29}$$

$$Var[L_{chron}] = \frac{1}{\lambda^2} \tag{30}$$

We noticed that the variance of the chronological age is larger than of the replicative age:

$$Var[L_{repl}] = \frac{1}{\lambda^2}(\mu\lambda + \mu^2) = Var[L_{chron}] \cdot (\mu\lambda + \mu^2) \tag{31}$$

$$Var[L_{chron}] > Var[L_{repl}] \tag{32}$$

Here, we assumed that the following holds: $\mu(t), \lambda(T) < 0.5$ for all times t and for all reasonable temperatures

T, so $(\mu\lambda + \mu^2) < 1$. We used the law of total variance to calculate the variance of the replicative life span: $Var(Y) = E[Var(Y|X)] + Var(E[Y|X])$. In conclusion, the variance of the chronological age is larger than the variance of the replicative age and both variances decrease with an increasing population size.

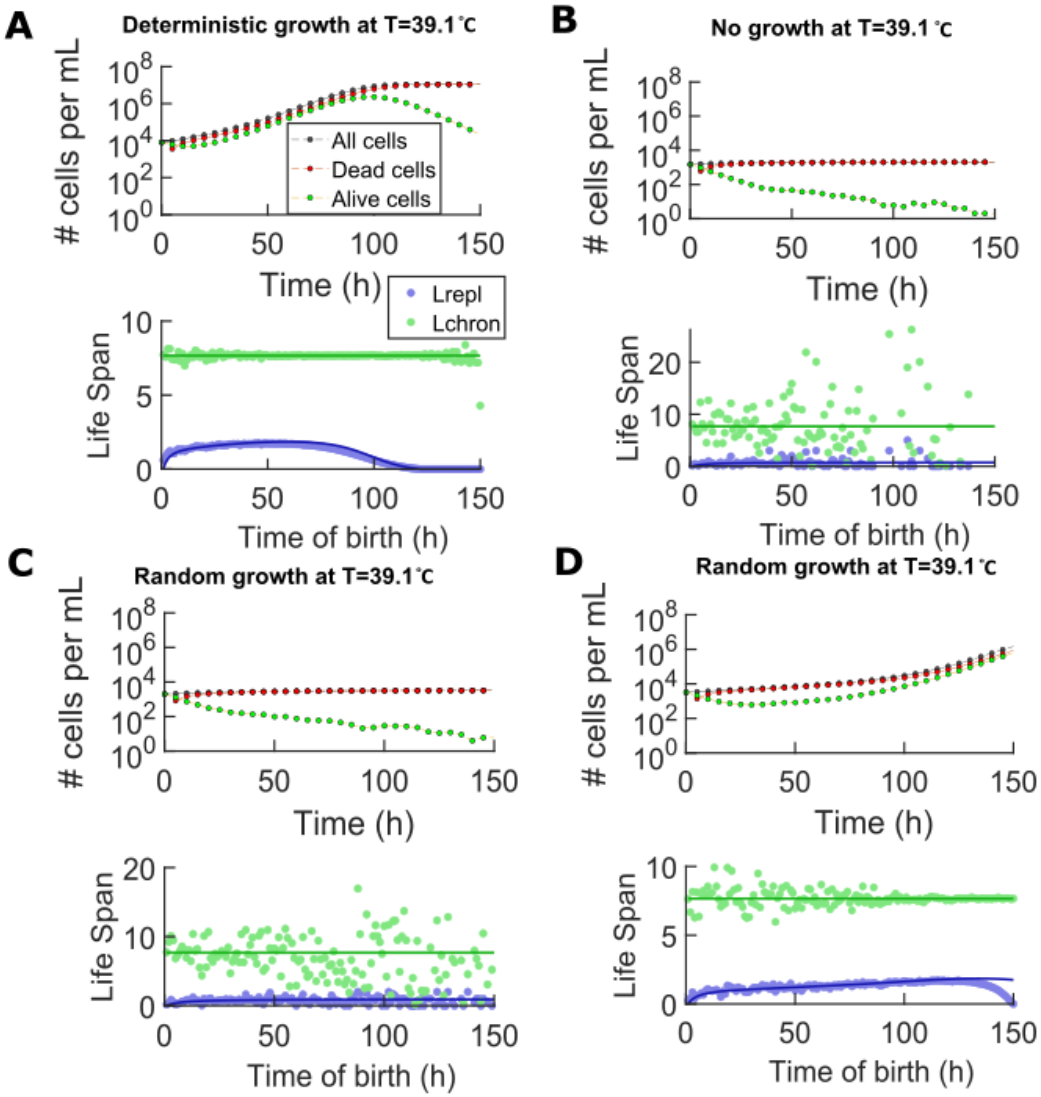

Figure 15: The growth behaviour of single cells in populations that show three different types of growth at $T = 39.1℃$: A) deterministic growth, $A_0 = 10000$ cells/mL, **B)** non-growth, $A_0 = 1500$ cells/mL, **C)** random growth resulting in extinction, $A_0 = 2400$ cells/mL and **D)** random growth resulting in growth, $A_0 = 2400$ cells/mL. The expectation values of L_{chron} and L_{repl} are indicated over time using a full line. L_{chron} and L_{repl} are averaged over the cells born at a certain time point and are indicated as dots.

7 Conclusions

In this chapter, we introduced a mathematical model that describes the growth behaviour of yeast populations at high temperatures, by describing the behaviour of single cells in the population (via a bottom-up approach). Using the model, which is consistent with previously published work and experimental results [8], we reproduced the three types of growth and the phase diagram of growth.

As described above, the mathematical model has several advantages over a previously used mathematical model [8]. Firstly, it is more realistic, because it is continuous in time rather than using fixed, discrete time steps. Also, it allows us to study single cells (and their replicative and chronological age) within the population. Using the latter feature of the model, we found that the chronological age of the cells is on average approximately 8

hours, which is short compared to the duration of the simulation (~ 150 hours) and the replicative age does not exceed two, meaning that a cell replicates at most twice in its life. These results suggest that the turnover of cells in a population is high, meaning that cells are replaced at a quick rate.

Importantly, the mathematical model reproduces experimental results from co-existence experiments. By using the estimated parameters of the strains and by using the same conditions as in experiment, the outcome of the model matches the experimental results qualitatively. The main finding of this chapter is that the mathematical model reproduces the two outcomes of a co-existence experiment that we obtained experimentally (the strong strain profiting from the weak strain and the strong strain helping the weak strain) and that it predicts a third outcome, where both strains help each other to grow. All three outcomes can be obtained from simulation of the model by varying a single parameter (any of T_0, T_{max} or K) between the two strains that are mixed in the population (Figure 12). We found that the outcomes of the model are robust against the choice of parameters and initial conditions, meaning that a rather broad range of parameter values or initial cell densities result in one of the three scenarios (see Figure 13).

In the future, the model could be used as a tool to predict the outcome of a co-existence experiment. Then, we could aim to produce a desired, experimental outcome by matching the experimental conditions and strains to the successful conditions and parameters in the model (e.g. using Figure 13). For example, we could aim to obtain the unexplored third scenario (help each other) or the uncharted outcome of the cheater strain profiting from another strain (as in Figure 14). In experiments, a suitable choice of strains and initial conditions is crucial to obtain one of the three scenarios. This is illustrated by the fact that we have not obtained the third scenario experimentally. So, in experiments, the outcomes of a co-existence experiment are not as robust against the choice of parameters and conditions as in the model. We expect that this is caused by oversimplifications in our model. For example, we did not define interactions between the cells in our model, other than the interaction via the secretion of glutathione and the depletion of nutrients.

Additionally, we found a quantity γ_{repl}, which can predict the outcome of a co-existence experiment, together with the parameter μ_{max}, by using only the initial conditions and the parameters of both strains. The quantity γ_{repl} is a measure for the amount of offspring that a strain produces and μ_{max} is a measure for the rate at which the offspring is produced. Therefore, together, γ_{repl} and μ_{max} can be used to predict the outcome of a co-existence experiment with one variable parameter between the two strains. This can be useful, because we only need the physical properties of the cells and the initial conditions of the experiment to make a prediction. However, γ_{repl} can only predict the outcome if the initial densities of the strains are equal. In the future, we could seek for another quantity that can predict the outcome of co-existence experiments, also when we choose a different initial cell density for both strains or when we vary both γ_{repl} and μ_{max} between the two strains. Then, we could always predict the outcome of a co-existence experiment from the physical properties of the cells and the initial conditions.

Part 4

Cooperation in *E. coli* at high temperatures

1 Introduction

After having studied yeast, we will now study the prokaryotic bacterium *E. coli*, to discover whether density-dependent growth and cooperative behaviour at high temperatures is conserved among microbial species (prokaryotic and eukaryotic). *E. coli* populations mainly live in the colon of mammals, where they play an important role in the digestion of food. Also, *E. coli* is frequently used as a model organism in science. The temperature that is optimal for growth of *E. coli* populations is around 37℃. Above this temperature, *E. coli* cells can experience heat stress, a condition that exposes the cell to heat-induced damage.

When exposed to heat stress, the cell cycle of an *E. coli* cell arrests, causing growth to slow down [35]. Also, reactive oxygen species (ROS) form as a by-product of the respiratory chain, which can damage key components in a cell, such as DNA [36] and proteins [37]. Like most microbial species [38], *E. coli* cells use a heat shock response system to repair heat-induced damage. The conventional view states that the survival of an *E. coli* cell depends on its autonomous ability to repair heat-induced damage via the heat shock response system [38], as described next.

As a consequence of a rising temperature, the concentration of heat-induced sigma factor σ^{32}, one of the regulatory bacterial σ factors that collectively control the effectivity of transcription initiation at certain promoter sites [39], rapidly increases. Then, RNA polymerase (RNAP) can effectively bind to the promoters of heat shock genes, and initiate transcription, to create heat shock proteins (HSP) [39]. HSP act as molecular chaperones and refold proteins or degrade irreversibly damaged proteins in the cytoplasm, thereby promoting cell survival. A system of chaperone proteins categorized as HSP, called the DnaK chaperone system, act as negative modulators on σ^{32}, as they compete with RNAP to bind σ^{32} [40]. When bound to σ^{32}, they inactivate the σ^{32} factor and promote its degradation, thereby creating a negative feedback loop on their own production (see Figure 16) and regulating the cellular heat-shock response.

In this thesis, we studied the growth behaviour of *E. coli* populations at high temperatures, to investigate whether the cells cooperate with each other to battle heat. We found that the conventional view that the survival of an *E. coli* cell depends solely on the heat shock response system, is incomplete. Namely, we discovered that the ability of a population of *E. coli* cells to grow not only depends on temperature, but also on the initial population density. So, the survival of a cell also depends on the amount of neighbouring cells. This indicates that the cells cooperate with each other to collectively survive the heat.

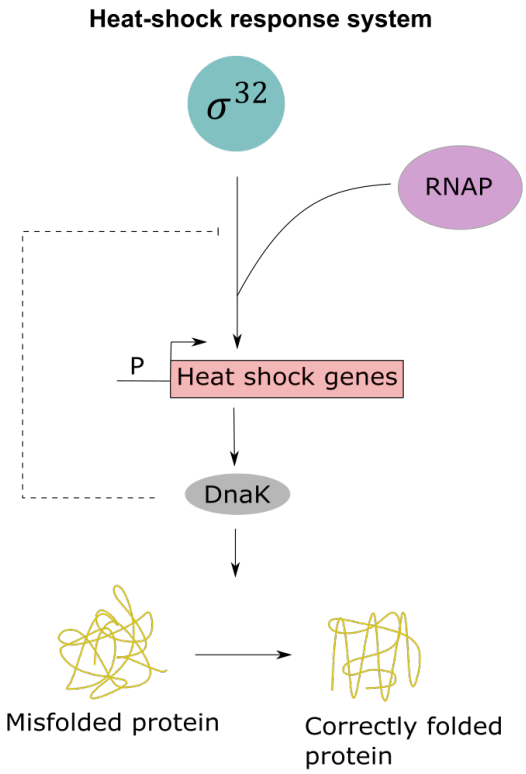

Figure 16: The *E. coli* heat shock response, involving sigma factor σ^{32}, which induces the transcription of heat shock genes, and the HSP DnaK, which regulates the heat shock response.

2 Results

To discover how an *E. coli* population copes with heat, we have grown cultures of *E. coli* (strain K12 MG1655) at a range of different high temperatures, having different initial cell densities. We measured the cell density of the culture over time using flow cytometry, a method that counts the cells in a certain liquid volume, including dead cells. The resulting growth curves of cultures grown at the optimal temperature of 37° C, give the optimal doubling time of an *E. coli* culture (see Figure 17A). We calculated the optimal doubling time for an *E. coli* population to be approximately 44 minutes, which corresponds to the optimal doubling time from literature [41]. Surprisingly, we found that the growth curves at 45.5℃ show that the growth behaviour of a population of *E. coli* cells is dependent on the initial cell density (see Figure 17B). Namely, the population with the highest initial density grows (blue curve), whereas the populations with lower initial densities do not (green and red curves). We did not find growing populations at 50° C for any of the tested initial cell densities (see Figure 17C).

We summarized the results of all growth experiments in a phase diagram (see Figure 17D). This phase diagram illustrates that the growth behaviour of a population of *E. coli* cells is not only dependent on temperature, but also on the initial cell density of the culture. A population with a large initial density is able to survive conditions that a population with a small initial cell density is unable to survive. We characterized a blue region in the phase diagram, representing growth of the population, which is located at low temperatures and large initial cell densities. Also, we characterized a red region, representing non-growth, which is located at high temperatures and low initial cell densities. In between the blue and the red region, we have no measurements of the population behaviour.

The grey region in the phase diagram indicates a lack of nutrients, which makes populations unable to grow. We found that the saturating cell density of a culture decreases for an increasing temperature (see Figure 17D),

because cells consume more energy per unit time at high temperatures to stay alive and to grow [42]. At the same time, the cultures grow slower at high temperatures. Therefore, the cells need more time to grow and use more energy and nutrients during their period of growth. So, the saturating cell density decreases with temperature.

We can view the growth behaviour of *E. coli* at high temperatures as a dynamical system. For a fixed temperature and at low temperatures ($<\sim 45℃$), the system contains one fixed point (a point that maps onto itself), located at the saturating cell density, as populations always grow until saturated (see Figure17D). This fixed point is stable, because once the system reached this point, it will remain there. At intermediate temperatures ($\sim 45℃ - 48℃$), the system contains three fixed points. One stable fixed point is located at saturating cell density. Another stable fixed point is located at zero cell density, representing a culture that has gone extinct. Additionally, an unstable fixed point is located in between the blue and red regions in the phase diagram, where a small fluctuation can lead to either growth or extinction of the population. At temperatures above $\sim 48℃$, growth is not possible. Therefore, there is only one stable fixed point in the system, located at zero cell density.

The fixed points change as a function of temperature and form boundaries (called phase boundaries) in the phase diagram, where we study various temperatures. The boundary between the grey region and the blue region is a stable phase boundary, consisting of stable fixed points. This boundary represents the saturating cell density of a culture. In between the blue and the red region, there is an unstable boundary, consisting of unstable, fixed points. The lower boundary of the blue region represents the minimum, initial density that results in guaranteed growth of the population. The upper boundary of the red region represents the maximum, initial density that results in guaranteed extinction of the population. The exact boundaries of the phase diagram and of the dynamical system need to be determined more precisely in follow-up experiments.

Most likely, two of the three phase boundaries (the top stable phase boundary and the middle unstable phase boundary) converge to a point, called the fold bifurcation point. At the fold bifurcation point, the two fixed points of the dynamical system come together and annihilate each other, leaving only the bottom stable, fixed point representing extinction. So, at temperatures above the fold bifurcation, no growth is possible at all. More experiments are required to determine the location of the fold-bifurcation point, but from our results we can estimate the fold-bifurcation point to be located at $\sim 48℃$ and initial density $\sim 10^7 - 10^8$ cells/mL. Around the expected location of the fold-bifurcation point, we have observed slight growth, followed by non-growth of the population (see Figure 17E, upper three curves), which is indicated in the phase diagram by pink data points (see Figure 17D).

From the growth curves, the maximum growth rate was estimated for each temperature (see Figure 17F). We found that the maximum growth rate decreases with temperature, as previously described [35]. We extrapolated the fitted line in the plot of the growth rates, to discover at which temperature the growth rate is expected to be zero in our experiments. This happens at a temperature of $\sim 47.1℃$, which is in line with experiments at similar temperatures, suggesting that the fold-bifurcation point is approximately located here (see Figure 17D). Overall, we found that the growth behaviour of a population of *E. coli* cells at high temperatures depends on the initial cell density of the population.

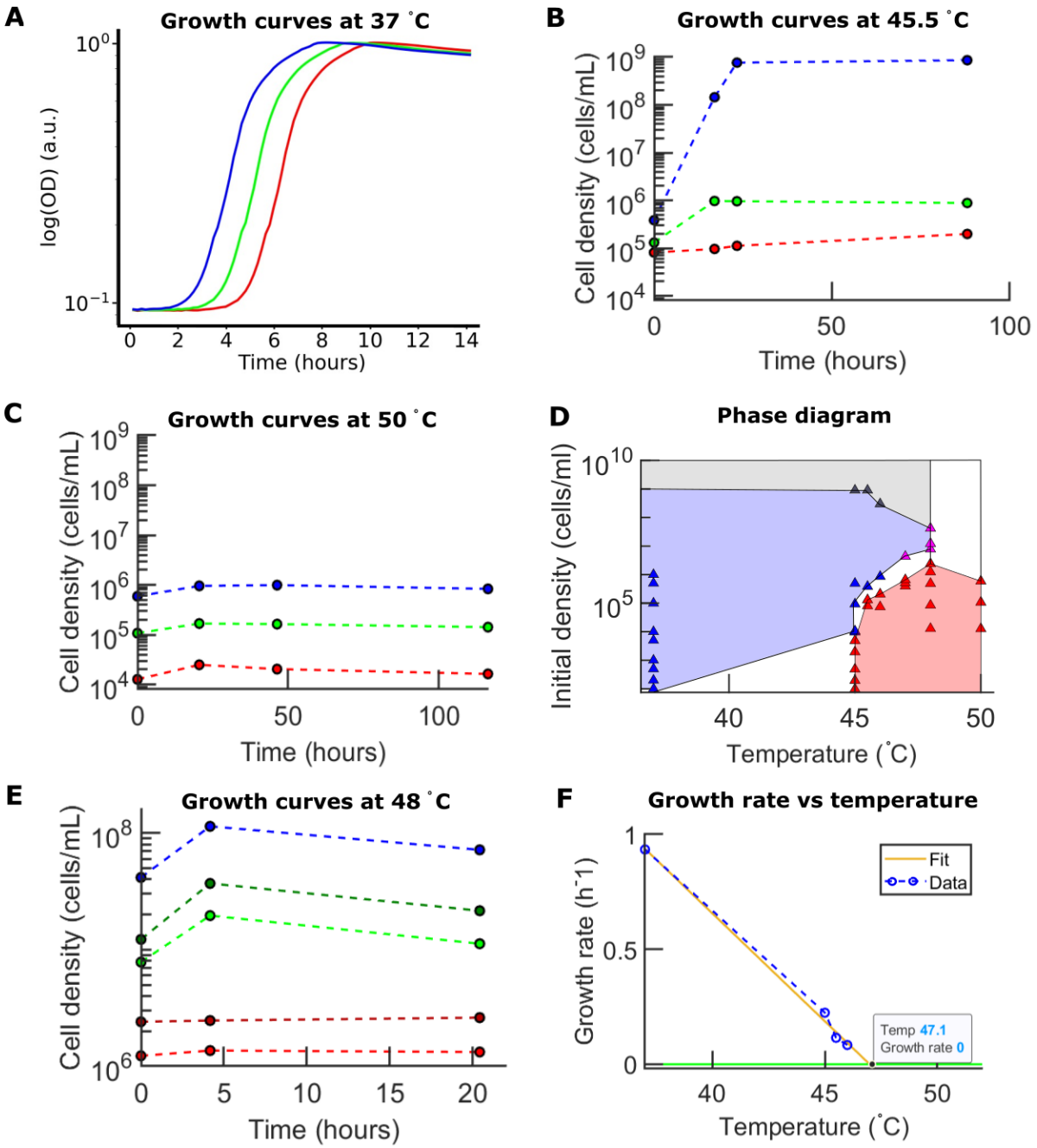

Figure 17: *E. coli* growth behaviour at high temperatures. A) A growing population of *E. coli* MG1655 cells over time at 37 ℃, with three different initial densities (serial dilution of 1:10). Each color has n=3 biological replicates. Data is obtained using a spectrophotometer. OD is measured at a wavelength of 600 nm and is directly proportional to the density of cells. An OD of 1.0 approximately corresponds to $5 \cdot 10^8$ cells/mL [43]. **B-C,E)** Population density over time measured using a flow cytometer (n=1 biological replicate) at **B)** 45.5 ℃ (initially $\sim 3.8 \cdot 10^5$ cells/mL (blue), $\sim 1.3 \cdot 10^5$ cells/mL (green), $\sim 8.1 \cdot 10^4$ cells/mL (red)) and **C)** at 50 ℃ (initially $\sim 5.9 \cdot 10^5$ cells/mL (blue), $\sim 1.1 \cdot 10^5$ cells/mL (green), $\sim 1.3 \cdot 10^4$ cells/mL (red)). **D)** Phase diagram summarizing all experiments. Blue triangles indicate population growth, whereas red triangles indicate non-growth. Grey triangle indicate the saturating cell density. Each data point has n=1 biological replicate. **E)** Population density over time at 48 $^\circ C$ (initially $\sim 4.2 \cdot 10^7$ cells/mL (blue), $\sim 1.2 \cdot 10^7$ cells/mL (dark green), $\sim 7.8 \cdot 10^6$ cells/mL (green), $\sim 2.4 \cdot 10^6$ cells/mL (dark red), $\sim 1.3 \cdot 10^6$ cells/mL (red)). **F)** Growth rates (h^{-1}) as a function of temperature, estimated from the growth curves. A linear fit is drawn through the data points.

3 Literature study

The result that *E. coli* populations grow in a density-dependent manner suggests that there is cooperative behaviour underlying this behaviour. Based on previous work [8], the cells might cooperate by secreting a molecule that detoxifies the growth medium, e.g. from reactive oxygen species (ROS). Then, a high initial cell density of a population would lead to a quick accumulation of the secreted molecule in the growth medium, so a population would be able to collectively survive heat stress. However, a low initial cell density would lead to a slow accumulation of the secreted molecule, causing the population to go extinct. Thus, this type of cooperative behaviour could explain density-dependent growth, which we observed in experiments. We sought to discover the method of cooperation that *E. coli* cells might use to collectively combat high temperatures. In this section, we describe our findings.

We sought molecules that could potentially facilitate density-dependent growth of *E. coli* populations at high temperatures. Previous work [44] found that at high temperatures, a population of *E. coli* cells can be rescued and stimulated to grow by adding indole. Indole is a small signalling molecule, synthesized from the amino acid tryptophan [45]. At 50 ℃, the researchers found that populations show growth in response to a low concentration (20 μM) of extracellular indole added to the growth medium [44]. So, extracellular indole improves survival and stimulates growth at high temperatures [44].

Furthermore, indole can be secreted via diffusion across the membrane [46], which is a crucial feature to explain density-dependent growth. Additionally, indole induces transcriptional changes in neighbouring cells, causing an upregulation of efflux pumps [47]. Efflux pumps are transport proteins in the cell wall of *E. coli* cells, which play a key role in the heat shock response system, via the removal of damaged proteins from the cell (see Figure 18). So, via the upregulation of efflux pumps, indole promotes survival of cells at high temperatures. Also, indole directly counteracts ROS, harmful molecules that cause oxidative stress, via a redox reaction [48] and indole is suggested to induce the expression of certain HSP [49], thereby stimulating the refolding or degradation of damaged proteins. Finally, the cytoplasmic pH decreases due to heat stress, which increases the toxicity of ROS [50]. Nevertheless, indole can regulate the cytoplasmic pH, by carrying protons across the cytoplasmic membrane [51], thereby reducing the toxicity of ROS. In conclusion, because indole can be secreted, indole is able to rescue cells at high temperatures and because indole is involved with the heat-shock response and ROS, indole might be the molecule that *E. coli* cells secrete to collectively combat heat stress.

4 Discussion

Our work demonstrates that *E. coli* populations grow in a density-dependent manner at high temperatures, revealing that the cells collectively combat heat. Based on previous work [8], we hypothesized that the cells secrete a public good, which detoxifies the growth medium (e.g. from ROS) and may be used by other cells to repair heat-induced damage. Based on literature, it is plausible that the small molecule indole is the public good in this cooperative behaviour. Indole is a well-studied signalling molecule in *E. coli*, with multiple functions. For example, indole regulates biofilm formation [52], the transition from stationary to exponential phase [53], and multiple stress responses [46]. Additionally, indole is a signalling molecule that can enable interaction between different microbial species and different biological kingdoms, fulfilling an important role in pathogenesis and immunity [45, 54]. We found that indole can upregulate efflux pumps [47], also in neighbouring cells, thereby promoting the removal of heat-damaged proteins from the cell (see Figure 18). Additionally, indole can induce

the expression of HSP [49] and deactivate ROS [23], which are harmful molecules that cause the primary stress resulting from heat: oxidative stress. So, indole could be the public good that enables cooperation between *E. coli* cells at high temperatures.

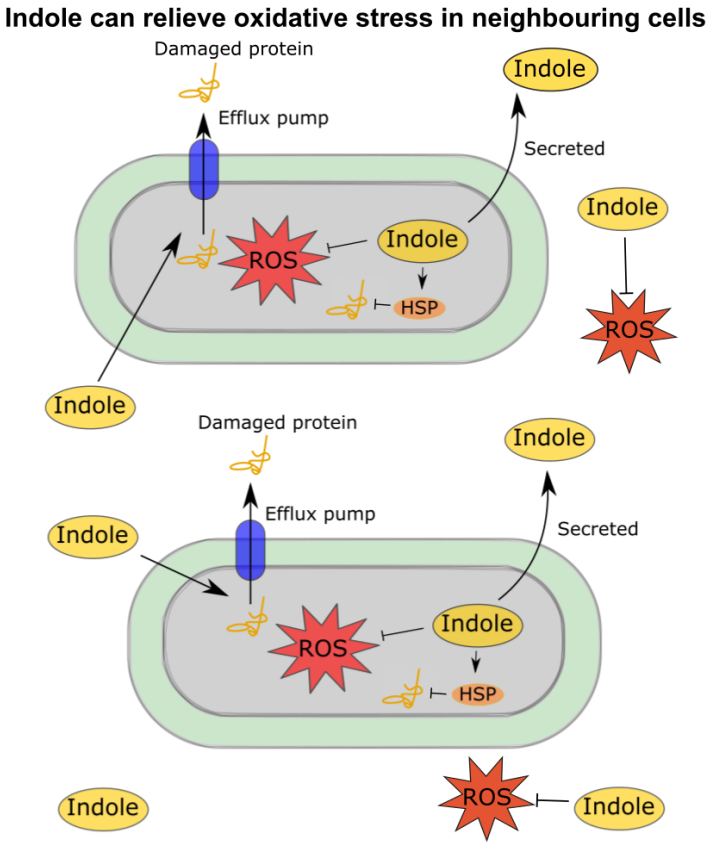

Figure 18: Indole plays a key role in relieving oxidative stress in the cell and in neigbouring cells, by counteracting ROS, inducing HSP and transcriptionally activating efflux pumps.

Even though indole meets all the requirements to be the public good, more experiments are required to confirm our hypothesis. In the following, we explain the experiments that we would do as part of this thesis, if we had the time and opportunity. Firstly, we would take more data points on the phase diagram, to characterize the growth behaviour in untested regions and the boundaries between the regions more precisely. Secondly, we would test whether random growth (growth after an unpredictable time, as observed in yeast populations growing at high temperatures [8]) exists in *E. coli* populations. We expect that random growth occurs in between the blue and the red region of the phase diagram (see Figure 17D). Therefore, we would do growth experiments in this region of the phase diagram with several replicates, to discover whether the populations grow after a variable time of stasis. Confirming the existence of random growth experimentally, would improve our understanding of the growth behaviour at high temperatures and would verify our theory about the dynamical system having an unstable phase boundary located in between the blue and the red region.

Next, we would try to discover the method of cooperation that the cells use at high temperatures. To this end, we would test whether the ability to grow is resided in the intracellular or in the extracellular medium. We can test this via a medium transfer experiment (see Figure 19), in which we add the growth medium from a population of cells, grown at a high temperature for some time, to fresh cells (right, bottom tube). The fresh cells have an initial density that normally would not result in growth, so if they start growing in spent medium, the cells must have secreted a molecule into the medium before, which gives the fresh cells the ability to grow. However, if the

fresh cells are unable to grow in the spent medium, the medium does not contain secreted factors that stimulate growth. Secondly, in a different experiment, we would refresh the medium of a population of cells, grown at a high temperature for some time, and dilute the cells (left, bottom tube). If the cells lose their ability to grow as a consequence, they lack some secreted factor in the medium that was present before. However, if the cells keep growing, secreted factors in the medium have no influence on the growth ability of the cells and instead, some intracellular factor might dictate the ability to grow.

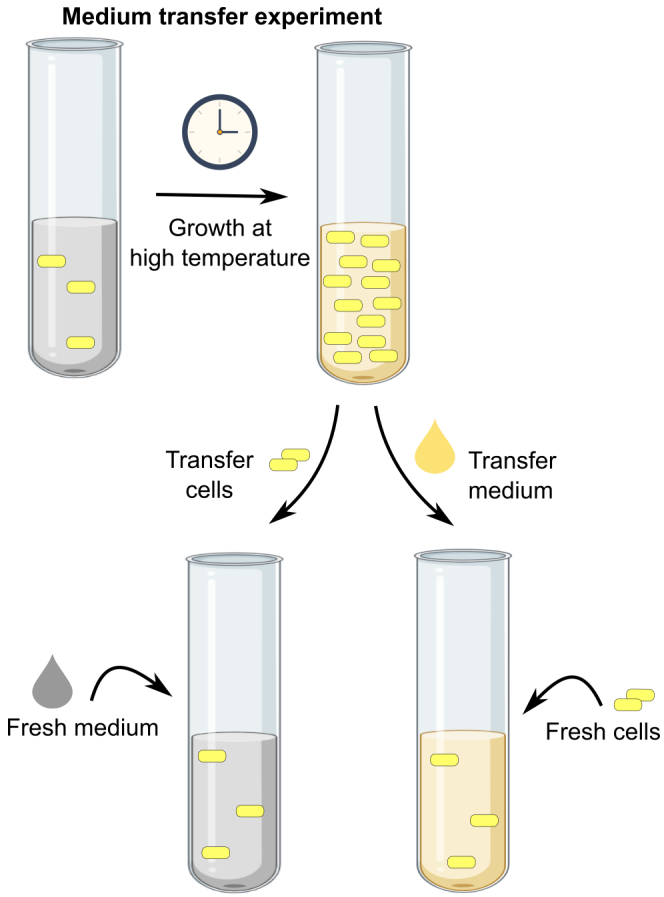

Figure 19: Medium transfer experiment to discover whether intracellular or extracellular factor(s) determine the ability to grow at high temperatures.

If we discover that the ability to grow is not in the extracellular medium, but rather determined by intracellular factors, then we would start with the following experiment to test whether the ability to grow is, for example, determined by a mutation. Starting with a sufficiently large initial population size, a mutant cell that is able to grow at high temperatures due to a mutation, might be present in the population by chance, enabling survival and growth of the population. Therefore, we would test whether a heat-tolerant mutation dictates the ability to grow, by taking a sample from a population that grew at high temperature, and transferring these cells to fresh medium, resulting in a sufficiently low initial density that would normally not grow (according to the phase diagram). If the ability to grow is determined by a mutation, then the transferred population will still show growth, even at low initial cell densities that normally result in extinction. However, if the transferred population stops growing after diluting, then we can rule out the possibility of a heat-tolerant mutant determining the ability to grow.

We expect that the ability to grow is a secreted factor in the extracellular growth medium. Then, we could determine which molecule (or which molecules) in the growth medium give(s) the cells the ability to grow at high temperatures. First, we would test the potential of the small molecule indole, by adding it to the growth

medium after a period of non-growth. If the cells are able to grow as a consequence, indole is sufficient to stimulate growth and survival of the population at high temperatures. Then, we would test whether indole is essential for growth at high temperatures, by adding an inhibitor of indole (such as L-bishomotryptophan [55]) to the growth medium of a growing culture, and observing the effect on the growth behaviour of the population. If the population becomes unable to grow after the inhibitor was added, then indole is essential for growth at high temperatures. Alternatively, we could create a mutant strain, that is unable to produce indole. We would do this by deleting the tnaA gene, which is essential for indole production, as it encodes the predecessor of indole, tryptophan. The mutant strain would then be unable to produce indole. If this strain is unable to grow at high temperatures, under conditions that promote growth in the wild-type strain, then indole is necessary for growth at high temperatures. These experiments could confirm that indole is not only sufficient, but also essential for survival of the population at high temperatures.

Furthermore, there is no consensus on the conditions under which indole is produced by *E. coli* cells. A study that describes *E. coli* populations under antibiotic stress [56] shows that only unstressed, growing cells produce indole [56]. However, other studies [44, 57] show that instead, the production of indole increases under stress conditions such as high temperatures. In the future, we hope to settle this ambiguity with our results. If the cells indeed use indole as a public good to collectively survive heat, then the production of indole most likely increases at high temperatures.

If the experiments with indole are unsuccessful, we could choose to start a broad search for the secreted molecule(s). To identify the type of molecule that is secreted into the medium by the cells and that gives the population the ability to grow, we would perform a transcriptome analysis (via RNA-sequencing) on *E. coli* populations in different parts of the phase diagram. Then, we would compare our analysis to a transcriptome analysis of a population growing at the optimal temperature of 37℃. By determining which genes are transcriptionally up- or downregulated, we could determine the type of stress that *E. coli* cells experience at high temperatures. For example, we could find that genes associated with processes that can cause oxidative stress (such as aerobic metabolism [58]) are downregulated at high temperatures compared to at optimal temperature. Downregulating these genes may decrease the formation of reactive oxygen species (ROS) [58], enabling the cells to survive and replicate. This would suggest that *E. coli* cells experience oxidative stress at high temperatures. Then, a molecule that can relieve oxidative stress, such as an antioxidant [59], might be (one of) the secreted molecule(s), giving cells the ability to grow at high temperatures. Thus, by identifying groups of genes that change expression at high temperatures we could reason to which class of molecules the secreted molecule(s) might belong.

Part 5

Summary and outlook

Microbial cooperation is the phenomenon of microbial cells working together to obtain a common advantage. Cooperative behaviour in microbial populations is specifically observed under stressful environmental conditions, such as high temperatures. In this thesis, we studied population behaviour at high temperatures for two different model organisms: *S. cerevisiae* and *E. coli*.

The yeast *S. cerevisiae* secretes the antioxidant glutathione (a so-called public good) at high temperatures, which deactivates toxic, reactive oxygen species (ROS) in the environment [25]. A previous study [8] shows that a population with a low initial cell density is unable to produce enough glutathione to detoxify the medium, causing the cells to be unable to grow and the population to go extinct. Conversely, a population with a high initial cell density is able to detoxify the medium, causing the population to grow to the saturating cell density. Thus, the cells in a population of yeast cooperate with each other via the secretion of glutathione to survive high temperatures.

Motivated by the result that cells in a population cooperate with each other to survive heat [8], we have shown that cells from two different strains also cooperate with each other. This brings us one step closer to the natural situation, where many different strains and species coexist within a microbial community, possibly cooperating to survive heat. We genetically engineered yeast strains to express a fluorescent protein at a relative level (their 'strength': a relatively stronger strain has a lower expression level and a relatively weaker strain has a higher expression level). We found that a so-called strong strain can grow under more harsh conditions (higher temperature and lower initial cell density) than a so-called weak strain, because the weak strain is genetically manipulated to produce a fluorescent protein. We then performed co-existence experiments where two genetically different strains share a common growth medium, revealing that two scenarios can arise: the strong strain profiting from the weak strain to grow or the strong strain helping the weak strain to grow. Furthermore, we extended a mathematical model for yeast growth at high temperatures [8] to include co-existence of strains. This model reproduces our experimental findings. Moreover, the model predicts the third scenario, where the strains help each other to grow.

In the future, a follow-up study is desirable. For example, the existence of the third scenario, where both strains help each other, could be confirmed experimentally. Also, the concept of this thesis might be extended to include more than two different yeast strains or even multiple microbial species. This would provide the first steps to studying how cells in natural microbial communities cooperate at high temperatures. Insights from these studies could be used to understand the impacts of climate change, which warms up natural habitats, on microbial communities. Eventually, our findings might suggest ways to help microbial communities overcome climate change. Since microbes are crucial to the health of ecosystems [60], an effective way to help microbial communities may be required to keep ecosystems healthy.

To discover whether cooperative behaviour, previously found in yeast at high temperatures [8], is conserved among microbial species, we studied the model organism *E. coli*. We found a striking similarity in growth behaviour between *E. coli* and *S. cerevisiae* at high temperatures. Namely, *E. coli* cells show the same density-dependent growth behaviour. Also, the phase diagrams that summarize the conditions for growth of *E. coli* and yeast populations at high temperatures, are very similar [8]. This indicates that cooperative behaviour may be conserved among different microbial species (both eukaryotic and prokaryotic). In addition, we suggest that the

small, secreted molecule indole might play a role similar to glutathione in yeast, stimulating survival and growth of *E. coli* populations at high temperatures. However, to confirm this, follow-up experiments are required. First, we need to test whether *E. coli* cells secrete a molecule into the extracellular medium that dictates the ability to grow. Then, we could test whether this secreted molecule could be indole that acts as a public good for the cells in the population. Finally, we could investigate whether indole is necessary and sufficient for survival and growth of a population at high temperatures.

Overall, the result that two microbial species use cooperation at high temperatures, suggests that more microorganisms cooperate in a similar manner to survive high temperatures. To test this hypothesis, the cooperative behaviour of other microbial species could be studied at high temperatures in the future. As glutathione and indole are molecules that are produced by many microbial species [61, 62] and because both glutathione and indole can relieve oxidative stress at high temperatures [25, 48], it is possible that other microbial species also secrete glutathione or indole to collectively survive heat.

To summarize, in addition to previous work on *S. cerevisiae* [8], a eukaryote, we have shown that the growth behaviour of *E. coli*, a prokaryote, is density-dependent at high temperatures. This finding suggests that cooperative behaviour with the goal to survive high temperatures, is conserved amongst microbial species. Moreover, we have shown that a mixed population of two different yeast strains can cooperate with each other. This indicates that natural, microbial communities, which consist of a variety of strains and species, may exhibit complex, cooperative behaviour when exposed to high temperatures. Together, these insights provide the first step to understanding how microbial communities cope with climate change warming up their natural habitats.

Part 6

Materials and Methods

In the following chapter, the materials and methods that were used in this thesis are described. This chapter is divided into two sections, one for the experiments with *S. cerevisiae* and one for the experiments with *E. coli*.

1 *S. cerevisiae*

We used the yeast *S. cerevisiae* as a model organism, which grows optimally at a temperature of $\sim 30\,^{\circ}C$, with a doubling time of about 2 hours [63]. In this thesis, we studied the growth of *S. cerevisiae* cultures at temperatures ranging from 38.0 to 39.5 ℃.

1.1 Strain information

Our system of yeast strains consists of a wild-type, haploid strain (from Euroscarf with the official strain name 20000A, which is isogenic to the laboratory-standard W303a strain, with the following genotype: MATa; HIS3-11-15; LEU2-3-112; URA3-1; TRP1 D 2; ADE2-1; can1-100) and several, genetically engineered, haploid strains that either express GFP or mCherry at a certain level. In this thesis, we discriminate between a first generation and a second generation of strains, where the first generation of strains was already available in the lab, whereas the second generation strains was constructed specifically for this work.

1.1.1 First-generation, GFP-expressing strains

The first-generation strains express GFP at a certain level, indicated by a relative expression strength (see Table 3 and Figure S1). The level of GFP expression is regulated by different constitutive promoters [64]. Our system also contains an inducible strain, called TT7, that normally expresses no or very little GFP, but can be induced to produce a high level of GFP, using a certain concentration of the small molecule doxycycline (see Figures S1 and S2).

Table 3: First generation of GFP-expressing strains and their characteristics: the promoters, their relative expression strength of GFP [64] and the strain names.

promoter	Relative expression strength	Strain name
pKEX2	4	DHY4
pTEF1(m7)	30	DHY3
pGPD1	200	DHY5
pTET07-GFP pADH1-rtTA	∼1-200 (inducible)	TT7

The strains DHY4, DHY3 and DHY5 were constructed by first inserting a functional ADE2 gene in the locus of the defective ADE2 gene of the wild type (20000A), using homologous recombination. After fixing the ADE2 gene, unlike the wild type, the strain can express adenine, so intermediate red pigment is not accumulated in the cell. Next, the GFP-expressing strains were constructed by integrating a constitutive promoter linked to GFP from a linearized yeast-integrating plasmid into the HIS3 locus via homologous recombination. The

GFP expression of the strain with the weakest GFP expression level is controlled by the constitutive promoter of the yeast KEX2 gene, which was placed 621 base pairs upstream of the ORF. This promoter causes the weakest level of GFP-expression ($\sim$1x). The strain with intermediate GFP expression level ($\sim$10x) contains the constitutive promoter (m7)-TEF1, controlling the GFP expression. The strain with the strongest GFP expression level ($\sim$100x) is controlled by the constitutive promoter pGPD1 (see Figure S1).

The strain with inducible GFP expression, TT7, which can be induced to express GFP using the small molecule doxycycline, was constructed from the wild-type strain 20000A, by first inserting pADH1-rtTA at the HO locus. Then, the defective ADE2 gene was replaced by a functional ADE2 gene using homologous recombination. Therefore, TT7 does not produce red pigment. Finally, pTET07-GFP was inserted at the LEU2 locus. The GFP expression in the TT7 strain is controlled by the promoter pTET07, which can be induced using the molecular complex rtTA-doxycycline. Doxycycline is a small molecule that can readily diffuse into the cells [65]. When it binds to the protein rtTA, a complex is formed, which stimulates GFP expression by binding to the operator.

1.1.2 Second-generation, GFP-expressing strains

To optimize the separation between strains in a co-existence experiment, a second generation of strains was constructed. The second-generation strains include strains constitutively expressing GFP and strains constitutively expressing mCherry. First, we describe the construction of the GFP-expressing strains. There are five different GFP-expressing strains, each with a different promoter, causing expression of GFP at a different level relative to the non-expressing strain (see Table 4). The names of the strains correlate with their relative expression level of GFP (see Table 4). Strain G1 shows the weakest GFP expression and strain G9 the strongest.

Table 4: Second generation of GFP-expressing strains and their characteristics: the plasmid used to construct them, the promoter's relative expression strength of GFP [64] and the strain name.

Backbone-promoter	Relative expression strength (a.u.) [64]	Strain name
Hy100E-pSTE5	7.5	G1
Hy95E-pTEF1(m3)	60-70	G6
Hy98E-pTEF1(m10)	70	G7
Hy94E-pTEF1	70-80	G8
Hy96E-pTEF1(m6)	90	G9

The second-generation, GFP-expressing strains were constructed via multiple GFP-plasmids (see Figure 20 step 1), each with a different promoter controlling GFP and with the gene for resistance to the antibiotic ampicillin. The GFP plasmids were transformed into competent *E. coli* $DH5\alpha$ cells, to amplify the plasmids (see Figure 20 step 2). We selected for the $DH5\alpha$ cells that had taken up the correct plasmid using LB plates with ampicillin (see Figure 20 step 3). Cells from the colonies on the LB Amp plates were grown overnight in LB medium, supplemented with ampicillin. The plasmids were extracted using a miniprep kit (GenElute) and nanodropped, which resulted in a concentration of $\sim$265-430 $\frac{ng}{\mu L}$ of the plasmid (see Figure 20 step 4). We linearized the plasmids using the restriction enzyme PmeI. Then, we grew a fresh culture of yeast cells in YPD medium. Subsequently, we used the linearized plasmids to transform the yeast cells with the GFP gene and the HIS marker. We followed the yeast transformation protocol available in the lab and finally, we streaked out the cultures on SD-His plates to select for the correctly transformed yeast (see Figure 20 step 5). Successful

transformants were checked by PCR, restreaked on YPD plates and stored.

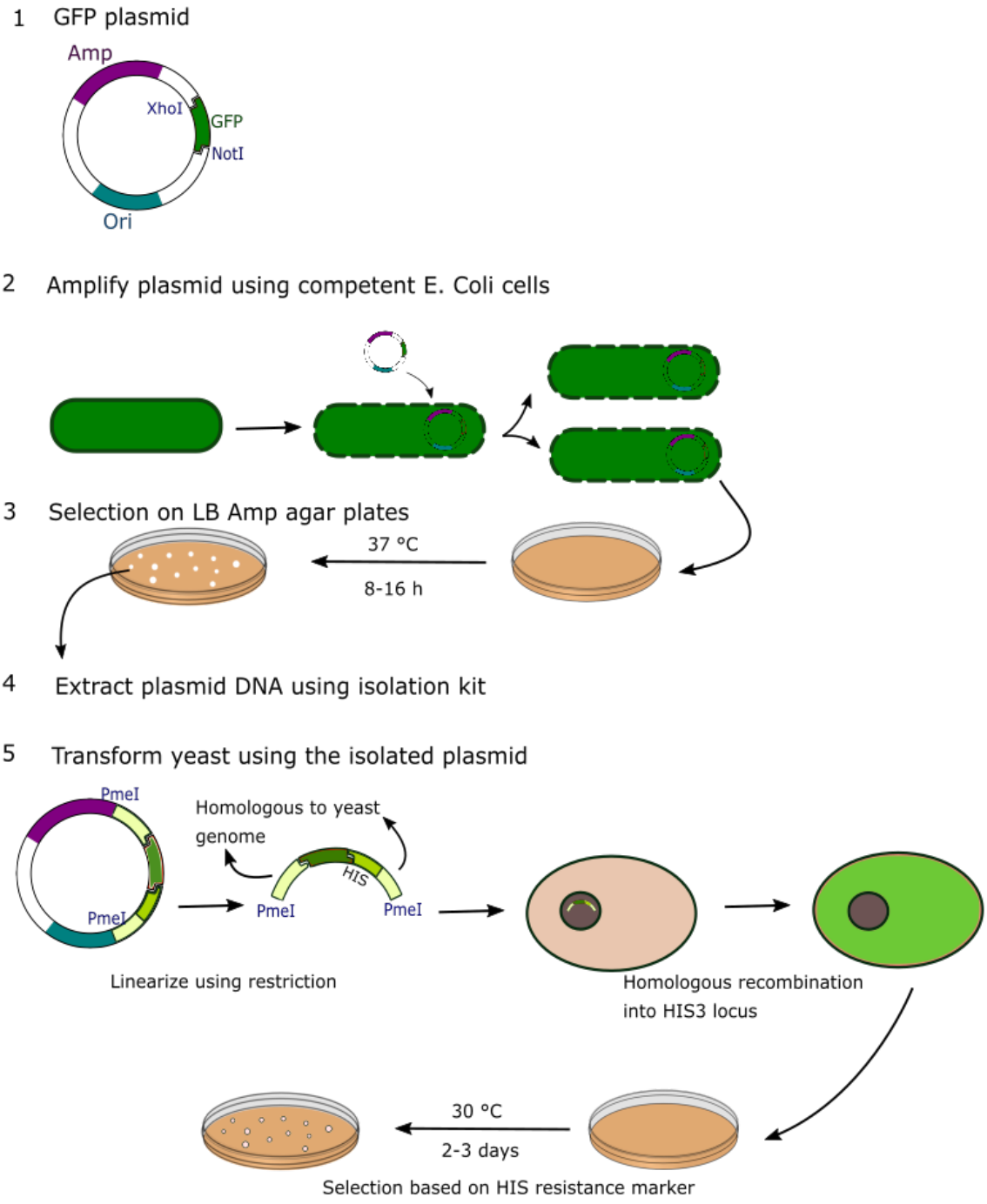

Figure 20: Construction of the second generation GFP-expressing strains. Each strain is constructed from a different plasmid, with a different constitutive promoter, resulting in five different GFP-expressing strains.

1.1.3 Second-generation, mCherry-expressing strains

There are five mCherry-expressing strains, each with a different promoter that causes a different mCherry expression level (see Table 5). Again, the strain names correlate with the relative expression level of mCherry. The strain with the weakest expression level is called R1 and the strain with the strongest expression level R9. These strains were constructed analogous with the second-generation GFP-expressing strains. Only here, the GFP gene on the plasmid was swapped with the mCherry gene, as described next.

Table 5: mCherry-expressing strains and their characteristics: which plasmid is used to build them, their relative expression strength of mCherry, based on [64].

Backbone-promoter	**Relative expression strength (a.u.) [64]**	**Strain name**
Hy100E-pSTE5	7.5	R1
Hy95E-pTEF1(m3)	60-70	R6
Hy98E-pTEF1(m10)	70	R7
Hy94E-pTEF1	70-80	R8
Hy96E-pTEF1(m6)	90	R9

We constructed the mCherry-expressing strains by cutting the mCherry fragment (yeast optimized) from the pTS96 plasmid using XhoI and NotI. The digestion product was run on an agarose gel. Next, the mCherry fragment was excised from the gel, purified and nanodropped (24 $\frac{ng}{\mu L}$). The mCherry fragment was ligated into the selected backbones using T4 ligase (in 1:3 backbone:insert ratio), to obtain the mCherry plasmids, that contained the selected promoters. The plasmid also contains the gene for resistance to the antibiotic ampicillin. Then, the ligation reaction was transformed into competent *E. coli* $DH5\alpha$ cells. We selected for the $DH5\alpha$ cells that took up a plasmid using LB plates with ampicillin. The plates contained about 10x more colonies than the self-ligation plates, where we did not add mCherry and the plasmid ligated to itself without the insertion of mCherry. Cells from colonies were grown overnight in LB supplemented with ampicillin. Then, we extracted the plasmid by miniprep (GenElute), nanodropped it ($\sim$265-430 $\frac{ng}{\mu L}$) and sent it for sequencing at Macrogen, with both a forward and a reverse reaction, starting from the promoter or the terminator, respectively. The sequencing results showed that the mCherry fragment was successfully ligated into each of the backbones. Finally, yeast transformation was performed analogous to the construction of the GFP-expressing strains.

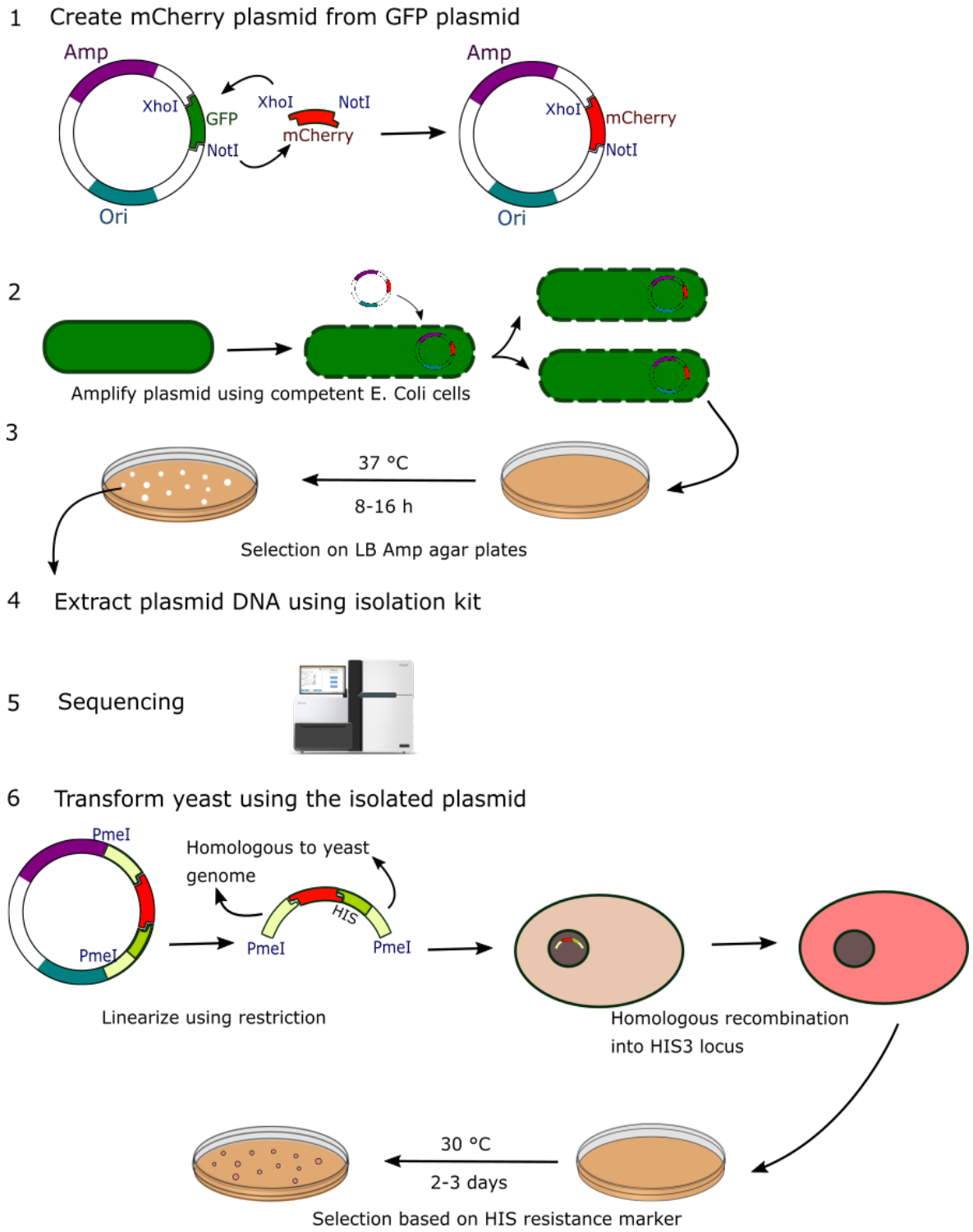

Figure 21: Construction of the second generation mCherry-expressing strains. Each strain is constructed from a different plasmid, with a different constitutive promoter, resulting in five different mCherry-expressing strains.

1.1.4 Cheater strain

The genes GSH1 and GSH2 in *S. cerevisiae* encode the synthesis of glutathione [8]. The gene GSH1 was knocked out to construct a so-called cheater strain, which is unable to produce glutathione itself, requiring an external source of glutathione [8].

We constructed the mCherry-expressing cheater strain by knocking out GSH1 from the wild type W303, and replacing it with the marker HygB. First, we amplified the marker HygB via PCR. Then, we designed primers

analogous to the GSH1 gene and performed transformation with HygB selection and supplementing glutathione. Only correctly transformed cells containing the hygromycin resistance gene could grow on the selection plate. We checked that GSH1 was successfully removed by PCR. Also, we checked that the strain was unable to grow without supplemented glutathione, as glutathione is essential for survival and growth. Next, we fixed the ADE2 gene, so the strain could synthesize adenine, and would not accumulate red pigment. Then, we selected for the ADE2 fix using SD-ADE+GSH agar plates. Finally, we transformed the strain to express mCherry, controlled by the constitutive promoter p(m3)TEF1. This promoter has a relative expression level of 60-70x and the strain is called CR6. Also, the strains express HIS as marker gene after the transformation. We selected for the correctly transformed cells on a SD-HIS+GSH agar plate.

1.2 Growth medium

During growth experiments, all yeast was cultured in minimal media consisting of: Yeast Nitrogen Base (YNB) medium, Complete Supplement Mixture (CSM), which contains all essential amino acids and vitamins, and 2% dextrose (2 g per 100 mL, which is a saturating concentration). This medium is called SD (synthetic defined) medium.

1.3 Growth experiments

We followed the growth, mCherry expression and GFP expression of yeast populations over time. As previouslly described [8], the initial cultures for the growth experiments were created by picking a single yeast colony from an agar plate stored at 4℃ (see Figure 22 step 1), which was then incubated in 5 mL SD medium at 30 ℃ for about 16 hours. Then, we took 20 μL of this overnight culture and diluted it 50x by adding 980 μL PBS buffer (Phosphate-Buffered Saline) (see Figure 22 step 2), which is an isotonic buffer that keeps the pH constant, commonly used in biological research. Subsequently, we sampled the diluted overnight culture using a flow cytometer (BD FACS Celesta with a High-Throughput Sampler), which reveals the culture's population density that can be used to calculate what volume of the overnight culture is required to produce the right initial cell density (cells/mL) for the experiment, using a custom-made Excel sheet (see Figure 22 step 3). We put the desired cell density in 25 mL SD medium (see Figure 22 step 4). Next, we mixed and put 5 mL of the culture in a well (see Figure 22 step 5). Specifically, 24 of these cultures can be grown simultaneously using a Whatman: 24-well x 10 mL assay collection and analysis microplate (also called 'brick'). In the brick, six different conditions were assessed with four replicates each to evaluate the reproducibility of the experiment. The bricks were sealed using a breathable film (Diversified Biotech: Breathe-Easy), covered with a custom-made, insulating Styrofoam cap and incubated in a thermostatic incubator (Memmert ICP26) (see Figure 22 step 6), that kept the temperature stable around the set value, with a standard deviation of 0.017℃. The bricks were constantly shaken on a plate shaker at 400 rpm throughout the entire experiment, to make sure the cultures remained well-mixed, nutrients and oxygen are homogeneously distributed and the yeast cells did not sink to the bottom of the brick.

We do not control for carryover glutathione from the overnight culture. However, we usually take overnight cultures of similar cell density to start our experiment, such that the amount of GSH in the culture should be in some constant, small range. Furthermore, the amount of carryover liquid is usually very small: typically we transfer only 200 μL from the overnight culture to over 25 mL culture, giving at least a 1:125 dilution. Therefore, the overnight culture contains < 2 μM GSH [8]. Thus, this is a carryover of less than 0.02 μM GSH, which is

more than an order of magnitude below the concentration detected in cultures that cannot grow because of the lack of GSH. Therefore, the carryover of glutathione can be neglected.

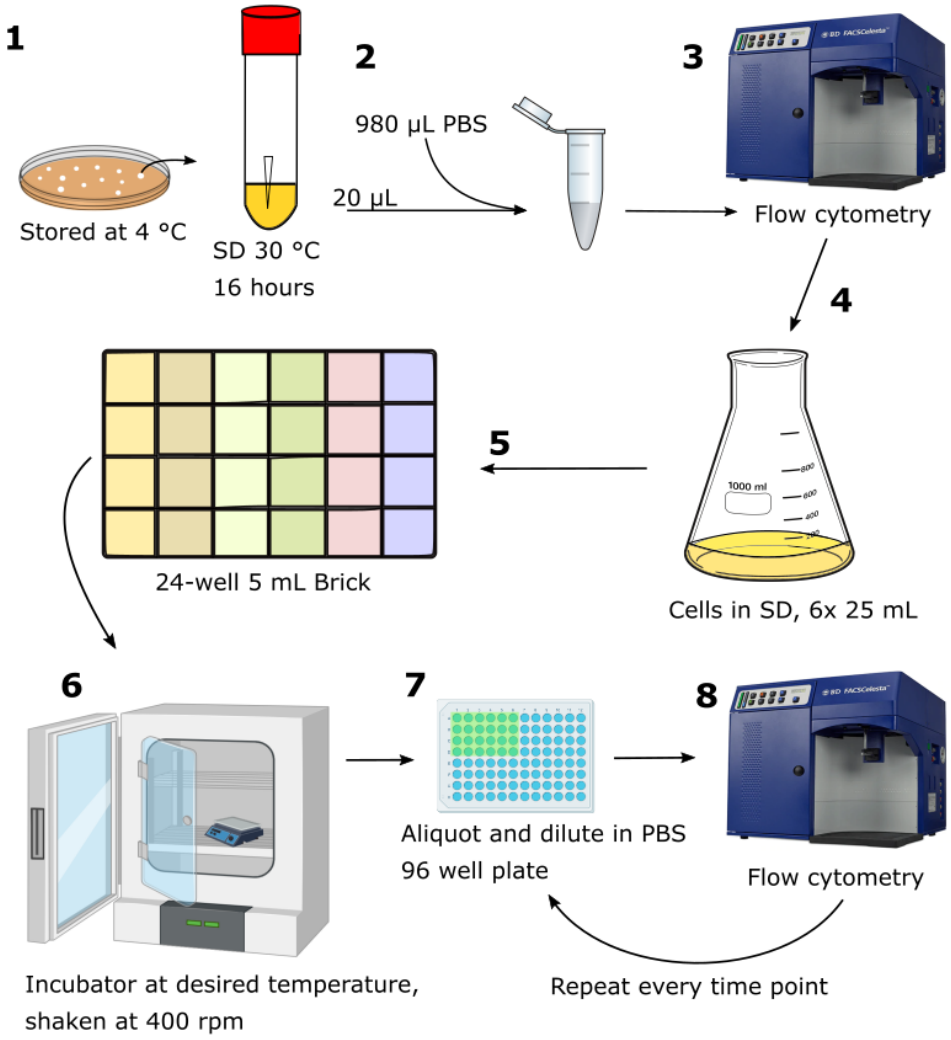

Figure 22: A typical growth experiment with *S. cerevisiae*.

In a co-existence experiment, we grew a pure culture of each of the two strains, as described above. The pure culture has an initial cell density equal to the minimal initial density of one of the strains in the mixture (strong strain), or equal to the total initial density of the mixture (weak strain). Also, we grew a mixed culture, which consists of both of the strains, mixed in the desired ratio. For the mixed culture, we followed a similar protocol as described above, but we added cells from to different strains to the initial culture.

1.4 Flow cytometry

To measure the population densities, we used a flow cytometer (BD FACS Celesta with a High-Throughput Sampler) with lasers (405 nm (violet), 488 nm (blue) and 561 nm (yellow/green)). We used a calibration of the FSC (forward scatter) and SSC (side scatter) gates that only detects yeast cells (including dead cells). For the first generation of yeast strains, this is: forward scatter photomultiplier tube voltage (FSC-PMT) = 681 V, side scatter photomultiplier tube voltage (SSC-PMT) = 264 V, GFP-channel photomultiplier tube voltage (Alexa-Fluor 488-PMT) = 485 V, mCherry-channel photomultiplier tube voltage (PE-TexasRed-PMT) = 498 V, and an FSC-threshold of 50000 (a.u). For the second generation of yeast strains, the calibration is different: forward scatter

photomultiplier tube voltage (FSC-PMT) = 375 V, side scatter photomultiplier tube voltage (SSC-PMT) = 233 V, GFP-channel photomultiplier tube voltage (Alexa-Fluor 488-PMT) = 500 V, mCherry-channel photomultiplier tube voltage (PE-TexasRed-PMT) = 590 V, and an FSC-threshold of 50000 (a.u).

Depending on the optical density of the culture (assessed by eye), we took 250 μL, 50 μL or 10 μL from each of the four wells in a column of the brick, supplemented it to 250 μL in total using PBS buffer from Fisher Bioreagents and sampled it in a 96-well plate (Sarstedt, Cat. #9020411) (see Figure 22 step 7). The number of events measured by the flow cytometer is proportional to the number of yeast cells present in the sample, when corrected for the dilution factor. Using a custom-made MATLAB script that analyses the results from the flow cytometer, we evaluated the growth of the cultures over time (see Figure 22 step 8).

2 *E. coli*

E. coli populations are optimally grown at a temperature of 37℃, where they double approximately every half hour [41]. In this thesis, we studied the growth behaviour of populations of *E. coli* at temperatures ranging from 45-50℃.

2.1 Strain information

We used a strain called K12 MG1655, which is a widely used wild-type strain in laboratories, with the following genotype: F- lambda- ilvG- rfb-50 rph-1.

2.2 Growth medium

All cultures were grown in autoclaved LB medium, which consists of distilled water, yeast extract, tryptone and NaCl.

2.3 Growth experiments

A typical growth experiment starts with preparing a culture of fresh cells by picking a colony from an agar plate stored at 4 ℃, which is then incubated in 5 mL LB medium at 37℃ for 2-3 hours (see Figure 23 step 1). Then, 20 μL of this culture was diluted 50x by adding 980 μL PBS buffer (see Figure 23 step 2). Next, this diluted culture was sampled using a flow cytometer (BD FACS Celesta with a High-Throughput Sampler), which counts the number of cells, revealing the culture's cell density (see Figure 23 step 3). The results from the flow cytometer were used to calculate the volume of the culture that is required to get the right initial cell density in the experiment, with a custom-made Excel sheet. The calculated concentration was put in an Erlenmeyer flask (VWR International, cat no 214-0423) filled with 100 mL of LB medium (see Figure 23 step 4). Six of these flasks were grown simultaneously in a water bath (Grant Instruments) with a thermostatic circulator (TC120-ST18), which keeps the temperature stable around a set value, with a standard deviation of 0.05 ℃ and a uniformity of the temperature in the bath of $\pm$0.1℃. The flasks were covered with a cap and contain an autoclaved magnetic stirrer (2MAG MIXdrive 6 High Temperature, coupled to a 2MAG MIXcontrol 20 control unit for MIXdrive), which constantly rotated at 400 rpm to keep the cultures well-mixed. A circular weight (Lead ring O form, VWR International, cat no 214-1942) was put around the flask necks, to prevent them from floating in the water bath (see Figure 23 step 5).

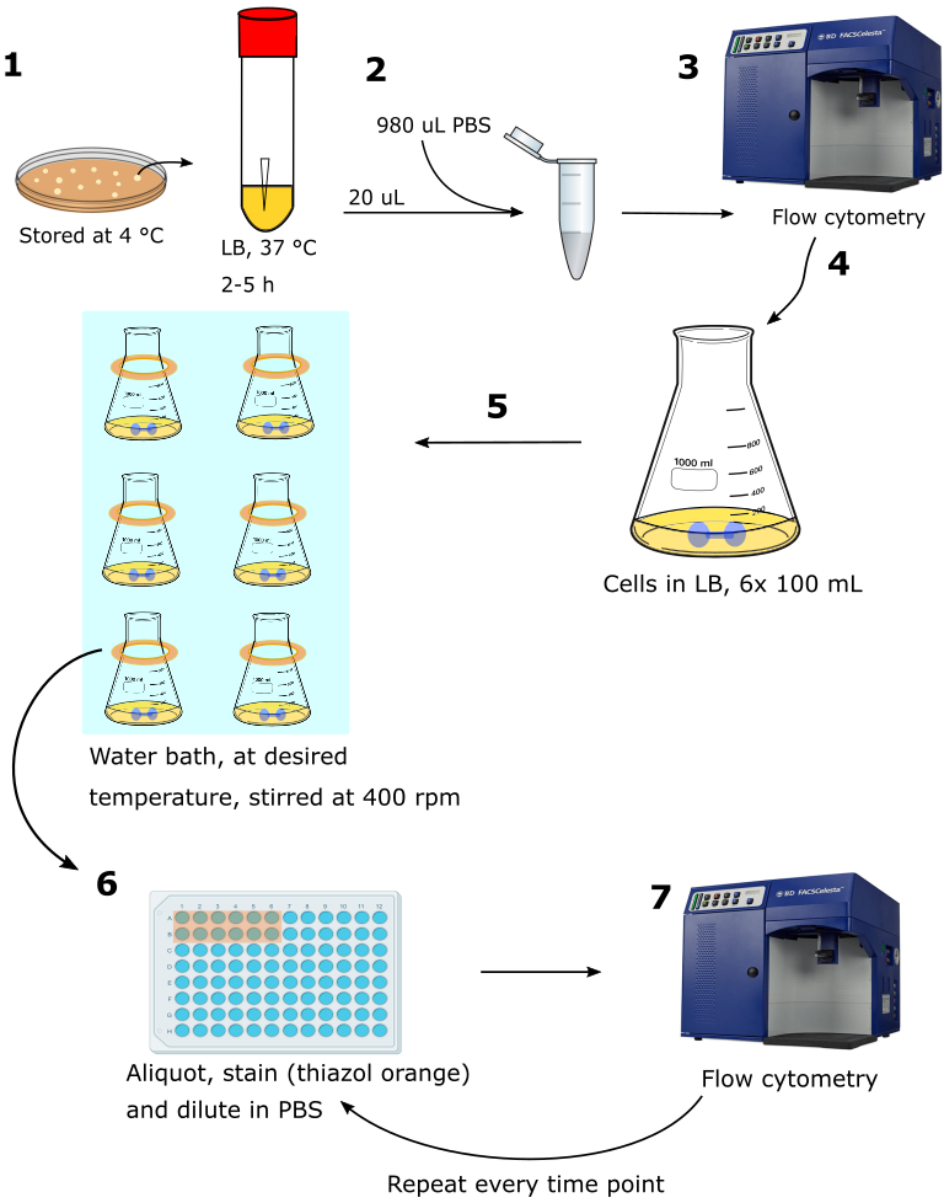

Figure 23: A typical growth experiment using *E. coli*.

2.4 Staining and flow cytometry

We used a flow cytometer (BD FACS Celesta with a High-Throughput Sampler) with lasers (405 nm (violet: Red), 488 nm (blue: PacificBlue) and 561 nm (yellow/green: AlexaFluor)) to measure the population densities at different time points. We used a calibration of the FSC (forward scatter) and SSC (side scatter) gates that mainly detects *E. coli* cells. The settings are: forward scatter photomultiplier tube voltage (FSC-PMT) = 500 V, side scatter photomultiplier tube voltage (SSC-PMT) = 350 V, GFP-channel photomultiplier tube voltage (Alexa-Fluor 488-PMT) = 725 V, mCherry-channel photomultiplier tube voltage (PE-TexasRed-PMT) = 725 V, and an SSC-threshold of 1000 (a.u).

Depending on the optical density of the culture at each time point (assessed by eye), we diluted the sample 1x, 25x or 500x, supplemented it to 250 μL in total using PBS buffer from Fisher Bioreagents and sampled it in a 96-well plate (Sarstedt, cat no 9020411). About five minutes before measuring, 0.150 μL 2 mM thiazole orange stain (390062-1G Sigma Aldrich) was added to the diluted sample, which is a stain that enters cells and stains

DNA, to visualize cells and separate them from other particles in the flow cytometer (see Figure 23 step 6). The number of events that is measured by the flow cytometer, gated in the FFC and SSC signal channels and in the yellow/green laser channel, is proportional to the number of cells present in the sample (see Figure 23 step 7). Using a custom-made MATLAB script that analyses the results from the flow cytometer, we evaluated the growth of the cultures over time and used the results to create growth curves.

2.5 Spectrophotometry

The growth curves at optimal temperatures (30℃ for yeast and 37℃ for *E. coli*) were characterized using a spectrophotometer (plate reader BioTek Synergy HTX microplate plate reader, model S1LFA). It measures OD values of liquid cultures over time. The OD value represents the optical absorption of light by the culture, excited by light with a wavelength of 600 nm. The OD is directly proportional to the cell density (for yeast: an OD value of 0.10 corresponds to approximately $1.2 \cdot 10^6$ cells/mL, for *E. coli*: an OD value of 1.00 corresponds to approximately $5 \cdot 10^8$ cells/mL). From a growth curve (log(OD) versus time in hours), we calculated the maximum growth rate, using a linear fit over six data points in MATLAB. The maximum growth rates were calculated in the region where the log(OD) is linearly proportional to the cell density (OD $\sim$ 0.1 - 0.45). Because the plate reader cannot detect OD values below 0.08 $\sim 10^6$ cells/mL for yeast and $\sim 4 \cdot 10^8$ cells/mL for *E. coli*, we used flow cytometry for most experiments throughout this thesis.

References

[1] R. D. Rolfe, “Interactions among microorganisms of the indigenous intestinal flora and their influence on the host,” *Reviews of Infectious Diseases*, vol. 6, no. 1, 1984.

[2] B. B. Jørgensen and A. Boetius, “Feast and famine — microbial life in the deep-sea bed,” *Nature Reviews Microbiology*, vol. 5, no. 10, pp. 770–781, 2007.

[3] E. L. Bruger and C. M. Waters, “Bacterial quorum sensing stabilizes cooperation by optimizing growth strategies,” *Applied and Environmental Microbiology*, vol. 82, no. 22, pp. 6498–6506, 2016.

[4] A. E. Little, C. J. Robinson, S. B. Peterson, K. F. Raffa, and J. Handelsman, “Rules of engagement: Interspecies interactions that regulate microbial communities,” *Annual Review of Microbiology*, vol. 62, no. 1, pp. 375–401, 2008.

[5] J. Gore, H. Youk, and A. van Oudenaarden, “Snowdrift game dynamics and facultative cheating in yeast,” *Nature*, vol. 459, no. 7244, pp. 253–256, 2009.

[6] S. Shibasaki, Y. Shirokawa, and M. Shimada, “Cooperation induces other cooperation: Fruiting bodies promote the evolution of macrocysts in dictyostelium discoideum,” *Journal of Theoretical Biology*, vol. 421, pp. 136–145, 2017.

[7] S. Smukalla, M. Caldara, N. Pochet, A. Beauvais, S. Guadagnini, C. Yan, and K. J. Verstrepen, “Flo1 is a variable green beard gene that drives biofilm-like cooperation in budding yeast,” *Cell*, vol. 135, no. 4, pp. 726–737, 2008.

[8] D. S. Laman Trip and H. Youk, “Yeasts collectively extend the limits of habitable temperatures by secreting glutathione,” *Nature Microbiology*, vol. 5, no. 7, p. 943–954, 2020.

[9] M. Cavaliere, S. Feng, O. S. Soyer, and J. I. Jiménez, “Cooperation in microbial communities and their biotechnological applications,” *Nature*, vol. 19, no. 8, pp. 2949–2963, 2017.

[10] J. Bull and W. Harcombe, “Population dynamics constrain the cooperative evolution of cross-feeding,” *PLoS One*, vol. 4, no. 1, 2009.

[11] B. Schink, “Energetics of syntrophic cooperation in methanogenic degradation,” *Microbiology and molecular biology reviews*, vol. 61, no. 2, pp. 262–280, 1997.

[12] S. Hummert, K. Bohl, D. Basanta, A. Deutsch, S. Werner, G. Theißen, and S. Schuster, “Evolutionary game theory: cells as players,” *Molecular BioSystems*, vol. 10, no. 12, pp. 3044–3065, 2014.

[13] B. J. Xavier, “Social interaction in synthetic and natural microbial communities,” *Molecular Systems Biology*, vol. 7, no. 1, pp. 483–495, 2011.

[14] C. J. Marx, “Getting in touch with your friends,” *Science*, vol. 324, no. 5931, pp. 1150–1151, 2009.

[15] F. Madeo, E. Fröhlich, M. Ligr, M. Grey, S. J. Sigrist, D. H. Wolf, and K. Fröhlich, “Oxygen stress: A regulator of apoptosis in yeast,” *Journal of Cell Biology*, vol. 145, no. 4, pp. 757–767, 1999.

[16] J. Verghese, J. Abrams, Y. Wang, and K. A. Morano, “Biology of the heat shock response and protein chaperones: Budding yeast (*saccharomyces cerevisiae*) as a model system,” *Microbiology and Molecular Biology Reviews*, vol. 76, no. 2, pp. 115–158, 2012.

[17] K. Foster and T. Wenseleers, “A general model for the evolution of mutualisms,” *Evolutionary Biology*, vol. 19, pp. 1283–1293, 2006.

[18] D. Wall, “Kin recognition in bacteria,” *Annual Review of Microbiology*, vol. 70, no. 1, pp. 143–160, 2016.

[19] F. F. Severin, M. V. Meer, E. A. Smirnova, D. A. Knorre, and V. P. Skulachev, “Natural causes of programmed death of yeast *Saccharomyces cerevisiae*,” *Biochimica et Biophysica Acta (BBA) - Molecular Cell Research*, vol. 1783, no. 7, pp. 1350–1353, 2008.

[20] D. Cerqueda-García, L. P. Martínez-Castilla, L. I. Falcón, and L. Delaye, “Metabolic analysis of chlorobium chlorochromatii cad3 reveals clues of the symbiosis in ‘chlorochromatium aggregatum’,” *The ISME Journal*, vol. 8, no. 5, p. 991–998, 2013.

[21] I. M. Cavalcanti, A. H. Nobbs, A. P. Ricomini-Filho, H. F. Jenkinson, and A. A. D. B. Cury, “Interkingdom cooperation between candida albicans, streptococcus oralis and actinomyces oris modulates early biofilm development on denture material,” *Pathogens and Disease*, 2016.

[22] L. Hall-Stoodley, J. Costerton, and P. Stoodley, “Bacterial biofilms: from the natural environment to infectious diseases,” *Nature Reviews Microbiology*, vol. 2, no. 2, pp. 95–108, 2004.

[23] K. A. Morano, C. M. Grant, and W. S. Moye-Rowley, “The response to heat shock and oxidative stress in *saccharomyces cerevisiae*,” *Genetics*, vol. 190, no. 4, pp. 1157–1195, 2011.

[24] X. Li, P. Fang, J. Mai, E. T. Choi, H. Wang, and X. Yang, “Targeting mitochondrial reactive oxygen species as novel therapy for inflammatory diseases and cancers,” *Journal of Hematology & Oncology*, vol. 6, no. 1, p. 19, 2013.

[25] A. K., B. S., and C. M. R., “Glutathione: new roles in redox signaling for an old antioxidant,” *Frontiers in Pharmacology*, vol. 5, pp. 1–12, 2014.

[26] M. Kafri, E. Metzl-Raz, G. Jona, and N. Barkai, “The cost of protein production,” *Cell Reports*, vol. 14, no. 1, pp. 22–31, 2016.

[27] Uniprot, “Green fluorescent protein gene - gfp - aequorea victoria (jellyfish),” 2020, *https://www.uniprot.org/uniprot/P42212* (accessed on 27-03-2020).

[28] Uniprot, “Mcherry - mcherry fluorescent protein - anaplasma marginale - mcherry gene & protein,” 2020, *https://www.uniprot.org/uniprot/X5DSL3* (accessed on 27-03-2020).

[29] R. Higuchi-Sanabria, W. M. Pernice, J. D. Vevea, D. M. A. Wolken, I. R. Boldogh, and L. A. Pon, “Role of asymmetric cell division in lifespan control in *Saccharomyces cerevisiae*,” *FEMS Yeast Research*, vol. 14, no. 8, pp. 1133–1146, 2014.

[30] V. Longo, G. Shadel, M. Kaeberlein, and B. Kennedy, “Replicative and chronological aging in *Saccharomyces cerevisiae*,” *Cell Metabolics*, vol. 16, no. 1, pp. 18–31, 2012.

[31] M. Bibinger, “Notes on the sum and maximum of independent exponentially distributed random variables with different scale parameters,” *bioRxiv (preprint)*, 2013.

[32] L. You, “Toward computational systems biology,” *Cell Biochemistry and Biophysics*, vol. 40, p. 167–184, 2004.

[33] F. A. Haight, *Handbook of the Poisson Distribution*. John Wiley & Sons, 1967.

[34] R. D. Chaudhari, J. D. Stenson, T. W. Overton, and C. R. Thomas, “Effect of bud scars on the mechanical properties of *Saccharomyces cerevisiae* cell walls,” *Chemical Engineering Science*, vol. 84, pp. 188–196, 2012.

[35] A. Farewell and F. C. Neidhardt, “Effect of temperature on in vivo protein synthetic capacity in *Escherichia coli*,” *Journal of Bacteriology*, vol. 180, no. 17, pp. 4704–4710, 1998.

[36] B. Mendoza-Chamizo, A. Løbner-Olesen, and G. Charbon, “Coping with reactive oxygen species to ensure genome stability in *Escherichia coli*,” *Genes*, vol. 9, no. 11, 2018.

[37] B. Ezraty, A. Gennaris, F. Barras, and J. F. Collet, “Oxidative stress, protein damage and repair in bacteria,” *Nature Reviews Microbiology*, vol. 15, no. 7, pp. 385–396, 2017.

[38] K. Richter, M. Haslbeck, and J. Buchner, “The heat shock response: Life on the verge of death,” *Molecular Cell*, vol. 40, no. 2, pp. 253–266, 2010.

[39] H. J. Chung, W. Bang, and M. A. Drake, “Stress response of *Escherichia coli*,” *Comprehensive Reviews in Food Science and Food Safety*, vol. 5, no. 3, pp. 52–64, 2006.

[40] F. Arsène, T. Tomoyasu, and B. Bukau, “The heat shock response of *Escherichia coli*,” *Comprehensive Reviews in Food Science and Food Safety*, vol. 55, no. 3, pp. 3–9, 2000.

[41] B. Gibson, D. J. Wilson, E. Feil, and A. Eyre-Walker, “The distribution of bacterial doubling times in the wild,” *Proceedings of the Royal Society B: Biological Sciences*, vol. 285, no. 1880, 2018.

[42] J. Soini, C. Falschlehner, C. Mayer, D. Böhm, S. Weinel, J. Panula, A. Vasala, and P. Neubauer, “Transient increase of atp as a response to temperature up-shift in *Escherichia coli*,” *Microbial Cell Factories*, vol. 4, no. 9, 2005.

[43] K. Stevenson, A. F. Mcvey, I. B. N. Clark, P. S. Swain, and T. Pilizota, “General calibration of microbial growth in microplate readers,” *Scientific Reports*, vol. 6, no. 38828, 2016.

[44] J. Liu and D. Summers, “Environmental factors affecting indole production in *Escherichia coli*,” *PLoS One*, vol. 12, no. 12, 2017.

[45] W. Chu, T. R. Zere, M. M. Weber, T. K. Wood, M. Whiteley, B. Hidalgo-Romano, and R. J. C. ... Mclean, “Indole production promotes *Escherichia coli* mixed-culture growth with pseudomonas aeruginosa by inhibiting quorum signaling,” *Applied and Environmental Microbiology*, vol. 78, no. 2, pp. 411–419, 2011.

[46] C. Chimerel, U. F. Keyser, S. Piñero-Fernandez, and D. K. Summers, “Indole transport across *Escherichia coli* membranes,” *Biophysical Journal*, vol. 100, no. 3, 2011.

[47] S. S. Grant and D. T. Hung, “Persistent bacterial infections, antibiotic tolerance, and the oxidative stress response,” *Virulence*, vol. 4, no. 4, pp. 273–283, 2013.

[48] J. Kim, H. Hong, A. Heo, and W. Park, “Indole toxicity involves the inhibition of adenosine triphosphate production and protein folding inpseudomonas putida,” *FEMS Microbiology Letters*, vol. 343, no. 1, pp. 89–99, 2013.

[49] J. Kim and W. Park, “Indole inhibits bacterial quorum sensing signal transmission by interfering with quorum sensing regulator folding,” *Microbiology*, vol. 159, no. 12, pp. 2616–2625, 2013.

[50] L. M. Maurer, E. Yohannes, S. S. Bondurant, M. Radmacher, and J. L. Slonczewski, “ph regulates genes for flagellar motility, catabolism, and oxidative stress in *Escherichia coli* k-12,” *Journal of Bacteriology*, vol. 187, no. 1, pp. 304–319, 2005.

[51] A. Zarkan, S. Caño-Muñiz, J. Zhu, K. A. Nahas, J. Cama, U. F. Keyser, and D. K. Summers, “Indole pulse signalling regulates the cytoplasmic ph of e. coli in a memory-like manner,” *Scientific Reports*, vol. 9, no. 1, 2019.

[52] H. Hirakawa, T. Kodama, A. Takumi-Kobayashi, T. Honda, and A. Yamaguchi, “Secreted indole serves as a signal for expression of type iii secretion system translocators in enterohaemorrhagic *Escherichia coli* o157:h7,” *Microbiology*, vol. 155, no. 2, pp. 541–550, 2009.

[53] C. Chimerel, C. M. Field, S. Piñero-Fernandez, U. F. Keyser, and D. K. Summers, “Indole prevents *Escherichia coli* cell division by modulating membrane potential,” *Biochimica et Biophysica Acta (BBA) - Biomembranes*, vol. 1818, no. 7, pp. 1590–1594, 2012.

[54] J. Lee, T. K. Wood, and J. Lee, “Roles of indole as an interspecies and interkingdom signaling molecule,” *Trends in Microbiology*, vol. 23, no. 11, pp. 707–718, 2015.

[55] Q. T. Do, G. T. Nguyen, V. Celis, and R. S. Phillips, “Inhibition of *Escherichia coli* tryptophan indole-lyase by tryptophan homologues,” *Archives of Biochemistry and Biophysics*, vol. 560, pp. 20–26, 2014.

[56] H. H. Lee, M. N. Molla, C. R. Cantor, and J. J. Collins, “Environmental factors affecting indole production in *Escherichia coli*,” *Nature*, vol. 467, no. 7311, pp. 82–85, 2010.

[57] T. H. Han, J.-H. Lee, M. H. Cho, T. K. Wood, and J. Lee, “Environmental factors affecting indole production in *Escherichia coli*,” *Research in Microbiology*, vol. 162, no. 2, pp. 108–116, 2011.

[58] S. M. Chiang and H. E. Schellhorn, “Regulators of oxidative stress response genes in *Escherichia coli* and their functional conservation in bacteria,” *Archives of Biochemistry and Biophysics*, vol. 525, no. 2, pp. 161–169, 2012.

[59] M. Subramanian, M. Goswami, S. Chakraborty, and N. Jawali, “Resveratrol induced inhibition of *Escherichia coli* proceeds via membrane oxidation and independent of diffusible reactive oxygen species generation,” *Redox Biology*, vol. 2, pp. 865–872, 2014.

[60] R. Cavicchioli, L. R. Bakken, M. Baylis, C. M. Foreman, D. M. Karl, B. Koskella, D. B. M. Welch, J. B. H. Martiny, M. A. Moran, V. I. Rich, B. K. Singh, L. Y. Stein, F. J. Stewart, M. B. Sullivan, E. A. Webb, and N. S. Webster, “Scientists’ warning to humanity: microorganisms and climate change,” *Nature Reviews Microbiology*, vol. 17, no. 9, pp. 569–596, 2019.

[61] S. D. Copley and J. K. Dhillon, “Lateral gene transfer and parallel evolution in the history of glutathione biosynthesis genes,” *Genome Biology*, vol. 3, no. 5, 2002.

[62] J. H. Lee and J. Lee, “Indole as an intracellular signal in microbial communities,” *FEMS Microbiology Reviews*, vol. 34, no. 4, pp. 426–444, 2010.

[63] B. L. A. Carter and M. N. Jagadish, “The relationship between cell size and cell division in the yeast *Saccharomyces cerevisiae*,” *Experimental Cell Research*, vol. 112, no. 1, pp. 15–24, 1978.

[64] H. Youk and W. A. Lim, “Secreting and sensing the same molecule allows cells to achieve versatile social behaviors,” *Science*, vol. 343, no. 6171, 2014.

[65] T. Maire, T. Allertz, M. A. Betjes, and H. Youk, “Dormancy as a spectrum measuring spore’s proximity to death and to replicative life,” *bioRxiv (preprint)*, 2019.

Part 7

Supplementary information

S1 Experimental results yeast

In this section, supplementary information regarding the experiments with *S. cerevisiae* is presented and discussed.

S1.1 First-generation strains

First, we will discuss supplementary information about the first-generation strains. We determined the relative, mean GFP expression of the first-generation strains (see Figure S1), including the base-level of the wild type strain W303 and of the inducible TT7 strain (maximally induced to express GFP and non-induced). The expression level is regulated by the corresponding constitutive promoter (indicated in the legend).

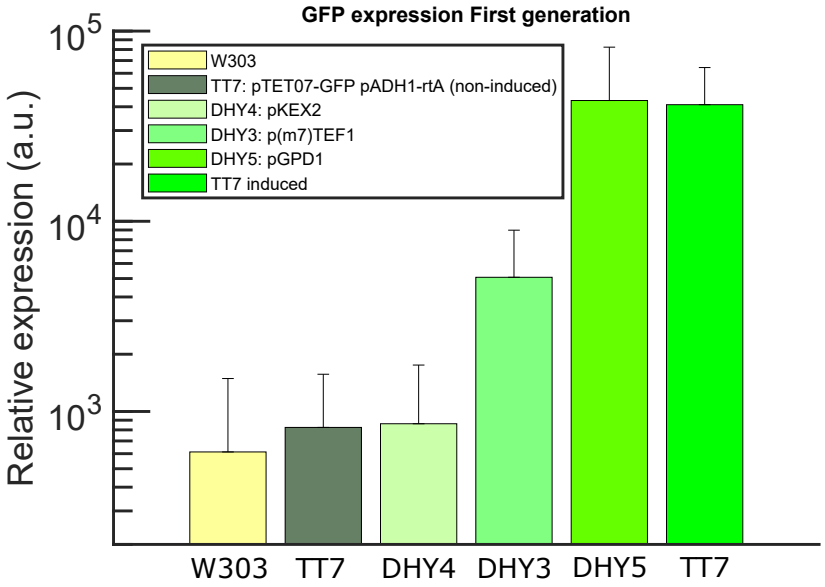

Figure S1: Relative, mean GFP expression level of the first-generation strains at $30\,℃$. Data is obtained using flow cytometry and represents the geometric mean expression level in a population of cells. The strain names and the promoters that regulate the relative GFP expression levels are indicated in the legend. The error bars represent the standard deviation within the population.

The GFP expression of the strain TT7 is induced by doxycycline. Doxycycline binds to the protein rtTA, forming a complex that binds the operator, stimulating the expression of GFP. We measured the GFP expression as a function of doxycycline concentration at a high temperature (see Figure S2). The resulting curve is roughly sigmoidal. Using this curve, the GFP expression of the inducible strain can be regulated.

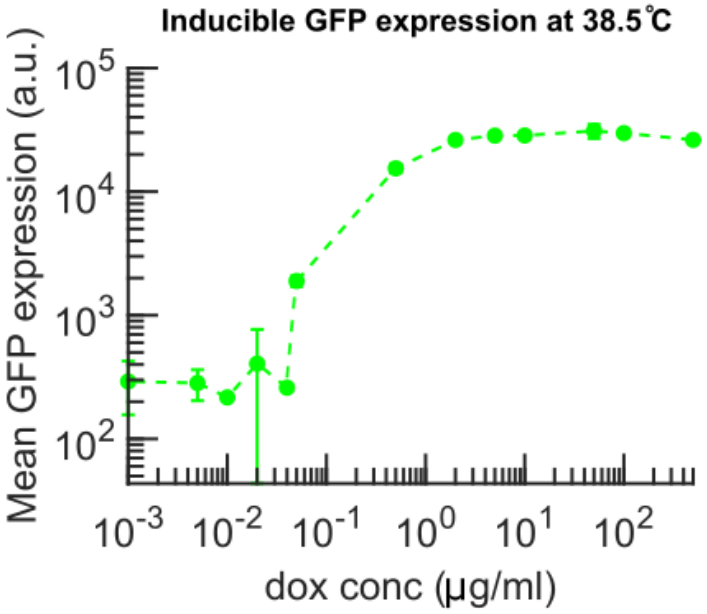

Figure S2: Inducible GFP expression of strain TT7 as a function of the concentration of inducer doxycycline at $38.5℃$. Data is obtained using flow cytometry after an incubation time of $\sim$ 7 hours, with n=4 biological replicates. The error bars represent the standard deviation over the biological replicates.

For some of the first-generation strains, the wild type and two GFP-expressing strains, the phase diagram of growth was characterized [8] (see Figure S3). Indeed, the expression of a fluorescent protein, such as GFP, causes the phase diagram of the strain to shift. For example, the region of non-growth starts at a lower temperature and the maximum temperature at which growth is observed, decreases. So, a higher initial population density is required at the same temperature when a strain expresses GFP at a higher level.

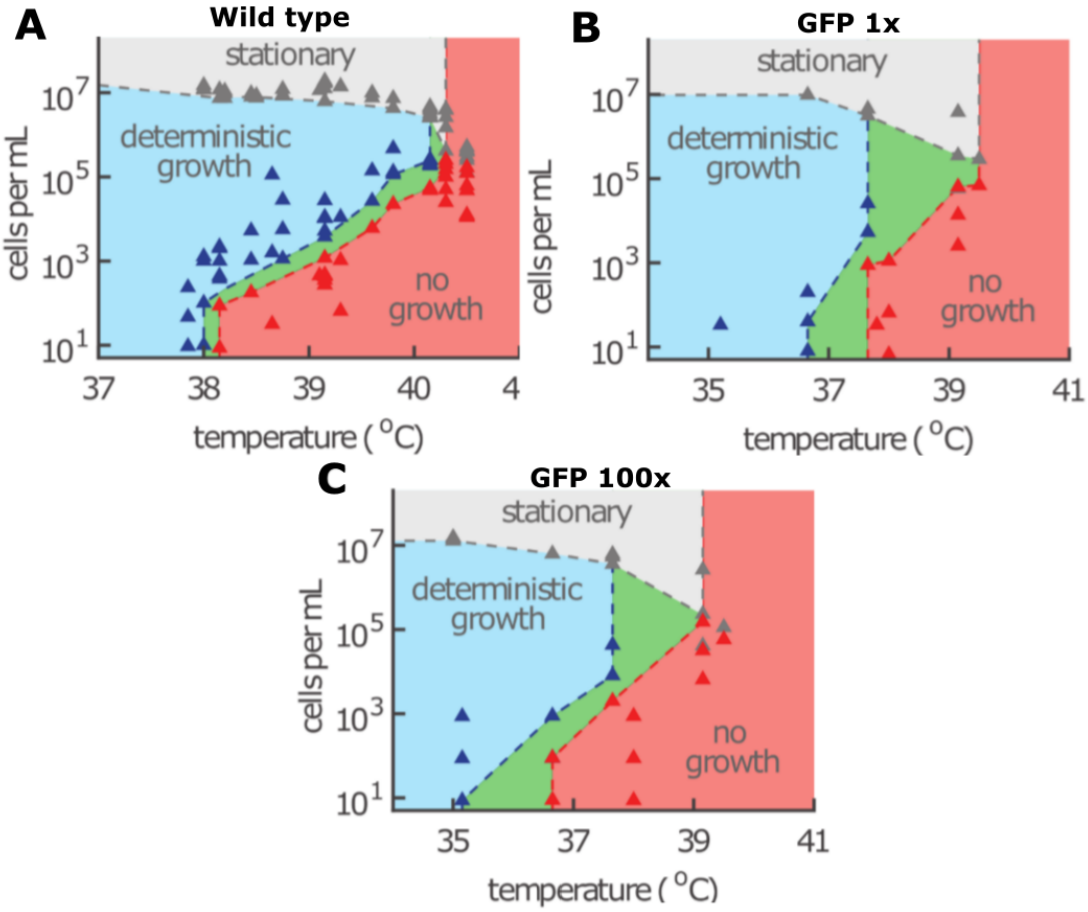

Figure S3: Growth at various temperatures and initial cell densities can be summarized in a phase diagram. A) W303 (wild type) strain, **B)** Weakest GFP-expressing strain (DHY4), **C)** Strongest GFP-expressing strain (DHY5). Adopted from [8]. The blue region represents deterministic growth, where all cultures grow. The green region represents randomly growing cultures, that grow after an unpredictable time of stasis. The red region represents cultures that do not grow, regardless of how often one repeats the experiment. The grey region represents a lack of nutrients.

S1.2 Second-generation strains

We measured the growth rate and GFP and mCherry expression level of the strains at the optimal temperature of 30℃. The average expression levels of the strains were determined by measuring the fluorescence of cells in a population using flow cytometry. Beside the mean, relative expression levels (see Figure 5A,B), the expression levels of the second-generation strains were also characterized in the form of a histogram (see Figure S4A,B). These histograms give more information about the spread and overlap of the GFP and mCherry expression levels of the strains. The expression levels can change slightly with a changing temperature.

We additionally characterized the growth rate of the strains at the optimal temperature of 30℃ using the optical density (OD) of a growing culture, measured using a spectrophotometer (see Figure S4C,D). Using these growth curves, we calculated the maximum growth rates of the strains (see Table S6). The fluorescence of the strains in the other channel (i.e. the mCherry fluorescence of the GFP-expressing strains and the GFP

fluorescence of the mCherry-expressing strains) is consistently at base level (see Figure S4E,F).

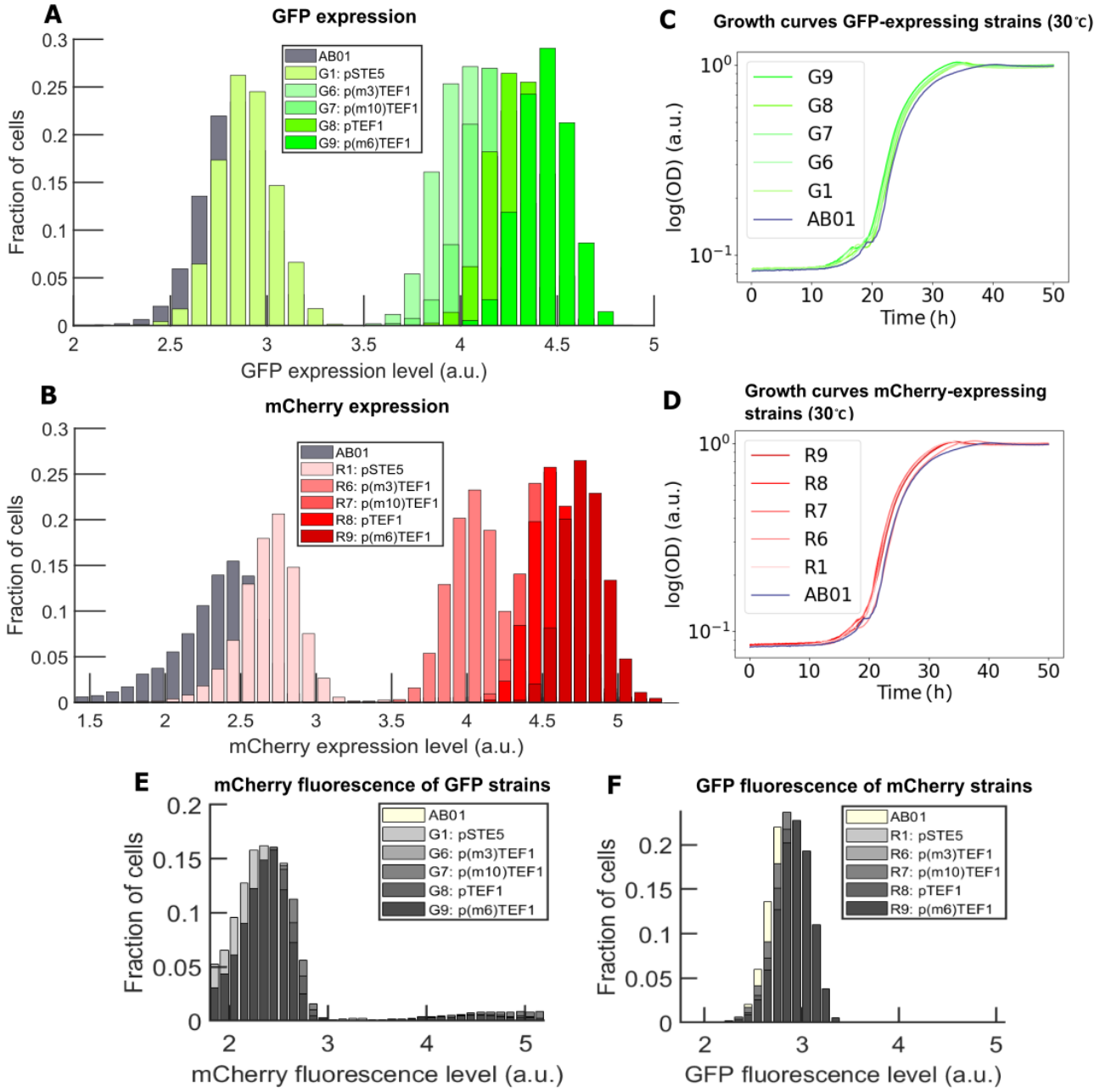

Figure S4: Expression levels and growth curves of the second-generation strains at $30℃$. A) Data is obtained using flow cytometry. Relative GFP expression of the second generation of GFP-expressing strains, **B)** Relative mCherry expression of the mCherry-expressing strains. **C)** Growth of the GFP-expressing strains at $30℃$. Data is obtained using a spectrophotometer that measures the OD OD (optical density) every 10 minutes. The OD value represents the absorption of light with a wavelength of 600 nm. It is directly proportional to the density of cells. An OD of 0.10 corresponds to approximately $1.2 \cdot 10^6$ cells/mL. **D)** Growth of the mCherry-expressing strains at $30℃$. **E)** The (base level) mCherry expression of the GFP-expressing strains. **F)** The (base level) GFP expression of the mCherry-expressing strains.

We calculated the maximum growth rates and the minimum doubling times of the second-generation strains (Table S6) from the growth curves (see Figure 5D,E). Also, we determined the minimum doubling times via the following formula, where $t_{D,min}$ is the minimum doubling time and μ_{max} is the maximum growth rate.

$$t_{D,min} = \frac{ln(2)}{\mu_{max}} \tag{33}$$

The maximum growth rates of the strains are also shown in Figure 5F,G.

Table S6: Maximum growth rates and minimum doubling times of the second-generation strains, calculated from the growth curves.

Strain	**Max growth rate (h^{-1})**	**Min doubling time (min)**	**Strain**	**Max growth rate (h^{-1})**	**Min doubling time (min)**
G1	0.29	142	R1	0.39	106
G6	0.35	121	R6	0.36	113
G7	0.35	121	R7	0.44	95
G8	0.34	122	R8	0.37	104
G9	0.33	124	R9	0.35	112
AB01 (parent strain)	0.43	97	AB01 (parent strain)	0.43	97

S1.3 Separation of strains in a co-existence experiment

In this section, we show how we separate the two strain in a co-existence experiment, based on their fluorescence (see Figure S5).

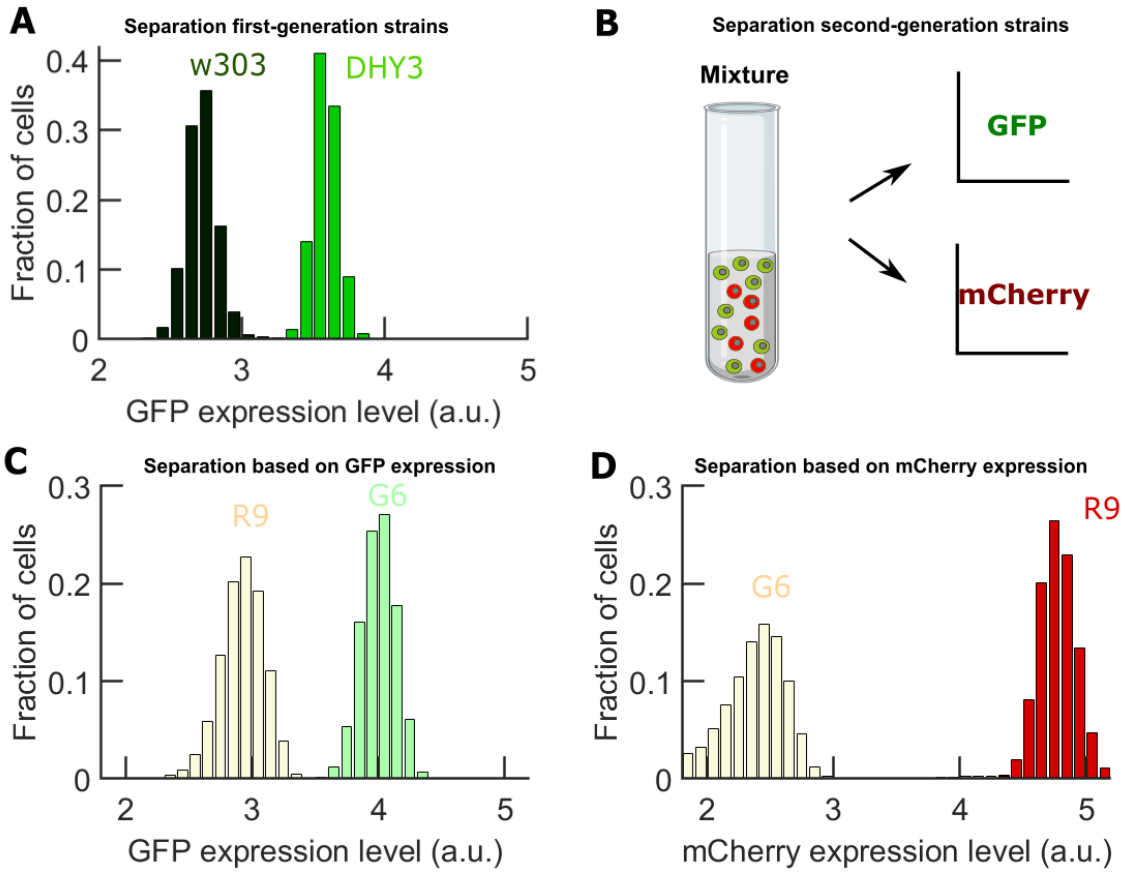

Figure S5: Separation of strains in a co-existence experiment. A) First-generation strains are separated using the GFP channel only. Here, the example of a frequently used combination of strains is given as an example: the wild type strain w303 and the GFP-expressing strain DHY3 (relative level of GFP expression 10x). **B)** Two second-generation strains in a mixed culture are separated using both the GFP and the mCherry channel. Here, a frequently used combination of strains is given as an example: R9 (expressing mCherry in the highest level, relative 9x) and G6 (expressing GFP in an intermediate level, relative 6x). The strains are separated using **C)** the flowcytometer data in the GFP channel and **D)** in the mCherry channel.

S2 Mathematical model

In the following section, supplementary information regarding the mathematical model, which simulates yeast growth at high temperatures and is used to simulate co-existence experiments, is introduced.

S2.1 Summary of the model

First, we will recall the mathematical model for yeast growth at high temperatures described in part 3 of this thesis and briefly define its parameters and variables.

The model assumes that the waiting times for cell replication (X_i) and cell death (Y_i) of a single cell (labeled $i = \{1, \dots, A_t\}$) can be modelled as exponentially distributed random variables, where the parameter μ is the growth rate and λ is the death rate.

$$X_i \sim Exp(\mu) \tag{34}$$

$$Y_i \sim Exp(\lambda) \tag{35}$$

On the population-level, we are interested in the minimum of the waiting times, corresponding to the first cell in the population to replicate or die, which is also exponentially distributed.

$$Z_t = min_i(X_i) \sim Exp(\mu A_t) \tag{36}$$

$$Q_t = min(Y_i) \sim Exp(\lambda A_t) \tag{37}$$

For simplicity, we look at the number of replications (W_t) and deaths (Q_t) that occur in a time step δt, with a population size A_t, which are modelled as follows:

$$W_t \sim Poisson(\mu A_t \delta t) \tag{38}$$

$$Q_t \sim Poisson(\mu A_t \delta t) \tag{39}$$

The population size over time is described as follows by a stochastic equation:

$$A_{t+\delta t} = A_t + W_t - D_t \tag{40}$$

Glutathione is accumulated over time, via the following equation, where M_t is the concentration of glutathione.

$$M_{t+\delta t} = M_t + A_t \cdot \delta t \tag{41}$$

The growth rate μ depends on the concentration of glutathione in the medium via a Hill function with Hill coefficient $n = 1$ and on the available nutrients via the carrying capacity C:

$$\mu(t) = \mu_{max} \frac{M_t}{K + M_t} \Big(1 - \frac{M_t}{C}\Big) \tag{42}$$

The death rate depends linearly on temperature:

$$\lambda(T) = \mu_{max} \frac{T - T_0}{T_{max} - T_0} \tag{43}$$

In Table S7, the definition of all parameters and variables is summarized.

Table S7: Definition of the parameters and variables used in the model

Parameter	Definition	Typical value	Variable	Definition
A_0	The initial population size of strain 1	∼1000 cells/mL	A_t	The number of living cells of strain 1
B_0	The initial population size of strain 2	∼1000 cells/mL	B_t	The number of living cells of strain 2
T	The temperature	$39℃$	$N_{A,t}$	The total number of cells of strain 1
μ_{max}	The maximum growth rate	0.25 h^{-1}	$N_{B,t}$	The total number of cells of strain 2
K	The sensitivity to glutathione	30000 units/mL	M_t	The concentration of glutathione/ The number of depleted nutrient units
C	The carrying capacity	$2 \cdot 10^7$ units/mL	W_t	The number of born cells during a time step δt
cc	The saturating cell density	10^7 cells/mL	D_t	The number of cells that died during a time step δt
T_0	The minimum temperature at which populations with a low initial density can die	$37.9℃$	μ	The growth rate
T_{max}	The maximum temperature, above which no population growth is possible	$40.2℃$		
λ	The death rate, dependent on temperature	0.12 h^{-1}		
n	The Hill coefficient	1		

Now, we will discuss how the values of the parameters are determined from experimental data to calculate the growth rate and the death rate in the model. Most of the parameters can easily be estimated using experimental data (namely the parameters T_0, T_{max}, C and μ_{max}). The minimum and maximum temperature (T_0 and T_{max}) are used to calculate the death rate λ (see equation 43). Their values are estimated from the experimental phase diagram of the yeast strain (e.g. see Figure S3). The minimum temperature T_0 is the temperature at which growth becomes density-dependent. In other words, in the model it is the minimum temperature T_0 above which death starts to play a role. The maximum temperature T_{max} is the temperature above which no growth is possible at all, regardless of the initial cell density.

The parameters C, μ_{max}, K and n are used to calculate the growth rate (via equation 42). The carrying capacity C corresponds to the density of nutrient units in total available in the medium. It is related to the saturating cell density cc that a culture can maximally reach, which we can read off from an experimental growth curve (e.g. see Figure 5D-E). The saturating cell density is typically in the order of 10^7 cells/mL, but differs per temperature and per strain. The maximum growth rate (μ_{max}) is determined by calculating the maximum slope of the experimental growth curve of a particular strain, grown at a temperature of $\sim 36℃$, where yeast cells start to secrete glutathione [8].

The other parameters (namely K and n) are not easily determined from experiment, but they are required to calculate the growth rate μ (via equation 42). We chose to keep the Hill coefficient n equal to 1 throughout this

thesis, unless stated otherwise, because this is the standard value in a Hill curve. The sensitivity to glutathione (K) can shift the Hill response curve to the left or to the right. The larger K, the more the curve is shifted towards higher glutathione concentrations (see supplementary Figure S7D), and the more glutathione the population of this strain needs to grow. The value of K is by definition the glutathione concentration at which the probability of birth is equal to $\frac{1}{2}\mu_{max}$. We chose the value of K such that the experimental results match the simulation results: K is chosen to be equal to 30000 for the wild-type strain.

S2.2 Separate deterministic part from noise

One of the advantages of the described model compared to the previous model [8] is that we can split its behaviour in a deterministic part and a stochastic part. In this section, we will demonstrate this.

For a large parameter a, the Poisson distribution $Poisson(a)$ can appropriately be approximated by a normal distribution $N(\mu = a, \sigma = a)$ [33]. This is easily verified via a simulation (see Figure S6A-C). For small parameter a (i.e. $a < 20$), the distributions do not match, as the Poisson distribution only contains integer values, whereas the normal distribution is continuous (see Figure S6A). Nevertheless, for large values of the parameters in our model $\mu A_t \delta t$ and $\lambda A_t \delta t$, we can replace the Poisson distributions by normal distributions. Then, we rewrite the stochastic equation describing the population size over time (equation 6), by replacing the Poisson distributions by normal distributions.

$$A_{t+\delta t} = A_t + W_t - D_t = \tag{44}$$

$$A_t + N(\mu A_t \delta t, \mu A_t \delta t) - N(\lambda A_t \delta t, \lambda A_t \delta t) = \tag{45}$$

Now, we rewrite the stochastic equation by combining the two normal distributions into one and by using the calculation rules of the normal distribution.

$$A_{t+\delta t} = A_t + N((\mu - \lambda) A_t \delta t, (\mu + \lambda) A_t \delta t) \tag{46}$$

$$= A_t + (\mu - \lambda) A_t \delta t + N(0, (\mu + \lambda) A_t \delta t) \tag{47}$$

Next, we split up the stochastic equation in a deterministic part: $A_t + (\mu - \lambda) A_t \delta t$ and a stochastic part: $N(0, \sqrt{(\mu - \lambda) A_t \delta t})$. The stochastic part represents the stochastic noise in the model, which has a mean of zero. This results in the following differential equation, where ϵ_t represents the stochastic noise.

$$\frac{A_{t+\delta t} - A_t}{\delta t} = \frac{dA}{\delta t} = (\mu - \lambda) A_t + \frac{1}{\delta t} \cdot N(0, (\mu + \lambda) A_t \delta t) \tag{48}$$

$$\frac{dA}{\delta t} = (\mu(t) - \lambda) A_t + \epsilon_t \tag{49}$$

We obtain the following solution to the deterministic part of the differential equation. The growth rate μ is dependent on time, because it depends on the concentration of glutathione, secreted by the cells, in the medium.

$$A_t = A_0 e^{(\mu(t) - \lambda)t}, \tag{50}$$

Here, $\mu(t) - \lambda(T)$ could simply be called the net growth rate μ_{net}. If $\mu(t) > \lambda(T)$, the population grows, whereas if $\mu(t) < \lambda(T)$, the population goes extinct.

We compared the size of the noise term ϵ_t to the deterministic part of the differential equation, for various

different, independent trials (see Figure S6D). We observe that the ratio of the noise term over the deterministic term fluctuates around 0 and that the magnitude of the noise is about $1 - 15\%$ of the deterministic part. This means that a large part of the population dynamics is determined by stochastic noise and different simulations could give qualitatively different results.

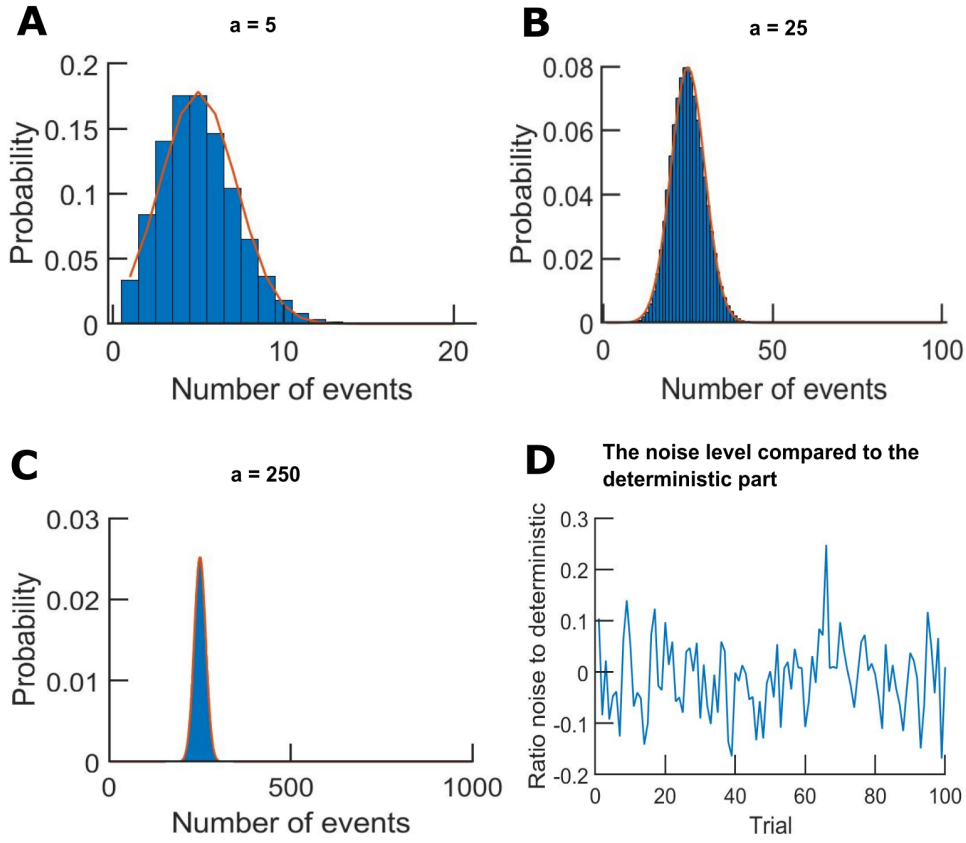

Figure S6: The Poisson distribution (blue histogram) and the normal distribution (red line) are equal for a large parameter. A) $a = 5$, **B)** $a = 25$, and **C)** $a = 250$. **D)** Comparison of the magnitude of the noise part versus the deterministic part of the differential equation (equation 49).

S2.3 Response curve of the growth rate to glutathione

In the model described in this thesis, we have chosen the Hill function as a response curve of the growth rate to the extracellular glutathione concentration. As an alternative to the Hill function response curve, a response curve that is independent of the extracellular glutathione concentration M_t, could have been chosen. In that case, the Hill term in the formula for the growth rate disappears, and we end up with the following formula. Here, the scaling factor μ_{max} and the term that incorporates a carrying capacity: $1 - \frac{M_t}{C}$, remain.

$$\mu(t) = \mu_{max}(1 - \frac{M_t}{C}) \tag{51}$$

This formula scales the growth rate solely based on the carrying capacity (see Figure S7A). This type of response would result in growth behaviour that shows no density dependence (see Figure S7B). All cultures grow, no matter their initial density. Thus, this response is not realistic.

Alternatively, a response curve that scales with the extracellular glutathione concentration M_t can be chosen. Specifically, we chose the growth rate to scale with the logarithm of $\frac{M_t}{K}$. When $M_t < K$, the growth rate is defined to be zero (otherwise it would be negative), and when $M_t > K$, the growth rate will increase linearly as a function

of $log(M_t)$ (see Figure S7A). This results in the following formula for the growth rate μ.

$$\mu(t) = \mu_{max} log(\frac{M_t}{K})(1 - \frac{M_t}{C}) \tag{52}$$

Using this alternative response curve, we obtain the three types of growth: deterministic growth, random growth and non-growth (see Figure S7C). However, random growth only occurs for a limited range of initial densities. Therefore, this response is not completely realistic.

Overall, the Hill function response curve (see Figure S7D) recapitulates the experimentally observed growth behaviour best. Namely, it shows deterministic growth (indicated in blue), random growth (indicated in green) and no growth (in red) at the same temperature for different initial cell densities (see Figure S7E). Even though the linear response curve also shows these three types of growth for a few specific initial densities, the Hill function response curve is most realistic and is used throughout this thesis.

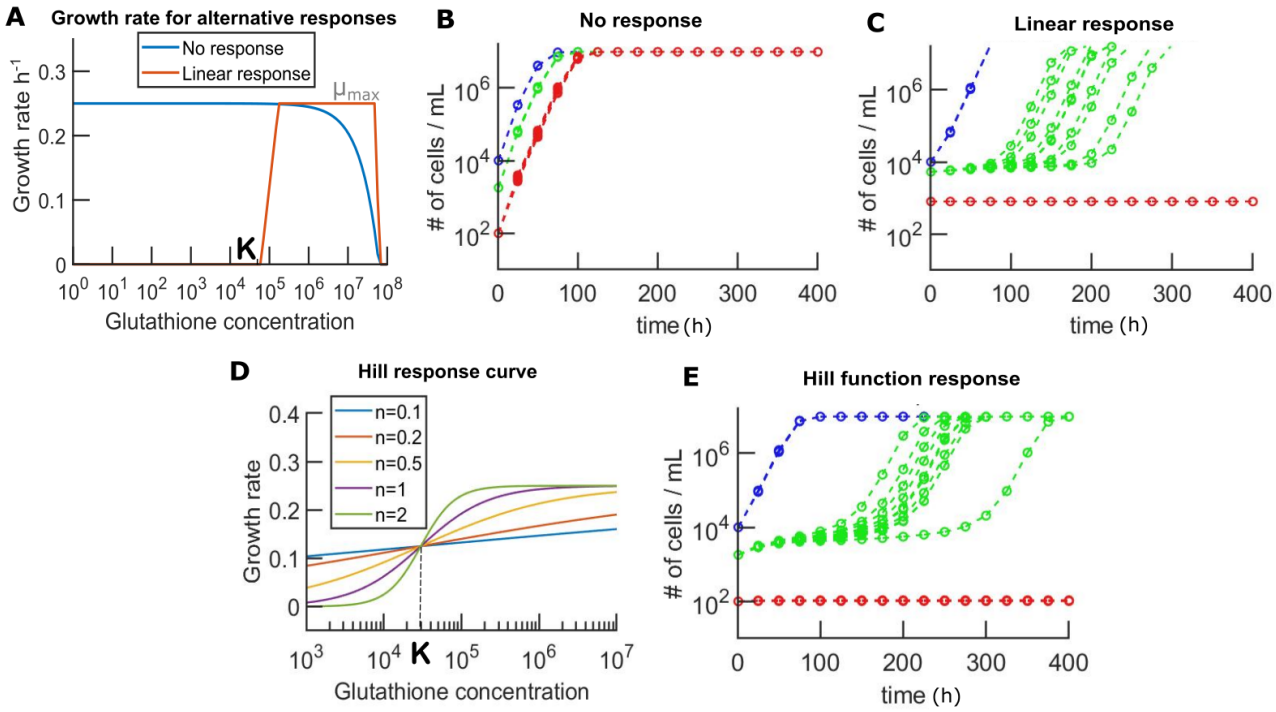

Figure S7: Alternative response curves in the model. A) Growth rates (in h^{-1}) as a function of the extracellular glutathione concentration (units per mL), resulting from an alternative type of response curve. **B)** Growth behaviour at $T = 39.1℃$ as a result of a non-responsive growth rate, which does not respond to the extracellular glutathione concentration, containing 10 simulated replicates per colour. **C)** Growth behaviour at $T = 39.1℃$ resulting from a linearly increasing growth rate (linear response to the concentration of glutathione), containing 10 simulated replicates per colour. **D)** The Hill curve response curve. Increasing the Hill coefficient n results in a more step-like response curve. The parameter K represents the concentration of glutathione that is required for growth, representing the point where $\mu = \frac{1}{2} \cdot \mu_{max} = 0.125$ **E)** Growth behaviour at $T = 39.1℃$, resulting from a Hill response function with Hill coefficient $n = 1$, showing deterministic (blue curves), random (green curves) and no growth (red curves), each with 10 simulated replicates.

S2.4 Phase boundaries and the fold bifurcation point

Our model of yeast growth at high temperatures can be viewed as a dynamical system, a system that is in an evolving, time-dependent state, described by the temperature and the cell density of the population. For a fixed temperature $T_0 < T < T_{max}$, the dynamical system has three fixed points (points that are mapped onto itself), two stable fixed points (black dots) and one unstable fixed point (white dot) in between (see Figure S8). Once the system reaches one of the stable fixed points, it cannot leave that point anymore. One of the stable fixed points is reached when the population density is equal to the saturating cell density, and the other stable fixed point when the population goes extinct (population size equal to zero). The unstable fixed point is reached at intermediate cell density, where random growth occurs. A small deviation from the unstable fixed point causes the population to either grow to the saturating density or to go extinct.

At a temperature equal to or above T_{max}, there is only one, stable fixed point, located at population density zero (see Figure S8), because at these temperatures, a culture is guaranteed to go extinct regardless of its initial cell density. At a temperature equal to or below T_0, there is also only one, stable fixed point, but now it is located at the saturating cell density, because the population will always be able to grow regardless of the initial cell density.

For varying temperatures, the fixed points become phase boundaries in the phase diagram (see Figure S8). The boundary between carrying capacity (grey) and deterministic growth (blue) is a stable phase boundary, because it consists of stable fixed points. This boundary represents the saturating cell density of a culture, called (cc). The region of random growth as a whole represents an unstable boundary, because it consists of unstable fixed points, where a small perturbation leads to either extinction or growth. The boundary between deterministic growth (blue) and random growth (green) represents the minimum, initial cell density, resulting in guaranteed growth of the population. The boundary between random growth (green) and non-growth (red), represents the maximum, initial population density that results in guaranteed extinction. Finally, there is a stable phase boundary, consisting of stable fixed points, located at zero cell density (for $T > T_0$). Most boundaries, but especially the boundaries surrounding the random growth regime, are highly sensitive to temperature (see Figure S8).

Two of the three phase boundaries (one stable and one unstable) converge to a single point, called the fold bifurcation point (indicated in pink), which occurs at temperature T_{max} for a certain initial cell density. At the fold bifurcation point (in the case of Figure S8 located at temperature $T_{max} = 40.2℃$, initial density of cells $A_0 \sim 10^6$ cells/mL), the two fixed points of the dynamical system come together and annihilate each other. At the fold-bifurcation point, the death rate is equal to the growth rate ($\lambda(T) = \mu_{max}$). At temperatures higher than T_{max}, the death rate exceeds the growth rate ($\lambda(T) \geq \mu_{max}$), so no growth is possible at all.

Exactly at the fold bifurcation point, interesting dynamics arise, because at T_{max}, the death rate is equal to the maximum growth rate: $\lambda(T) = \mu_{max}$. In the beginning of an experiment, after accumulation of glutathione, $M_t << C$ and the carrying capacity C does not play a role yet, so $\mu(t) \cong \mu_{max} = \lambda$ for a sufficiently large population size. Then, at the fold bifurcation point, the following equation holds (see equation 49).

$$\frac{dA}{\delta t} = A_t(\mu(t) - \lambda) + \epsilon_t \cong \epsilon_t \tag{53}$$

So, the change in population size solely depends on stochastic noise, called ϵ_t.

After some time, when M_t has increased, the carrying capacity starts to play a role, so μ decreases below

μ_{max} and eventually goes to 0, while λ remains constant. Therefore, the population decays exponentially, until the population has vanished:

$$\frac{dA}{\delta t} = A_t(\mu - \lambda) + \epsilon(t) \rightarrow -A_t\lambda + \epsilon(t) \tag{54}$$

In conclusion, at the fold bifurcation point, slight growth is possible at the start of the experiment, but thereafter, the population is guaranteed to go extinct.

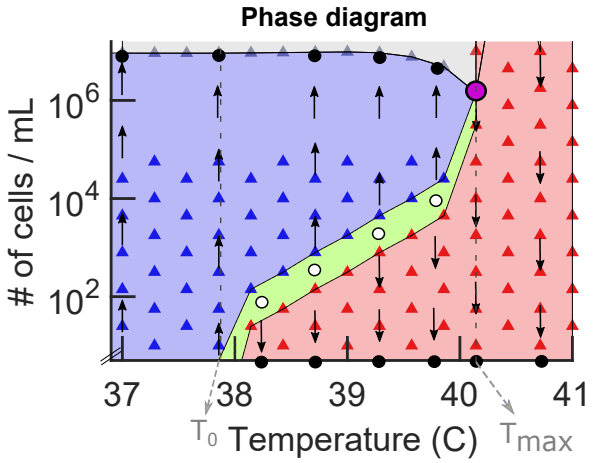

Figure S8: Phase diagram of the dynamical system of yeast growth at high temperatures. Each data points represents 10 simulated replicates. The phase diagram indicates the conditions (initial cell density and temperature) at which deterministic (blue region), random (green region) or non-growth (red region) occurs. Also, it indicates the fixed points (stable fixed points as black dots and unstable fixed points as white dots), phase boundaries (minimum of blue data points, maximum of red data points) and the fold-bifurcation point in the system (pink dot). Arrows indicate the behaviour of the dynamical system after the start of the experiment.

S2.5 Condition for non-growth of a pure culture

In this section, we will seek for a condition on the initial cell density that results in non-growth of a pure culture, which is useful to predict the initial cell densities in an experiment that result in a desired outcome: growth or non-growth. Here, the carrying capacity C is ignored, because, as explained in the section above, the decision of growth or non-growth is made long before the carrying capacity is reached. So, we can write the growth rate μ in the following way, assuming the Hill coefficient n is equal to 1.

$$\mu(t) \approx \mu_{max}\frac{M_t}{K + M_t} \tag{55}$$

We call the final concentration of glutathione that is accumulated by the culture M_{lim} - i.e. M_{lim} is the final concentration of glutathione in the medium, measured at $t \rightarrow \infty$. Thus, for all times t, $M_t \leq M_{lim}$, as glutathione is only secreted in the model and not taken up or degraded. We seek for an upper bound for M_{lim}, by using the fact that $\mu(t) < \lambda(T)$ for a non-growing culture, even when the concentration of glutathione in the medium is equal to M_{lim}.

$$\mu(t = \infty) = \mu_{max}\frac{M_{lim}}{K + M_{lim}} < \lambda(T) \tag{56}$$

Using the resulting inequality (see equation 56), by rearranging, we can describe the final concentrations of

extracellular glutathione, which result in non-growth.

$$(M_{lim} - \frac{\lambda(T)}{\mu_{max}})M_{lim} < \frac{\lambda(T)}{\mu_{max}}K \tag{57}$$

$$M_{lim} < \frac{\frac{\lambda(T)}{\mu_{max}}K}{1 - \frac{\lambda(T)}{\mu_{max}}} \tag{58}$$

$$M_{lim} < \frac{\lambda(T)K}{\mu_{max} - \lambda(T)} \tag{59}$$

This inequality describes an upper bound for M_{lim} that results in non-growth. So, cultures with a final concentration of glutathione $M_{lim} < \frac{\lambda(T)K}{\mu_{max}-\lambda(T)}$, are unable to grow.

Now, we seek for a lower bound for M_{lim}, so we can combine both expressions into a condition for non-growth of a pure culture. To that end, we calculate the glutathione concentration that is accumulated by a non-growing population. Initially, a non-growing population dies exponentially with rate λ, since the concentration of glutathione and the growth rate are equal to 0 in the beginning of the experiment, resulting in a net growth rate of $-\lambda$ (see equation 50). This results in the following differential equation (see equation 60), with its solution (equation 61). Here, we used $A(0) = A_0$ as boundary condition.

$$\frac{\delta A}{\delta t} = -\lambda(T) \cdot A \tag{60}$$

$$A(t) = A_0 \cdot e^{-\lambda t} \tag{61}$$

The cells constantly produce and secrete glutathione: one unit per cell per time step. Therefore, over time, the growth rate increases rather than remaining constant, which causes the net growth rate to increase to a value slightly larger than $-\lambda$, but still negative. Therefore, the true concentration of glutathione is larger than predicted by exponential decay, because there are some cell replications, and the resulting daughter cells secrete glutathione, in addition to the initial A_0 cells in the population. We calculate the accumulated concentration of glutathione (M_τ) at time $t = \tau$ for an exponentially decaying population as follows.

$$M_\tau = \int_0^\tau A_t \delta t = \int_0^\tau A_0 \cdot e^{-\lambda t} \delta t = [\frac{A_0}{-\lambda} e^{-\lambda t}]_0^\tau = \frac{A_0}{-\lambda} e^{-\lambda \tau} + \frac{A_0}{\lambda} \tag{62}$$

Now, we take the limit $\tau \to \infty$, to get the final concentration of glutathione in an exponentially dying culture, which we call M_{lim} again.

$$M_{lim} = \lim_{\tau \to \infty} M_\tau = \frac{A_0}{\lambda} \tag{63}$$

The final concentration of glutathione that an exponentially dying population accumulates, M_{lim}, is a lower bound for the actual, accumulated concentration of glutathione, because in reality, a population does not die exponentially but there are some cell replications before extinction, resulting in daughter cells that secrete glutathione, in addition to the initial A_0 cells. Thus,

$$M_{lim} > \frac{A_0}{\lambda} \tag{64}$$

Combining equation 59 and 63, we have an upper bound and a lower bound for M_{lim}.

$$\frac{A_0}{\lambda} < M_{lim} < \frac{K \cdot \lambda}{\mu_{max} - \lambda} \tag{65}$$

Now, we remove M_{lim} to get the following inequality (see equation 66). Then, we rearrange to get an inequality that describes the condition for the initial number of cells A_0 that results in non-growth in a pure culture.

$$\frac{A_0}{\lambda} < \frac{K \cdot \lambda}{\mu_{max} - \lambda} \tag{66}$$

$$A_0 < \frac{\lambda^2 K}{\mu_{max} - \lambda}, \qquad \text{(Condition for non-growth)} \tag{67}$$

This condition can be used to predict the initial cell density of a pure cultures that results in the desired outcome: growth or non-growth, depending on the scenario we aim to obtain. So, using this condition can contribute to establishing a successful co-existence experiment.

S2.6 Impact of the parameters

In this section, we explore the role of each parameter in the model further, by studying their effect on the phase diagram. First, we study the effect on the phase diagram for a single strain and then, we study the effect of the parameters on the outcome of a co-existence experiment.

S2.6.1 Single strain

In this subsection, we study the change in the phase diagram of a strain (see Figure S9B-F), caused by a change in one of the parameters. We compare the resulting phase diagrams to the phase diagram of the wild type strain (see Figure S9A). First, we study the effect of T_0 and T_{max}, which determine the death rate of a strain. Increasing the value of T_0 causes the temperature at which death starts to play a role, to increase (see Figure S9B). Then, the phase boundaries shift towards higher temperatures and become steeper, causing the strain to become fitter. Increasing the value of T_{max} causes the temperature above which no growth is possible to increase (see Figure S9C). So, increasing T_{max} causes the phase boundaries to shift towards higher temperatures and become less steep, making the strain fitter.

The other four parameters (K, n, C and μ_{max}) determine the growth rate of a strain. So, changing one of these parameters might have an effect on the phase diagram. Firstly, increasing the value of K, results in an increased required concentration of glutathione for growth. Therefore, cultures with an initial density well below K, become unable to grow, as they go extinct before a large enough concentration of glutathione is built up. Thus, the phase boundaries in the middle of the phase diagram shift slightly upwards (see Figure S9D). Secondly, the parameter n determines the steepness of the Hill function (see Supplementary Figure S7D). Decreasing the value of n (from 1 to 0.1), causes the phase boundaries to become steeper. Namely, the Hill function becomes more linear for a low Hill coefficient and thus the growth rate becomes more or less constant, causing the ability to grow to become only dependent on temperature and (almost) independent of the initial cell density (see Figure S7D). Thirdly, decreasing the value of C causes the entire phase diagram to be shifted downwards (see Figure S9F), as the saturating cell density is decreased. Lastly, studying the effect of the value of the residual parameter μ_{max} on the phase diagram is not considered useful. Namely, μ_{max} does not change the qualitative growth behavior, only the rate at which it happens, since μ_{max} scales both the growth and death

rate up or down.

In conclusion, we can tune the shape of the phase diagram by varying one of the parameters, but the qualitative behaviour remains the same, except for the case in which the Hill coefficient n is drastically changed (Figure S9E).

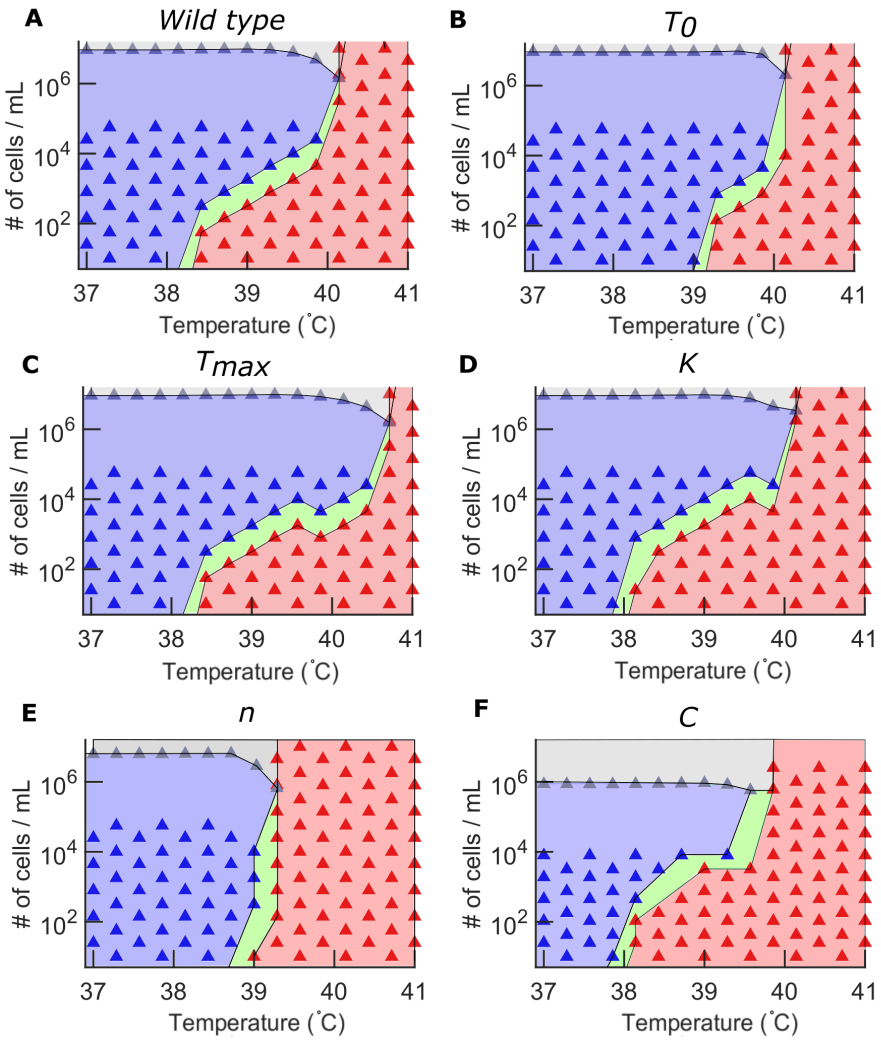

Figure S9: Changing one of the parameters results in a different phase diagram. A) Wild type strain: $T_0 = 37.9℃, T_{max} = 40.2℃, K = 30000, n = 1, C = 2 \cdot 10^7$, **B-F)** Hypothetical strain, which differs from the wild type in the following parameter: **B)** $T_0 = 39℃$, **C)** $T_{max} = 40.8℃$, **D)** $K = 90000$, **E)** $n = 0.1$, **F)** $C = 2cc = 2 \cdot 10^6$. Each data point represents 10 simulated replicates.

S2.6.2 Two strains in a co-existence experiment

Now that we have studied the phase diagram of a particular strain as a function of initial density and temperature (Figure S9), we will study the outcome of a co-existence experiment as a function of the strain parameters. In a co-existence experiment, we simulate two strains in a mixture, sharing a common environment. The strains differ from each other in properties via one or multiple parameters. To clarify the role of each parameter in the model, we defined many different, hypothetical strains, each with a different growth behaviour. We tested many possible combinations of strains (called strain 1 and strain 2), within a reasonable parameter range, where the initial cell densities of both strains are fixed. Then, we studied the resulting growth behaviour (see Figure S10). The growth behaviour of the strains in the mixture is indicated using a color scheme (defined in Figure S10A). Here, yellow means that both strains can grow equally large in population size, whereas red means that only

strain 1 can grow and green means that only strain 2 can grow in the mixture of both strains. Blue means that both strains are unable to grow in the mixture. By studying the resulting phase diagrams for each parameter (see Figure S10B-E), we derived the impact of the parameters of the strains on the outcome of the co-existence experiment (e.g. having strains in a blue region results in both strains not growing and going extinct).

First, we studied the parameters that influence the death rate of the strains (T_0 and T_{max}). We observed that a large value for T_0 is beneficial for the growth of the strain in the mixture (see Figure S10B). A strain is guaranteed to grow if $T_0 \geq T = 39℃$, because then the death rate can be neglected ($\lambda = 0$) (see equation 12). On the boundary ($\sim 37℃$), interesting outcomes appear and only one of the two strains is able to grow in the mixture. Also, we found that a large T_{max} is beneficial for growth of a strain (see Figure S10C). In the phase diagram for T_{max}, we observed a change in color when crossing $T_{max} = 39℃$. Namely, a strain is unable to grow when $T_{max} \leq T = 39℃$, because then, the death rate $\lambda(T)$ exceeds the maximum growth rate μ_{max}.

Next, we studied the parameters that influence the growth rate of the strains (μ_{max}, K, C and n). The maximum growth rate μ_{max} does not have an influence on the outcome of a co-existence experiment (see Figure S10D). Namely, if it is larger than a certain threshold value $\mu_{max} \sim 0.01$, then both strains are able to grow. We conclude that μ_{max} only has an influence on the rate of growth, but not on the ability of the strain to grow in the mixture. Also, we observed that a low K, corresponding to the minimum concentration of glutathione required for growth, is beneficial for growth (see Figure S10E). Above a certain threshold ($K \sim 100000$), no growth is possible, because the concentration of glutathione M_t does not exceed $K \sim 100000$ before the population goes extinct.

The phase diagrams of the other parameters influencing the growth rate (C and n) are not shown, because they do not provide new insights. The phase diagram of C is not interesting, because the decision of growth or non-growth is made before the culture runs out of nutrients. Namely, the initial cell density ($\sim 10^3$) and the carrying capacity ($\sim 10^7$) of the cultures differ approximately by a factor of 10^4. So, for the culture to run out of nutrients, the cells would have to live sufficiently long such that they use up $C = 2 \cdot 10^7$ units of nutrients. With only 10^3 cells in the culture, this takes up a long time: $\frac{2 \cdot 10^7}{10^3} = 2 \cdot 10^4$ time steps. This is much longer than the average simulation (~ 500 time steps). Thus, we can safely conclude that the decision of growth or non-growth is made before the carrying capacity is reached and we can simplify $\mu(t)$ (see equation 55). The phase diagram of n also does not give interesting results, because varying n only results in a changing growth behaviour of a single strain for a small region in the phase diagram (see Figure S9E) and only if the value of n is changed drastically (e.g. from 1 to 0.1).

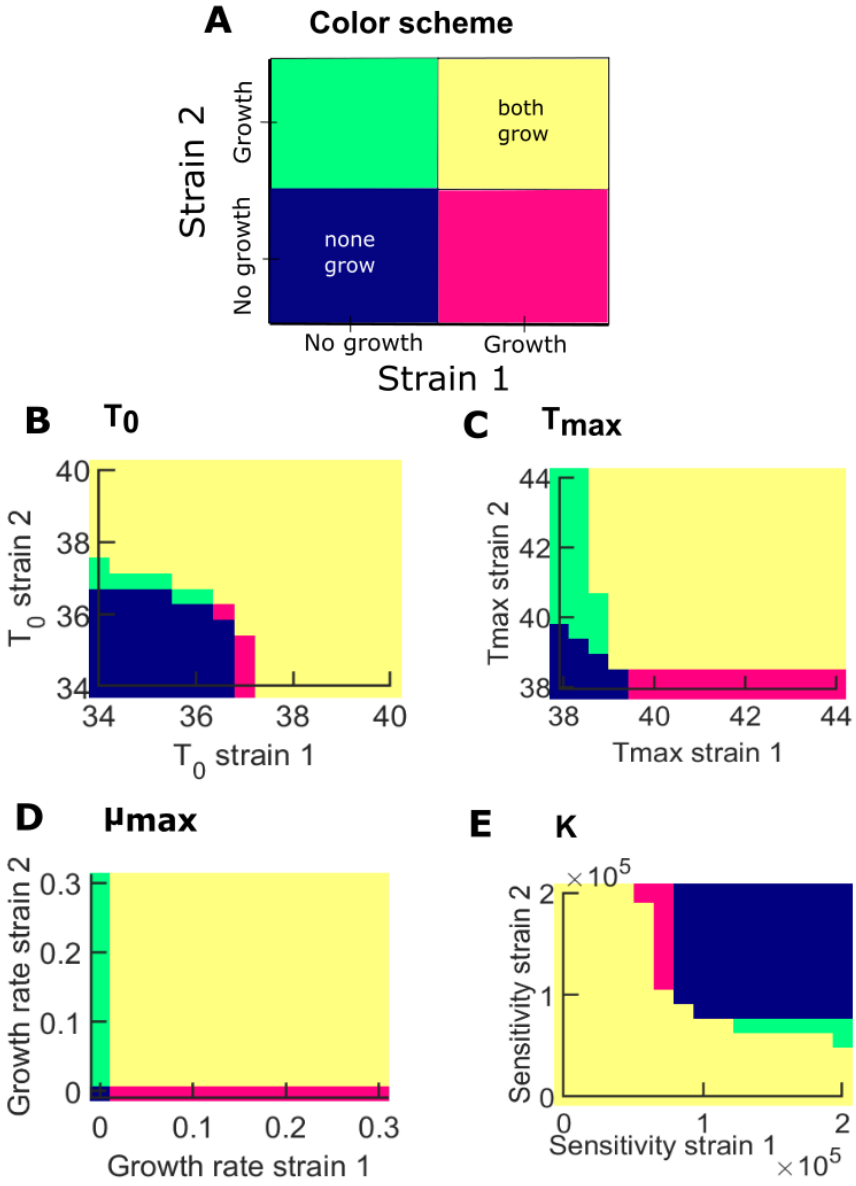

Figure S10: Changing one of the parameters can tune the outcome of a growth experiment with a mixed population at $T = 39℃$. Initial cell densities are kept constant: $A_0 = 1000$ (strain 1), $B_0 = 1000$ (strain 2). **A)** Color scheme that indicates the growth behaviour of the mixture of two strains: both strains do not grow (blue), both strains grow (yellow), only strain 1 grows (red) and only strain 2 grows (green). In **B)** only T_0 is varied between the two strains, **C)** only T_{max} is varied between the two strains, **D)** only μ_{max} is varied between the two strains, **E)** only K is varied between the two strains.

S2.7 Alternative genetic composition: two strains expressing a fluorescent protein

The outcomes of the model as described in Figure 12 are also obtained using a different combination of strains, with different parameters. Instead of using the wild type strain in combination with a strain that expresses a fluorescent protein (Figure 12) in a co-existence experiment, we could also use a different genetic composition: two strains that both express a fluorescent protein, but not at the same level. The strain with the highest expression level is the weak strain and the strain with the lowest expression level is the strong strain. The three scenarios were obtained by varying one parameter (in this case T_0) between the strains and adjusting only the initial cell densities (see Figure S11).

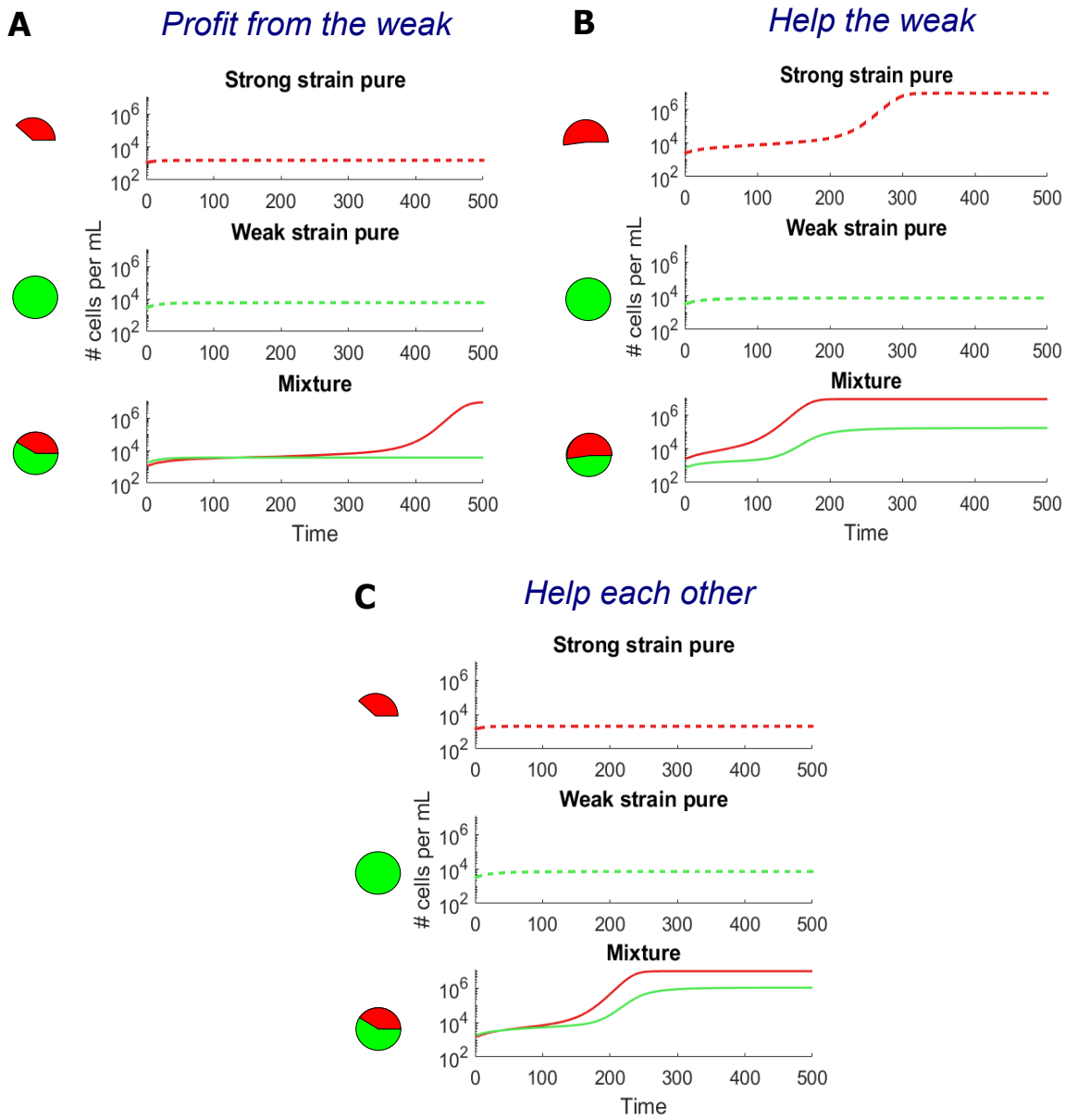

Figure S11: Simulation results with two strains that both express a fluorescent protein at $T = 39\,℃$. The graphs represent the population densities over time, representing an outcome of the co-existence experiment predicted by the model. We simulated both of the strains as a pure culture in a mixture. In this example, T_0 is chosen to be varied between the strains (two strains that each express a fluorescent protein at a certain level). $T_0^1 = 37.2℃$ and $T_0^2 = 36.5℃$. Then, we varied the initial cell densities of the two strains to obtain the three scenarios (profit from the weak, help the weak and help each other). **A)** Scenario 1 (profit from the weak): initially $A_0 = 1200$ cells/mL and $B_0 = 1900$ cells/mL. **B)** Scenario 2 (help the weak): initially $A_0 = 1700$ cells/mL and $B_0 = 1500$ cells/mL. **C)** Scenario 3 (help each other): initially $A_0 = 1500$ cells/mL and $B_0 = 1800$ cells/mL.

S2.8 Varying multiple parameters

Instead of varying only one of the parameters between the two strains, multiple parameters could be varied. This results in the same three scenarios (compared to Figure 12) as outcome of the model (see Figure S12), therefore, we conclude that it is sufficient to study the behaviour resulting from varying only one parameter between the two strains.

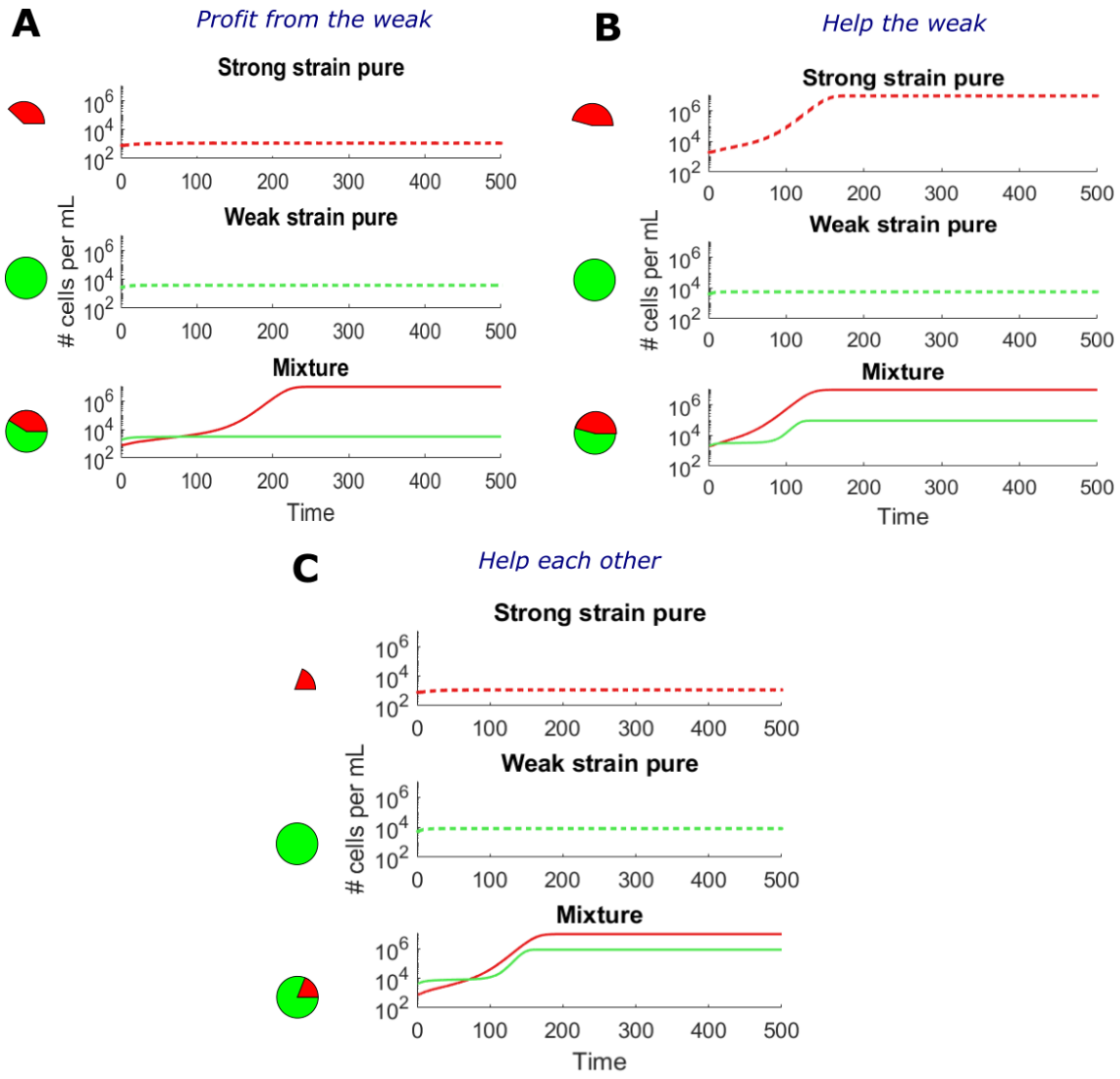

Figure S12: Varying two parameters between the strains at $T = 39℃$. The graphs represent the population densities over time, representing an outcome of the co-existence experiment predicted by the model. We simulated both of the strains as a pure culture and both strains in a mixture. Here, the parameters T_0 and μ_{max} are varied between the two strains. $T_0^1 = 37.9℃$ and $T_0^2 = 36.5℃$, $\mu_{max}^1 = 0.2h^{-1}$ and $\mu_{max}^2 = 0.5h^{-1}$. Then, we varied the initial cell densities to obtain the three scenarios (profit from the weak, help the weak and help each other to grow). **A)** Scenario 1 (profit from the weak): initially $A_0 = 800$ cells/mL, $B_0 = 2000$ cells/mL. **B)** Scenario 2 (help the weak): initially $A_0 = 2000$ cells/mL, $B_0 = 2200$ cells/mL. **C)** Scenario 3 (help each other): initially $A_0 = 800$ cells/mL, $B_0 = 4500$ cells/mL.

S3 MATLAB Code

In this section, the MATLAB code that was used for the most important figures in the chapter about the mathematical model is attached. The following code was used to plot the growth curves of two strains, pure and in a mixture (e.g. see Figure 12).

```
%% Parameters
n_cultures=10;
%Parameters strain 1 (strong)
mu1=0.25; % max growth rate
k1=30000; % sensitivity to glutathione
r1=1; % secretion rate
Tmin1=37.9; % minimal temp
Tmax1=40.2; % maximal temp
n1=1; % Hill coefficient
cc1 = 10^7; % saturating density
C1=2*cc1/mu1; % carrying capacity

%Parameters strain 2 (weak)
mu2=0.25; % max growth rate
k2=30000; % sensitivity to glutathione
r2=1; % secretion rate
Tmin2=36.5; % minimal temp
Tmax2=40.2; % maximal temp
n2=1; % Hill coefficient
cc2 = 10^7; % saturating density
C2=2*cc1/mu2; % carrying capacity

% Initial conditions
A0=1000;
B0=2200;
T=39.0;
tmax=500; % number of time steps
i=1;
if T<=Tmin1
    lambda1=0;
else
    lambda1=mu1*((T-Tmin1)/(Tmax1-Tmin1));
end
if T<=Tmin2
    lambda2=0;
else
    lambda2=mu2*((T-Tmin2)/(Tmax2-Tmin2));
end

M=zeros(1,tmax);
Nb1=zeros(1,tmax);
Nd1=zeros(1,tmax);
A=zeros(1,tmax);
NA=zeros(1,tmax);
NA(:,1)=A(:,1);
B=zeros(1,tmax);
```

```
NB=zeros(1,tmax);

A2=zeros(1,tmax);
NA2=zeros(1,tmax);
B2=zeros(1,tmax);
NB2=zeros(1,tmax);

Nb2=zeros(1,tmax);
Nd2=zeros(1,tmax);
mu=zeros(1,tmax);
%% Strain 1 pure
params = ['Tmin=','Tmax=','K=','c=','n=','mu_max='];
%Loop over t
figure(1)
subplot(3,1,1)
ylim([100 10^7.1])
xlim([0 tmax])
font_name = 'Helvetica';
font_size_tick = 14;
font_size_label = 14;
set(get(gca,'XAxis'),'FontSize', font_size_tick, 'FontName', font_name);
set(get(gca,'YAxis'),'FontSize', font_size_tick, 'FontName', font_name);
set(gca, 'LineWidth', 1.5);
set(gca, 'Layer', 'top');
set(gca, 'YTick', [10^2 10^4 10^6]);
set(gca, 'YTickLabel',['10^{2}'; '10^{4}'; '10^{6}']);
hold on
set(gca,'YScale','log');
title('Strong strain pure','FontSize',font_size_tick,'FontName',font_name)
dt=1;

A(:,1)=A0; %set initial density
for t=2:tmax
    if (A(t-1) < cc1)
        M(t)=max(0,M(t-1)+r1*A(t-1)*dt); % concentration glutathione
        %Strain 1
        mu(t-1)=max(0,mu1*(M(t-1)^n1/(k1^n1+M(t-1)^n1))*(1-M(t-1)/C1)); % growth rate
        Nb1(t-1)=max(0,poissrnd(mu(t-1)*A(t-1)*dt)); % number of births in timestep dt
        if T<Tmin1
            Nd1(t-1)=0;
        else
            Nd1(t-1)=max(0,poissrnd(lambda1*A(t-1)*dt)); % number of deaths in timestep dt
        end
        A(t)=max(0,A(t-1)+Nb1(t-1)-Nd1(t-1)); % update population: alive cells

        NA(t)=max(0,NA(t-1)+Nb1(t-1)); % update population: all cells
    end
    if (NA(t) >= cc1 || A(t) == 0) % if the strain reached carrying capacity or went extinct,
    stop
        for t=t:tmax
            NA(t)=NA(t-1);
        end
```

```
        break
    end
end
plot(1:tmax,NA,'.--','Color',[0.9 0.9 0.1],'LineWidth',1.5);

%% Strain 2 pure

figure(1);
subplot(3,1,2)
ylim([100 10^7.1])
xlim([0 tmax])
ylabel('# cells per mL')

set(get(gca,'XAxis'),'FontSize', font_size_tick, 'FontName', font_name);
set(get(gca,'YAxis'),'FontSize', font_size_tick, 'FontName', font_name);
set(gca, 'LineWidth', 1.5);
set(gca, 'Layer', 'top');
set(gca, 'YTick', [10^2 10^4 10^6]);
set(gca, 'YTickLabel',['10^{2}'; '10^{4}'; '10^{6}']);
hold on
set(gca,'YScale','log');
title('Weak strain pure','FontSize',font_size_tick,'FontName',font_name)

NB=zeros(1,tmax);
B(:,1)=A0+B0; % set initial density
NB(:,1)=B(:,1);
for t=2:tmax
    if (B(t-1) < cc2)
        M(t)=max(0,M(t-1)+r2*B(t-1)*dt); % concentration glutathione
        %Strain 2
        mu(t-1)=max(0,mu2*(M(t-1)^n2/(k2^n2+M(t-1)^n2))*(1-M(t-1)/C2)); % growth rate
        Nb2(t-1)=max(0,poissrnd(mu(t-1)*B(t-1)*dt)); % number of births in timestep dt
        if T<Tmin2
            Nd2(t-1)=0;
        else
            Nd2(t-1)=max(0,poissrnd(lambda2*B(t-1)*dt)); % number of deaths in timestep dt
        end
        B(t)=max(0,B(t-1)+Nb2(t-1)-Nd2(t-1)); % update population: alive cells

        NB(t)=max(0,NB(t-1)+Nb2(t-1)); % update population: all cells
    end
    if (NB(t) >= cc2 || B(t) == 0) % if the strain reached carrying capacity or went extinct,
    stop
        for t=t:tmax
            NB(t)=NB(t-1);
        end
        break
    end
end
plot(1:tmax,NB,'.--','Color',[0.3 0.9 0.3],'LineWidth',1.5);

%% Mixture
```

```
149
150 figure(1);
151 subplot(3,1,3)
152 set(get(gca,'XAxis'),'FontSize', font_size_tick, 'FontName', font_name);
153 set(get(gca,'YAxis'),'FontSize', font_size_tick, 'FontName', font_name);
154 set(gca, 'LineWidth', 1.5);
155 set(gca, 'Layer', 'top');
156 ylim([100 10^7.1])
157 xlim([0 tmax])
158 set(gca, 'YTick', [10^2 10^4 10^6]);
159 set(gca, 'YTickLabel',['10^{2}'; '10^{4}'; '10^{6}']);
160 hold on
161 set(gca,'YScale','log');
162 title('Mixture','FontSize',font_size_tick,'FontName',font_name)
163
164 A2(:,1)=A0; % set initial densities
165 B2(:,1)=B0;
166 NA2(:,1)=A2(:,1);
167 NB2(:,1)=B2(:,1);
168 for t=2:tmax
169     M(t)=max(0,M(t-1)+r1*A2(t-1)*dt+r2*B2(t-1)*dt); % concentration glutathione mixture
170     %Strain 1
171     mu(t-1)=max(0,mu1*(M(t-1)^n1/(k1^n1+M(t-1)^n1))*(1-M(t-1)/C1)); % growth rate
172     Nb1(t-1)=max(0,poissrnd(mu(t-1)*A2(t-1)*dt)); % number of births in timestep dt
173     if T<Tmin1
174         Nd1(t-1)=0;
175     else
176         Nd1(t-1)=max(0,poissrnd(lambda1*A2(t-1)*dt)); % number of deaths in timestep dt
177     end
178     A2(t)=max(0,A2(t-1)+Nb1(t-1)-Nd1(t-1)); % update population: alive cells
179
180     NA2(t)=max(0,NA2(t-1)+Nb1(t-1)); % update population: all cells
181     %Strain 2
182     mu(t-1)=max(0,mu2*(M(t-1)^n2/(k2^n2+M(t-1)^n2))*(1-M(t-1)/C2)); % growth rate
183     Nb2(t-1)=max(0,poissrnd(mu(t-1)*B2(t-1)*dt)); % number of births in timestep dt
184     if T<Tmin2
185         Nd2(t-1)=0;
186     else
187         Nd2(t-1)=max(0,poissrnd(lambda2*B2(t-1)*dt)); % number of deaths in timestep dt
188     end
189     B2(t)=max(0,B2(t-1)+Nb2(t-1)-Nd2(t-1)); % update population: alive cells
190
191     NB2(t)=max(0,NB2(t-1)+Nb2(t-1)); % update population: all cells
192     if B2(t)<10 % number of cells does not change after extinction
193         NB2(t)=NB2(t-1);
194         B2(t)=0;
195     end
196     if B2(t-1)==0 % once the strain is extinct, it cannot revive
197         B2(t)=0;
198     end
199 end
```

```
if (NA2(t) >= cc1 || A2(t) == 0 || NB2(t) >= cc2 || B2(t) == 0) % if the strain reached
    carrying capacity or went extinct, stop
    ii=t;
    for t=t:tmax
        NA2(t)=NA2(t-1);
    end
    for t=ii:tmax
        NB2(t)=NB2(t-1);
    end
end
%Plot
xlabel('Time')
plot(1:tmax,NA2,'Color',[0.9 0.9 0.1],'LineWidth',1.5);
plot(1:tmax,NB2,'Color',[0.3 0.9 0.3],'LineWidth',1.5);
```

The following code was used to calculate the replicative and chronological age of the cells and to plot this over time (see Figure 15).

```
% Parameters
mu1=0.25; % maximum growth rate
k1=30000; % sensitivity to glutathione
r1=1; % secretion rate
n=1; % Hill coefficient
Tmin1=37.9; % minimum temp
Tmax1=40.2; % maximum temp
cc = 10^7; % saturating density
X = 1:tmax; % time points
C = 1/mu1*(cc+sum((1/2).^X*cc)); % carrying capacity
%Conditions
T=39.1;
tmax=150;
dt=1;
n_cells=8000; % set initial density here
At = n_cells;
Mt = r1 * At; % concentration glutathione
mut = mu1*(Mt^n/(k1^n+Mt^n))*(1-(Mt/C)); % growth rate

if mut < 0
    mut = 0;
end
lambdat = mu1*((T-Tmin1)/(Tmax1-Tmin1));
if lambdat < 0
    lambdat = 0;
end
Mt = 0;
timestep=0.1;
B=ones(1,n_cells);
D=1+exprnd(1/lambdat,[1,n_cells]); % When will the cells die?
W1=1+exprnd(1/mut,[1,n_cells]); % When will the cells first replicate?
Lrepl=zeros(1,n_cells); % Replicative life span
Lchron=D-B; % Chronological life span
Ats = [n_cells]; % Alive cells
Nts = [n_cells]; % All cells
```

```
Dts = [0]; % Dead cells
ts = 0; % Time
for t=linspace(1,round(tmax/timestep),round(tmax/timestep)) % loop over time
    Ats(length(Ats)+1) = At;
    Mt = Mt + timestep * r1 * At *dt; % glutathione concentration
    mut(t) = mu1*(Mt^n/(k1^n+Mt^n))*(1-(Mt/C)); % growth rate
    if mut(t) < 0
        mut(t) = 0;
    end
    disp(t*timestep)
    ts = ts+timestep;
    deaths = (ts <= D) & (D < (ts+timestep));
    At = sum(D>(ts+timestep)); % alive cells
    births = (ts <= W1) & (W1 < (ts+timestep)) & (ts+timestep < D);
    nr_old = length(B);
    nr_new = sum(births);
    At = At + nr_new; % new population size (alive cells)

    Dts(length(Dts)+1) = Dts(end)+sum(deaths); % number of deaths
    Nts(length(Nts)+1) = Nts(end)+sum(births); % number of cells

    B((nr_old+1):(nr_old+nr_new)) = W1(births == 1); % array of time of births
    D((nr_old+1):(nr_old+nr_new)) = W1(births == 1) + exprnd(1/lambdat,[1,nr_new]); % array of
    time of deaths
    W1((nr_old+1):(nr_old+nr_new)) = W1(births == 1) + exprnd(1/mut(t),[1,nr_new]); % array of
    first replication times
    Lrepl((nr_old+1):(nr_old+nr_new)) = 0;
    Lchron((nr_old+1):(nr_old+nr_new)) = D((nr_old+1):(nr_old+nr_new)) - B((nr_old+1):(nr_old+
    nr_new));
    W1(births == 1) = W1(births == 1) + exprnd(1/mut(t),[1,nr_new]); % add new cell to array
    time of births
    Lrepl(births == 1) = Lrepl(births == 1) + 1; % add new cell to Lrepl
end

average_over = 1;
draweach = 50;

Lrepl_curr=[];
Lchron_curr=[];
for t=1:average_over:tmax % Calculate the averages over the cells born at a time point (dots in
     plot)
    Lrepl_curr(length(Lrepl_curr)+1) = mean(Lrepl( (t<=B) & (B<(t+average_over)) ));
    Lchron_curr(length(Lchron_curr)+1) = mean(Lchron( (t<=B) & (B<(t+average_over)) ));
end
Nts(end)=sum(Lrepl)+n_cells;

% Figure settings bottom
subplot(2,1,2)
cur_pos = get(gcf,'position');
cur_w = 450;
cur_h = 320;
set(gcf,'units','pixels','position',[cur_pos(1),cur_pos(2),cur_w,cur_h]);
```

```
hold on
xlabel('t')
ylabel('Amount of cells');
font_name = 'Helvetica';
font_size_tick = 24;
font_size_label = 24;
set(get(gca,'XAxis'),'FontSize', font_size_tick, 'FontName', font_name);
set(get(gca,'YAxis'),'FontSize', font_size_tick, 'FontName', font_name);
set(gca, 'Layer', 'top');
xlabel('Time of birth', 'FontName', font_name, 'FontSize',font_size_label);
ylabel('Life Span', 'FontName', font_name, 'FontSize',font_size_label);
set(gca, 'YMinorTick','Off');
set(gca, 'TickLength', [0.03, 0.03]);
set(gca, 'LineWidth', 1.5);

% Plot bottom
% dots
plot(1:average_over:tmax,(Lrepl_curr),'o','MarkerFaceColor',[0.5 0.5 0.9],'MarkerEdgeColor'
    ,[0.5 0.5 0.9] )
hold on
plot(1:average_over:tmax,(Lchron_curr),'o', 'MarkerFaceColor',[0.5 0.9 0.5], 'MarkerEdgeColor'
    ,[0.5 0.9 0.5] )
% lines
plot(linspace(1,round(tmax),round(tmax/timestep)),mut/lambdat,'LineWidth',2, 'Color',[0.1 0.1
    0.7])
hold on
plot(linspace(1,round(tmax),round(tmax/timestep)),1/lambdat*ones(1,round(tmax)/timestep),'
    LineWidth',2, 'Color',[0.1 0.7 0.1]);
legend('Lrepl','Lchron','FontSize',18)

% Figure settings top
subplot(2,1,1)
cur_pos = get(gcf,'position');
cur_w = 450;
cur_h = 320;
set(gcf,'units','pixels','position',[cur_pos(1),cur_pos(2),cur_w,cur_h]);
hold on
xlabel('t')
ylabel('Amount of cells');
font_name = 'Helvetica';
font_size_tick = 24;
font_size_label = 24;
set(get(gca,'XAxis'),'FontSize', font_size_tick, 'FontName', font_name);
set(get(gca,'YAxis'),'FontSize', font_size_tick, 'FontName', font_name);
set(gca, 'Layer', 'top');
xlabel('Time', 'FontName', font_name, 'FontSize',font_size_label);
ylabel('# cells per mL', 'FontName', font_name, 'FontSize',font_size_label);
set(gca, 'TickLength', [0.03, 0.03]);
set(gca, 'LineWidth', 1.5);
xlim([0 tmax])

% Plot top
```

```
x = 1:draweach:length(Ats);
plot(x*timestep,Nts(x),'o--','Color',[0.3 0.3 0.3],'MarkerFaceColor', [0.3 0.3 0.3],'
    MarkerEdgeColor', 'k','MarkerSize',4)
hold on
plot(x*timestep,Dts(x),'o--','MarkerFaceColor', 'r','MarkerEdgeColor', 'k','MarkerSize',4)
plot(x*timestep,Ats(x),'o--','MarkerFaceColor', 'g','MarkerEdgeColor', 'k','MarkerSize',4)
set(gca,'YScale','log');
set(gca,'YLim',[1,10^8]);
xlabel('Time')
ylabel('# cells per mL')
xlim([0 tmax])
set(gca, 'YTick', [10^0 10^2 10^4 10^6 10^8]);
set(gca, 'YTickLabel',['10^{0}'; '10^{2}'; '  10^4'; '  10^6'; '  10^8']);
legend('All cells','Dead cells','Alive cells','FontSize',18)
set(gca, 'YMinorTick','Off');
```

The following code was used to plot the phase diagram of a strain (see Figure 10D).

```
%% Phase diagram Poisson

%Parameters
mu1=0.25; % maximum growth rate
k1=30000; % sensitivity to glutathione
r1=1; % secreation rate
Tmin1=37.9; % minimal temperature
Tmax1=40.2; % maximal temperature
n=1; % Hill coefficient
tmax=1000; % number of time steps
cc = 10^7; % saturating density (cells/ml)
X = 1:tmax;
C = 1/mu1*(cc+sum((1/2).^X*cc)); % carrying capacity
dt=1; % time step duration

%Initial conditions
draw_each = 25;
n_cultures = 10;
Tsteps = 15;
density_pts=9;
A0_array1=round(logspace(1,7,density_pts)); % range of initial densities
A0_array2=round(logspace(1.4,7.4,density_pts));
T_array=linspace(37,41,Tsteps); % range of temperatures

deterministic=0; % counters
random=0;
non=0;

figure(2); % figure settings
cur_pos = get(gcf,'position');
cur_w = 450;
cur_h = 320;
set(gcf,'units','pixels','position',[cur_pos(1),cur_pos(2),cur_w,cur_h]);

clf
```

```
hold on
set(gca,'YScale','log');

font_name = 'Helvetica';
font_size_tick = 18;
font_size_label = 18;

set(get(gca,'XAxis'),'FontSize', font_size_tick, 'FontName', font_name);
set(get(gca,'YAxis'),'FontSize', font_size_tick, 'FontName', font_name);

set(gca, 'Layer', 'top');
xlabel('Temperature', 'FontName', font_name, 'FontSize',font_size_label);
ylabel('# of cells / mL', 'FontName', font_name, 'FontSize',font_size_label);
set(gca, 'YMinorTick','Off');
set(gca, 'TickLength', [0.05, 0.05]);
set(gca, 'LineWidth', 1.5);

set(gca, 'YTick', [10^2 10^4 10^6 10^8]);
set(gca, 'YTickLabel',['10^{2}'; '10^{4}'; '10^{6}'; '10^{8}']);
set(gca,'XLim',[37-0.1 41]);

% For drawing the colored polygons
poly_growth_T = [36 36];
poly_growth_D = [cc 0.1];

poly_nogrowth_T = [37];
poly_nogrowth_D = [0.1];

poly_carr_T = [37 37];
poly_carr_D = [10^10 cc];
tmax_obs = 0;

for j=1:Tsteps % loop over temperature
    T=T_array(j);
    if (T<Tmin1)
        lambdat=0;
    elseif (T>=Tmin1)
        lambdat=mu1*((T-Tmin1)/(Tmax1-Tmin1)); % death rate
    end
    if lambdat<0
        lambdat=0;
    end

    last = 1;
    growth_min = 10^7;
    growth_max = 0;
    nogrowth_min = 10^7;
    nogrowth_max = 0;
    non = 0;
    deterministic = 0;
    cur_carr = 10^10;
    for ii=1:density_pts % loop over initial densities
```

```
        if (mod(j,2)==0)
            A0 = A0_array1(ii);
        else
            A0=A0_array2(ii);
        end

        Ntcc = 0;
        Atc = 0;
        for i = 1:n_cultures % loop over a certain number of replicates
            At = A0;
            Nt = A0;
            Mt=0;
            mut=0;
            lambdat=0;
            Nt_old=Nt;
            t_old=1;
            mut_max = 0;
            for t=1:tmax
                if (At > 0 && Mt < C)
                    Mt = Mt + r1 * At * dt; % update glutathione concentration
                    mut = mu1*(Mt^n/(k1^n+Mt^n))*max((1-(Mt/C)),0); % growth rate
                    if mut > mut_max
                        mut_max = mut;
                    end
                    if mut < 0
                        mut = 0;
                    end
                    lambdat = mu1*((T-Tmin1)/(Tmax1-Tmin1));
                    if lambdat < 0
                        lambdat = 0;
                    end
                    Nb1t = poissrnd(mut*At*dt); % draw # births from Poisson distr
                    Nd1t = poissrnd(lambdat*At*dt); % draw # deaths from Poisson distr
                    At = At + Nb1t - Nd1t; % update population size
                    if At < 0
                        At=0;
                    end
                    Nt = Nt + Nb1t;
                    if (mod(t,draw_each)==0)
                        Nt_old = Nt;
                        t_old = t;
                    end
                end
            end
            drawnow
            if (mut_max >= lambdat && Nt/A0 > 100) % count how many cultures reach cc
                Ntcc = Ntcc + 1;
            elseif (mut_max < lambdat) % count how many cultures die
                Atc = Atc + 1;
            end

            if (Nt/A0 > 10)
```

```
                cur_carr = min(cur_carr,Nt); % carrying capacity
            end
        end
        if (Ntcc >= (n_cultures)) % deterministic growth
            deterministic=deterministic+1;
            plot(T,A0,'k^','LineWidth',2,...
                'MarkerEdgeColor',[.1 .1 .9],...
                'MarkerFaceColor',[.1 .1 .9],...
                'MarkerSize',6)
            growth_min = min(growth_min,A0);
            growth_max = max(growth_max,A0);

        elseif ((Atc >= n_cultures)) % no growth
            non=non+1;
            plot(T,A0,'k^','LineWidth',2,...
                'MarkerEdgeColor',[.9 .1 .1],...
                'MarkerFaceColor',[.9 .1 .1],...
                'MarkerSize',6)
            if (A0 < cur_carr) % keep track of the carrying capacity
                nogrowth_max = max(nogrowth_max,A0);
            end
        end
    end
    % colored polygons
    if (deterministic >= 1 && non >= 1)
        poly_growth_D = [cur_carr poly_growth_D growth_min];
        poly_growth_T = [T poly_growth_T T];
    elseif (deterministic >= 1)
        poly_growth_D = [cur_carr poly_growth_D 5];
        poly_growth_T = [T poly_growth_T T];
    elseif (last > 0)
        poly_growth_D = [cur_carr poly_growth_D cur_carr];
        poly_growth_T = [T poly_growth_T T];
        last = -1;
    end

    if (non == 0)
        poly_nogrowth_D = [0.1 poly_nogrowth_D 5];
        poly_nogrowth_T = [T poly_nogrowth_T T];
    end
    if (non >= 1 && deterministic >= 1)
        poly_nogrowth_D = [nogrowth_max poly_nogrowth_D 5];
        poly_nogrowth_T = [T poly_nogrowth_T T];
    elseif (non >= 1)
        poly_nogrowth_D = [10^10 nogrowth_max poly_nogrowth_D 5];
        poly_nogrowth_T = [T T poly_nogrowth_T T];
    end
    if (deterministic >= 1)
        poly_carr_D = [10^10 poly_carr_D cur_carr];
        poly_carr_T = [T poly_carr_T T];
    else
        poly_carr_D = [10^10 poly_carr_D cur_carr 10^10];
```

```
        poly_carr_T = [T poly_carr_T T T];
    end
    % Plot data points
    plot(T,cur_carr,'k^','LineWidth',2,...
        'MarkerEdgeColor',[.49 0.5 .63],...
        'MarkerFaceColor',[.49 0.5 .63],...
        'MarkerSize',6)
    ylim([5 10^7.2])
end
pgongrey = fill(poly_carr_T,poly_carr_D,[0.7 0.7 0.7],'FaceAlpha',0.3);
pgonred = fill(poly_nogrowth_T, poly_nogrowth_D,[0.9 0.1 0.1],'FaceAlpha',0.3);
pgonblue = fill(poly_growth_T,poly_growth_D,[0.1 0.1 0.9],'FaceAlpha',0.3);

plot(pgongrey,'FaceColor','black','FaceAlpha',0.3)
plot(pgonred,'FaceColor','red','FaceAlpha',0.3)
plot(pgongreen,'FaceColor','green','FaceAlpha',0.3)
plot(pgonblue,'FaceColor','blue','FaceAlpha',0.3)
```